

TECHNISCHE UNIVERSITÄT MÜNCHEN
III. Medizinischen Klinik, Hämatologie / Onkologie
Klinikum rechts der Isar

Stimulation and analysis of the vasculopoetic potential of Endothelial
Progenitor Cells by overexpression of Growth Factors via
retroviral transduction

Marc Albert Robert Rümmler

Vollständiger Abdruck der von der Fakultät für Medizin der Technischen
Universität München zur Erlangung des akademischen Grades eines
Doktors der Medizin
genehmigten Dissertation.

Vorsitzender: Univ.-Prof. Dr. D. Neumeier
Prüfer der Dissertation: 1. Priv.-Doz. Dr. R. A. J. Oostendorp
2. Univ.-Prof. Dr. B. Gänsbacher

Die Dissertation wurde am 19.11.2009 bei der Technischen Universität München
eingereicht und durch die Fakultät für Medizin am 24.03.2010 angenommen.

***Stimulation and analysis of the vasculopoetic
potential of Endothelial Progenitor Cells
by overexpression of Growth Factors
via retroviral transduction.***

Dedication:

*For my wife, for my family, for those who inspired me all my life and
for the ones that are no longer with us.*

Index

<i>Title:</i>	1
<i>Dedication:</i>	3
<i>Index</i>	4
<i>Pictures and figures</i>	7
<i>Tables</i>	9
<i>Abbreviations</i>	10
<i>I. Introduction</i>	12
1.1. Why to use Endothelial Progenitor cells for neo-vasculogenesis?	12
1.2. Aim of our study	13
1.3. How to reach this?	14
1.4. Choice of genes	15
1.5. Signaling	15
<i>II. Materials and Methods</i>	17
2.1. General methods of biochemistry and cell- or DNA analysis:	17
2.1.1. Genomic DNA Extraction out of the cells	17
2.1.2. RNA Extraction and c-DNA Synthesis	17
2.1.3. Reverse Transcription Polymerase Chain Reaction	17
2.1.4. Genomic DNA Polymerase Chain Reaction	18
2.1.5. Real Time-PCR	18
2.1.6. Protein extraction	18
2.1.7. Insulin-like-growth-factor-2 Enzyme-linked Immunosorbent Assay	19
2.1.8. Western Blot	19
2.2. Construction of the retroviral vector	20
2.2.1. Human IGF2 Insert	20
2.2.2. Human-AKT1	21
2.2.3. Human-Angiopoetin 1 (ANG1)	22
2.2.4. Human-PLGF	23
2.3. Ligation procedure	24
2.4. Producer and Target cell transfection	26
2.4.1. PT67 Producer Cells	26
2.4.2. Determination of the Virustiter produced by the PT67 Producer cells:	27
2.5. The cells that were used in our assays	27
2.5.1. Escherichia coli DH5 α	27
2.5.2. PT67 Producer Cells	27
2.5.3. Cord blood derived Endothelial Progenitor cells: CD34+ CBEC	28
2.5.4. HUVECs	28
2.5.5. Human umbilical vein stromal precursor cells (HVSC)	28
2.5.6. Human diploid fibroblasts	28
2.5.7. 3T3 Fibroblasts	28
2.6. Cell cultivation	28
2.6.1. PT67 Virus Producer cells	28
2.6.2. CD34+Endothelial Progenitor Cells	29
2.6.3. HUVECs:	29
2.6.4. HVSC	29
2.6.5. Human diploid Fibroblasts	29
2.7. Coculture	30
2.8. Cell Analysis	30
2.8.1. Cell growth	30
2.8.2 Cell morphology under IGF2 and TGFB1 stimulation	30

2.8.3. Survival.....	31
2.8.3.1. Cell survival under cytotoxic influence.....	31
2.8.3.2. Cell survival under nutrient restraint and growth factor restraint.....	31
2.8.3.3 Cell survival after UV-irradiation.....	31
2.8.4. Stimulation.....	31
2.8.4.1. IGF2.....	31
2.8.4.2. External TGFB1 stimulation.....	32
2.9. Coculture Analyze.....	32
2.9.1. Fixation and Immunohisto-staining.....	32
2.9.2. Tubuli-analyze.....	32
2.10. Statistic software analyze of the data sets.....	33
III. Results	34
3.1. Verification of the genetic alteration of the cells.....	34
3.1.1. Confirmation of transfection.....	34
3.1.2. Producer cells.....	35
3.1.2.1: Gene verification in the producer cells with PCR.....	35
3.1.2.2. Growth of the producer cells after retroviral transfection.....	35
3.1.3. Target cells.....	36
3.1.3.1: Proof of the vector integration into the DNA of the target cells.....	36
3.1.3.2. Proof of IGF2 transcription in the transfected target cells.....	37
3.1.3.2.1: mRNA / cDNA Proof with PCR and Realtime PCR.....	37
3.1.3.2.2. Proof of transcription of AKT1 and ANG1.....	38
3.1.3.3. Proof of protein translation by the target cells with ELISA.....	39
3.1.3.4. Determination of the viral titer.....	40
3.2. Consequences of the genetic alteration of the target cells.....	41
3.2.1. Growth.....	41
3.2.2. Cell survival.....	42
3.2.2.1. Cytotoxic stress.....	42
3.2.2.2: Growth factor withdrawal.....	43
3.2.2.3. Cell survival under FCS withdrawal.....	44
3.2.2.4. Cell survival under ultraviolet irradiation.....	45
3.3 Cell stimulation.....	45
3.3.1. IGF2 stimulation.....	45
3.3.2. TGFB1 Stimulation.....	48
3.4. A coculture assay of vessel formation.....	49
3.4.1. Cell growth and formation of a multilayer cell compound.....	50
3.4.2. Tubuli formation.....	50
3.4.3. Tubuli quality parameters: Length, Thickness, Crossing/Sprouting.....	53
3.4.3.1. Length.....	53
3.4.3.2. Thickness.....	54
3.4.3.3. Crossings/Sprouting.....	55
3.4.3.4. AKT1 in the Coculture assay.....	55
3.4.3.5. Cooperation project with the cardiology department to transplant the CBEC:.....	55
IV Discussion	57
4.1. Receptor growth cascades.....	57
4.1.1. Effects of AKT1 (Protein-kinase-B) activation.....	58
4.1.2. Insulin-receptor and its activation effects.....	59
4.1.3. The IGF1 Receptor.....	59
4.1.4. Mannose-6-phoshate receptors and Insulin-like Growth factor-2-receptor.....	60
4.2. Method verification.....	61
4.2.1. Affirmation of the viral construct.....	61
4.2.2. Producer cells.....	61
4.2.3. Target cells.....	62
4.2.3.1. Proof of IGF2 Transcription (mRNA/cDNA) in the transfected target cells with PCR and RT-PCR.....	62

4.2.3.2. Proof of transcription of AKT1 and ANG1	62
4.2.3.3. Proof of protein translation by the target cells	63
4.2.3.4. IGF2 supernatant Elisa	64
4.3. Consequences of the genetic alteration	64
4.3.1. Growth	64
4.3.1.2. Growth factor threshold theory	65
4.3.1.3. Possible transfection process induced cell damage	66
4.3.1.4. Cell Growth for AKT and Angiopoetin-1	66
4.3.2. Cell survival	67
4.3.2.1. Cytotoxic stress	67
4.3.2.2. Cell survival under Growth factor restraint	67
4.3.2.3. Cell survival under nutrient restraint	67
4.3.2.4. Cell survival under ultraviolet irradiation	68
4.3.3. Cell stimulation	69
4.3.3.1. External IGF2 stimulation	69
4.3.3.2. TGFB1 Stimulation	69
4.4. Coculture	70
4.4.1. Cell growth and building of a multilayer cell compound	70
4.4.2. Tubuli formation	70
4.4.3. Tubuli quality parameters: Length, Thickness, Crossing/Sprouting	71
4.4.3.1. Length	71
4.4.3.2. Thickness	71
4.4.3.3. Crossings/Sprouting	72
4.4.3.4. Coculture summary	72
V Conclusion and summary	73
VI Appendix	75
6.1. Typical cell appearance:	75
6.2. Growth curves of the different cell lines:	76
6.3. Network formation of CBEC:	78
6.4. UV-Apoptosis assay:	79
6.5. Growth curves of the external IGF2 stimulation:	81
6.6. Coculture cell sandwich layer:	82
VII Thanks	84
VIII Literature	85

Pictures and figures

Figure 1: Cloning pattern for IGF2 sequence integration into pLXSN vector

Figure 2: AKT1 cloning pattern sequence integration into pLXSN vector

Figure 3: Angiopoetin-1 cloning pattern

Figure 4: PLGF cloning pattern

Figure 5: Example from tubuli measurement with Image J

Figure 6: IGF2 native vs. transgene form in the PCR-gel electrophoresis for NB1591-94

Figure 7: PT67- PCR proof of Integration of plasmid e.g. for AKT1

Figure 8: PCR of genomic-DNA from the Target cells

Figure 9: Example of a Taqman[®] Real-Time PCR curve obtained from a IGF2 cDNA assay

Figure 10: Electrophoresis of PCR-Products from AKT1, ANG1 and IGF-receptor Primer

Figure 11: Elisa-Light-Absorption vs. Concentration of template IGF2 (NB1591-94,NB 1683)

Figure 12: G-418 Kill Curve 400 μ g/ml

Figure 13: G-418 Kill Curve with 1600 μ g/ml

Figure 14: Growth curve for NB 1591-94 FCS withdrawal

Figure 15: Comparison of average cell size for 50ng/ml IGF2 stimulation vs. parental cells

Figure 16: Picture of untreated parental endothelial cells after 2 weeks incubation

Figure 17: Picture of IGF2 treated cells and their morphology after 2 weeks of incubation

Figure 18: Growth curve of external IGF2 stimulation of NB1591-94

Figure 19, Growth Curve of external TGF-B1 Stimulation of NB1591-94

Figure 20: Tubuli vs. Cluster-formation depending on Insert IGF2 vs. parental $p=0.019$

Figure 21: Mean cluster formation of parental CBEC vs. HUVEC

Figure 22: Mean Tubular structure count in HUVEC vs. CBEC

Figure 23: Mean cluster count in HUVEC vs. CBEC

Figure 24: Mean of tubular structures for all assays:

Figure 25: Mean tubuli length depending on insert for NB 1591-94

Figure 26: Mean tubular thickness

Figure 27: Amount of tubular crossings of the different cells for NB1591-94

Figure 28: Overview of the intracellular pathway of the growth factors we used in our assays

Figure 29: Intracellular AKT1 involved cell cascades

Figure 30: NB1591-94 IGF2 pos. cells at 3 weeks of incubation with their typical appearance

Figure 31: NB1591-94 parental untreated cells after 3 weeks of incubation time

Figure 32: Growth curve for CBEC NB1591-94

Figure 33: Growth curve for CBEC NB1683

Figure 34: Growth curve for CBEC NB1166-67

Figure 35: Growth curve for CBEC NB1164-65

Figure 36: CBEC untreated forming tubular network under nutrient withdrawal

Figure 37: CBEC-pLXSN empty vector forming tubular network under nutrient withdrawal

Figure 38: CBEC NB 1164-65 Apoptosis Assay with ultraviolet irradiation

Figure 39: CBEC NB 1166-67 Apoptosis Assay with ultraviolet irradiation

Figure 40: CBEC NB 1591-94 Apoptosis Assay with ultraviolet irradiation

Figure 41: CBEC NB 1683 Apoptosis Assay with ultraviolet irradiation

Figure 42: CBEC NB 1166-67 Growth stimulation assay with external IGF2

Figure 43: CBEC NB 1166-67 Growth stimulation assay with external IGF2

Figure 44: Coculture cell sandwich layer with HUVEC and fibroblasts after 1 week

Figure 45: Cluster formed in Coculture assay by IGF2 overexpressing cells with fibroblasts

Figure 46: Typical tubular structures build by HUVEC in the Coculture assay

Tables

Table 1: Primers used for PCR

Table 2: Antibody for IGF2 Western Blot

Table 3: mRNA Clones used for analysis assays

Table 4: Statistic and growth curve results from PT-67 Growth Curve comparison

Table 5: Relative Quantity of cDNA copies of the cells (ddCT-Method compared to normalizer (H₂O))

Table 6: Relative Quantity of cDNA copies of the cells (ddCT-Method compared to normalizer (H₂O))

Table 7: Statistics of the different growth curves from the overexpressing cell lines

Table 8: Statistics with p-values of the kill curves for the different insert types

Table 9: Statistics for growth factor withdrawal assay

Table 10: P-values of nutrient withdrawal assay

Table 11: P-Values of the ultraviolet survival assays

Table 12: Statistics for external IGF2 Stimulation

Table 13: Statistics for external TGFB1 stimulation of NB 1591-94

Table 14: Statistics for the count of tubular structures depending on cell type or insert in CBEC NB 1591-94

Table 15: Statistics for tubular length depending on insert

Table 16: Statistics for tubular thickness depending on insert

Table 17: Receptor affinities of IGF2 (35)

Abbreviations

ANG1	Human Angiopoetin-1
AKT1	Human Protein kinase B
BP	Baisepairs = mean to measure DNA strand length
BSA	Bovine Serum Albumin
CD-	Cluster of differentiation, e.g. CD 34+, cellular surface marker
CXCR4	Stromal cell derived growth factor receptor
CREG	cellular repressor of E1A stimulated genes
CIP/KIP	cyclin dependant kinase inhibitors
CFU-EC	colony forming unit of endothelial cells
D-MEM:	Dulbeccos Media for cell culture nutrition
DNA:	Deoxyribonucleic acid
DH5 α	Escherichia coli cell line for plasmid amplification
EBM-2	Endothelial cell medium including 2%
CBEC	human endothelial Progenitor Cell
EcoRI	Escherichia coli Endonuclease I restriction enzyme
ELISA	Enzyme linked immunosorbent assay
eNOS	endothelial Nitrous Oxide
FCS	Fetal calf serum
G-	Geneticin
GSK-3 β	Glycogen synthase kinase 3 β
GLUT-4	Glucose Transporter 4
GDP	Guanosin-di-phosphat
GTP	Guanosin-tri-phosphat
HUVECs:	Human umbilical vein endothelial cells
HpaI	A restriction endonuclease
Inc.	Incorporated or Incorporation, standing for a form of company
IR	Insulin-receptor
IRS-1	insulin-receptor substrate-1
IGF1R	Insulin-growth-Factor-1-receptor
IGF1:	Human Insulin-like Growth factor 1
IGF2:	Human Insulin-like Growth factor II
IGF2-pos. cell:	Insulin-like Growth factor II overexpressing endothelial progenitor cell
LAD	left anterior derived coronary artery

LVEF	left ventricular ejection fraction
kD	kilo Dalton
HVSC	mesenchymal stem cells
M6P(-R)	Mannose-6-phosphat(-receptor)
MACS	magnetic-activated cell sorting
MEK	mitogen expressed kinase
MAP	mitogenig activated protein
NIH	National Institute of Health (of the United States of America)
pLXSN	Retroviral vector, part of the Retro-Pack ^o Transfection-System (51)
pOTB7	Delivery plasmid for most of our genes
PBS	Phosphate buffered saline
PT67	Producer cells that produce an infectious
p21	tumor suppressor protein
PCR	Polymerase chain reaction
PLGF	Platelet-derived growing factor
RNA	Ribonucleic acid
RT-PCR	Reverse Transcription polymerase chain reaction
RAS	rat sarcoma protein, part of an intracellular growth factor cascade
RAF	RAS activated factor
SH-PTP2:	A phosphatase to dephosphorylate several proteins of the metabolic pathways and mediating the fast responding Insulin effects
SOS-GRB	son-of-sevenless (sos) / growth-factor-bound (grb) complex
SDF-1	Stroma cell derived factor-1
Toe1	Target of EGR-1
Tie2	Angiopoetin receptor and tyrosine kinase
TGFB1	Transforming growth factor 1
Taq	Thermophilus aquaticus, produces the thermo-stable polymerase enzyme for the polymerase chain reaction
TRIzol	RNA purification reagent from Invitrogen ^o Incorporation
UV	ultra violet irradiation
UVSC	Umbilical vein stromal cells
VE-cadherin	vascular endothelial cadherin
VEGF	vascular endothelial Growth Factor
3T3-cells	Human fibroblast cell line

I. Introduction

1.1. Why to use Endothelial Progenitor cells for neo-vasculogenesis?

Cardiovascular diseases are the most important cause of mortality and morbidity in the modern post-industrial population (1). The great majority of cardiovascular diseases being summarized in this category have one basic principle: the chronic or acute lack of blood perfusion leading to ischemia and- or tissue remodeling with all its fatale consequences (2). Therefore, one of the best strategies of therapy for many of these illnesses is to treat the origin of their pathomechanisms to improve the vessel function of various organs of the human body. With the help of angiogenesis and vasculogenesis (explained below) induced vessel outgrowth, leading to an improved parenchyma perfusion, the circulus vitiosus of ischemia, organ dysfunction and increasing oxygen need could be stopped. The main problem that causes arteriosclerotic plaque progression is the development of turbulent blood flow, which leads to more and more cholesterol accumulation. These turbulences could therefore be reduced with the help of new smooth endothelium layers by re-establishing a laminar blood flow.

Vasculogenesis leads to vessel outgrowth through the mobilization and differentiation of endothelial progenitor cells (EPC), migrating into the ischemic areas from bone marrow, from the local environment (3), or artificially by external infusion. Angiogenesis on the other hand is the formation of new vessels and capillaries out of local existing vascular structures [4]. The process of vasculogenesis requires the recruitment and invasion of EPC. This is achieved by a complex interaction of processes. The ischemia-induced release of growth factors like vascular endothelial Growth Factor (VEGF) or Angiopoetin-1, and the secretion of chemoattractants like CXCL12 (better known as SDF-1, stroma cell derived factor-1) lead to the mobilization of CBEC from the bone marrow (5). That procedure is possibly controlled by the level of eNOS (endothelial Nitrous Oxide) in the bone marrow sinuses (6). The migration towards the place where the CBEC are needed is called homing and is, as is the invasion into the ischemic parenchyma out of the vessel in which they arrive, mainly enabled by the expression of CXCR4 (Stromal cell derived growth factor receptor) on mobilized EPC (7).

Multiple investigators have shown that CBEC are included in the CD34+ fraction of the pool of mononuclear cells derived e.g. from bone marrow or cord blood. Included in this fraction of CD34+ cells are two populations involved in the process of vasculogenesis. The first of these are progenitors for CD14+ proangiogenic precursor cells that secrete VEGF, which plays a decisive role in neovascularisation (5, 8). The second population does not

express CD14, but AC133, VEGF-Receptor2 (KDR) and vascular endothelial Cadherin (VE-Cadherin) (5). This second party of cells can be grown into colonies with endothelial alike morphology, the so called CFU-EC (colony forming unit-endothelial cells) (9, 10), reaching high numbers of population doublings (11).

Both of these CBEC could be shown to participate in damaged endothelium repair and neoangiogenesis (5), which makes both types of cells ideal targets for therapeutic neo-vasculo- or angiogenesis.

1.2. Aim of our study

In the present study, we decided to further investigate the restorative angio- and vasculopoetic capabilities of CBEC, particularly the CFU-EC, and the possibilities to improve those. Several investigators have already demonstrated the multiple benefits of CBEC-Infusion with CD34+ cells significantly increases the vessel density of ischemic heart muscle after myocardial infarction (12, 13). Even more interesting is the fact that CBEC transplantation after myocardial infarction can improve the left ventricular function, mainly resulting in better ejection fraction of the heart (12, 13). This effect was mostly supposed to be due to a better survival and reactivation of the so called hibernating myocardium (13), the cardiomyocytes of the peri-infarct area with reduced metabolism, surviving because of a minimal rest perfusion. If these cells receive reperfusion, they are able to gain back their capability of contraction so that the heart function improves. The CBEC transplantation also led to a reduced ventricular remodeling (13) with a greater share of contractile parenchyma. One great disadvantage of the CBEC is the limited cell number that can be harvested from adult patients. Furthermore the CBEC from adult donors have very limited in vitro expanding capacities. The resulting cell amount for re-transplantation remains very poor. These limitations could be overcome by a reliable technique to stimulate the growth of CBEC in vitro, with the result of sufficient autologous (cells from the patient itself) CBEC gained out of the aged patient, suffering from a cardiovascular disease, to restore his heart- and circulatory function.

1.3. How to reach this?

To gain CBEC, we have established a cell culture system in which endothelial like cells were grown out of a cohort of CD34+ cord blood cells. Unfortunately the frequency of CBEC that were able to form endothelial cell colonies (CFU-EC) out of this population was very low: 1 in 11.8×10^4 if grown on fibronectin and even lower if grown on gelatin (14). We were able to demonstrate that CFU-EC derived cells from cord blood (cord blood endothelial cells-CBEC) could be augmented up to amounts of over 10^{15} cells in the first 60 days of cell culture, in contrast to the CBEC extracted from aged patients. Some of the cells reached more than 50 population doublings. The CFU-EC derived cells expressed VEGF-R1, Tie1, CD31, CD105, and VE-cadherin in high levels. After culture, only low levels of CD34, VEGF-R2 and Tie2 were measurable. CD36, a marker of microvascular endothelium, was not detectable. In addition myeloid markers, such as CD14 and CD45 were also not detectable (14). These observations, as well as the morphology of the colonies and the ability to form tubules on MatriGel and in fibroblast cocultures (see below) qualify the CFU-EC-derived cells as endothelial cells.

We established a reliable protocol to transduce these CBEC with a retroviral vector system (pLXSN, s. methods) (15), so that we were able to include different genes into these cells. This could mean a way to improve the growth potential of adult patients' cells, as well as to increase the regenerative potency of the endothelial cells. Therefore we inserted the genes for human Insulin-like growth factor 2 (IGF2), human Protein Kinase B (AKT), human platelet-derived growing factor and human Angiopoetin-1 (ANG1) via the retroviral vector pLXSN into the cells.

Because the potential of the CBEC to regenerate ischemic parenchyma is limited to the repair and augmentation of the vessels, the next logical thought is to combine the endothelial progenitors with cells that would deliver the mesenchymal line of cell differentiation that could rebuild functional parenchyma. Those could be mesenchymal stem cells (HVSC) or Fibroblast progenitors, possessing the ability to restore heart or skeletal muscle to regain the specific organ's function. One could imagine even the combination with other progenitors to rebuild even more potential organs. Some approaches to that have already been done, e.g. Mangi et al. have injected AKT-overexpressing mesenchymal stem cells in rat hearts that had underwent myocardial infarction before. The HVSC were locally inserted into the peri-infarct area and were able to nearly completely restore the heart's blood pumping function, measured by the ejection fraction (16). They showed that the mesenchymal cells had differentiated into

expressing sarcomeric actin, a muscle cell protein, and connexin-43 gap junctions to correspond with their neighbor cells. The overexpression of AKT had shown a significant advantage in heart regeneration over the application of untreated HVSC (16).

1.4. Choice of genes

With the previously published observations in mind that were described above, we chose several genes to examine their effects on the growth, the differentiation and the vasculopoetic potency of the CBEC and HVSC. The genes were named before: human IGF2, human AKT, human Angiopoetin-1 and human PLGF. After the first tests, we focused our experiments on IGF2 and AKT1.

1.5. Signaling

The different growth factors achieve their effects through different ways of intracellular signaling. They have common parts or effectors but often differ in explicit points. Previous publications suggested that members of the insulin-like family of growth factors, such as IGF2, are attractive targets in improving therapeutic neo-vasculogenesis. The IGF2 Protein has three types of receptors and therein lays a key part of its effects (s. chapter results and discussion). The main receptor is the IGF2/Mannose-6-phosphat-receptor (M6P-R). It is a membrane associated receptor of about 220 kDa, consisting of only one glycopeptide chain, interacting with IGF2 and proteins linked to a Mannose-6-phosphat molecule at a carbohydrate side chain. The M6P-R occurs in two forms, namely as cation-dependent and cation-independent form. Only the cation-independent molecule functions as a receptor for IGF2 and is further described in the discussion chapter. M6P is a main adapter molecule for cell endocytosis and lysosomal transfer in the cell (17, 20).

Depending on the amount secreted, the IGF2 protein binds to another two receptors, the Insulin-receptor and the Insulin-growth-Factor-1-receptor (for further information see chapter discussion). All those receptors were described to stimulate cell growth and / or vasculo/ angiogenesis and we judged them ideal candidate genes to improve the clinical usability of endothelial progenitor- or mesenchymal stem cells by augmenting their proliferation and differentiation capabilities.

After the specific insert (IGF2, AKT1, PLGF, or ANG1) was cloned into the retroviral vector, the vector was sequenced to verify its insert orientation and the CBEC and HVSC were transfected with supernatant from the PT67 producer cell line. The vector integration

was checked by different Polymerase chain reaction techniques. To examine the effects of the integrated genes on the target cells in vitro, we studied the differences in cell growth, cell survival, cell function, cell differentiation and cell alteration (s. chapter methods) with the help of diverse techniques, always in comparison to an untreated parental control. The results we obtained are shown in the corresponding chapter.

Considering all these facts, the CBEC, first of all with the help of genetic alteration, are a very interesting and promising suspect of modern medical investigation.

The clinical use of CBEC is depending on several circumstances that must be elucidated to allow their application in medical routine. First of all the reduced cell growth must be increased to possess sufficient amounts of reliably working cells to be able to treat illnesses with cells from the patient himself. This would avoid the need of immunosuppressant medication, because the new tissue would not be recognized by the patient's immune system. The task is to find the best working in vivo growth stimulator for these cells. Next, the cells must be under stringent control that means they must be unable to lose their cellular and genetic program, their differentiation. Otherwise they could become tumor cells. The cell's gene expression profile and their degree of differentiation must clearly be identifiable to detect potential oncogenic cells to strictly avoid transplanting them. With all that in mind, we asked ourselves how we could achieve this; to let the cells grow better without turning them into uncontrollable oncogenic cells. To check their vasculopoietic abilities, we wanted to establish a reliable test assay to measure the tubular like structures and maybe the vessels that were formed by the genetically altered cells.

II. Materials and Methods

2.1. General methods of biochemistry and cell- or DNA analysis:

2.1.1. Genomic DNA Extraction out of the cells

The cells were dissolved from plate with trypsin, suspended in DNA buffer (Tris/EDTA, 1M HCl pH=8) and processed according to the phenol/chloroform/ isoamylalcohol extraction protocol of the NIH (23).

2.1.2. RNA Extraction and c-DNA Synthesis

The cells were lysed in TRIzol (Invitrogen, Cat.No. 15596-026) and totally genomic DNA-free RNA was obtained according to the manufacturer's protocol. The RNA was transformed to cDNA with Omniscript Reverse Transcriptase (Qiagen Cat. No. 205110) Kit, also following the manufacturer's handbook, delivered with the enzyme kit.

2.1.3. Reverse Transcription Polymerase Chain Reaction

For Reverse Transcription PCR the equivalent amount of 0.5 μ g RNA was used in the amplification assay using Taq polymerase (Invitrogen, Cat.No. 18038-018) and the primers shown below (table 1). The Products were amplified for 30 cycles at 93°C (30s.), 60°C (5°C below melting temperature of the primer pairs) (40s.) and 74°C (60s.). The products received were visualized on a 1.5% agarose gel with ethidium bromide, analyzed and recorded with the help of a GelDoc-System (Biorad GelDoc EQ).

<i>Gene:</i>	<i>Sense Primer:</i>	<i>Antisense Primer</i>	<i>Product size(bp)</i>
IGF2 recombined	GCT TCC AGA CAC CAA TGG GAA T	GAG ATT TTC GGG ATG GAA CCT GAT	671
IGF2 native	TCA CGT TCA CTC TGT CTC TCC CAC TA	GAG ATT TTC GGG ATG GAA CCT GAT	991
IGF2 recomb. Taqman	AGA TGG CCA GCA ATC GGA AGT	GAG ATT TTC GGG ATG GAA CCT GAT	137

IGF2 native Taqman	TCA CGT TCA CTC TGT CTC TCC CAC TA	GGG AGA ATT CGT CTG ATT GTC CAG	185
AKT1	TCTAGCCCCGCGGGCC	AGGATCCACAAGTTTGTACA	844
AKT1 Taqman	TCTAGCCCCGCGGGCC	AGAGAAAGAGAGAAGCC	156
PLGF	CCTCGCTCCCTTCAAGACGA	CGGAAGCTCCCAGGGGTCTGT	782
ANG1	AGCAACTGGAGCTGATGGAC	CATCTGCACAGTCTCTAAATGG	695
ANG1 Taqman	AGCAACTGGAGCTGATGGAC	ATTGCAGATGTAAAAATAGA	205
pLXSN	CCCTTGAACCTCCTCGTTCGACC	GCCCGCATGGACACCCAGACCG	854
pOTB7	GGAAACAGCTATGACCATG	GTAAAACGACGGCCAGT	689

Table 1: Primers used for PCR

2.1.4. Genomic DNA Polymerase Chain Reaction

The genomic DNA was gained as described above and used in the Polymerase Chain Reaction assay at a concentration of 0.5µg per well with similar conditions and primers as for the Reverse Transcription PCR described above (2.7.4).

2.1.5. Real Time-PCR

In this assay, the amount of coding- or genomic-DNA was decreased to 0.1µg DNA-equivalent. For the amplification a SYBR-Green PCR Master Mix (Applied biosystems, Prod. Nr. 4309155) was used according to the included protocol in a TaqMan Real-Time PCR Cycler. The 5' or 3'-primers were changed to shorten the resulting fragment length to about 150-250 basepairs.

The mathematic and statistical analysis to evaluate the included amount of cDNA in the cells was performed as described in the article of Yuan, Reed et al. (29).

The obtained values of the relative quantification were compared and analyzed with the help of the SPSS statistics software (see 2.7.14).

2.1.6. Protein extraction

Cells were grown and passaged as described above, at least up to a number of 1*10E8 per cell type. The cells then were dissolved in TRIzol (Invitrogen, s.RNA Extraction) and the protein phase separated with the help of phenol/chloroform wasn't discarded but the protein was

precipitated, cleaned and resolved. The supernatant protein was directly precipitated and subsequently treated the same way. In the photometer the concentration was determined and the protein was stored at -24°C until usage.

2.1.7. Insulin-like-growth-factor-2 Enzyme-linked Immunosorbent Assay

The cells were cultured as described previously and supernatant from the cell culture dishes was collected after the second medium changes at day one and three. Cells were collected and lysed in TRIzol (Invitrogen, s.RNA Extraction) and processed according to the TRIzol Protein extraction protocol with the use of phenol/chloroform phase separation. The concentration of the resulting cytoplasmatic and supernatant protein was measured and the amount adjusted for the needed ELISA protein equivalent. We used the DSL-Labs hIGF2 Elisa (hIGF2 Elisa with/without Extraction, DSL-Laboratories Inc., Cat.No.:DSL-10-9100) and the IGF2 cytoplasma and supernatant protein levels were quantified as described by the DSL-Elisa Handbook. The resulting light absorbance of the wells was measured in an Elisa Reader and analyzed with Magellan° software. Three samples of lysate and supernatant per cell line were analyzed and the average values were computed for NB 1591-94 and NB 1683. Furthermore, the ELISA protocol gave two possibilities to analyze the protein templates, named with and without protein extraction. The extraction step could be performed to eliminate contamination, but was only recommended for templates that were gained in vivo, not for cell culture use (see chapter 4.2.3.3).

2.1.8. Western Blot

The cytoplasmatic and supernatant protein was collected and processed as described for the ELISA. It was used according to a standard western blot protocol (<http://omrf.ouhsc.edu/~frank/Western.html>). The following Antibody was used to bind the IGF2 Protein.

Antibody/ Target:	From Company:	Catalogue & Lot Number:	Properties, Host:
1. Human IGF2	RnD Systems	BAF292, ACY023081	Biotinylated,goat

Table 02: Antibody for IGF2 Western Blot

2.2. Construction of the retroviral vector

The coding sequences described below were all obtained from commercial sources (see below) and amplified in DH5 α prior to further manipulations. First, before the digestion and ligation procedure, we performed the important check for internal restriction sites of the enzymes that are used in the subsequent steps of the cloning procedure. There may be restriction sites in the coding sequence of the insert and the insert would then be cut in multiple parts. Therefore, only those restriction endonucleases can be used, that cut in the multiple cloning site, but not in the coding sequence of the insert. Such a check can be performed with a DNA sequencing tool such as MacMolly (MacMolly Tetra software (version 2.1; Soft Gene, Berlin, Germany) and double-checked by digesting the plasmids obtained from the commercial sources. The choice of the right endonuclease pair is often difficult and time consuming, but it is decisive for the success of the cloning procedure. When only one endonuclease is used, as performed with the PLGF-sequence, the ligated insert has to be checked for correct orientation after the ligation procedure, because it would fit in both directions into the target DNA, but it would be of no use afterwards.

After ligation, the construct was amplified (with *Escherichia coli* DH5 α , Invitrogen Inc., Cat.No.18265-017, selected for high yielding clones), isolated, and purified (Plasmid Preparation Kit, MaxiPrep Quiagen Cat.No. 12162). All ligated inserts used in this study were sequenced (GATC Biolabs) (21) and the sequence was verified against the original sequence from the Mammalian Gene Collection (with the help of MacMolly Alignment Tool). For more detailed information, please see the chapter ligation procedure.

2.2.1. Human IGF2 Insert

The IGF2 Insert was obtained from the ATCC (MGC-8683, Image ID 2964584, BC000531) and delivered in the pOTB7 vector. The coding sequence [1378 basepairs(bp)] (plus a short sequence of 118bp from pOTB7 Vector) was isolated by digesting with the restriction enzymes EcoRI (position 165bp) plus HpaI (pos. 185bp) and ligated into the retroviral Vector pLXSN (Clontech K1060-B, GenBank M28248) at the corresponding restriction sites in the multiple cloning sites (pos.1471bp-EcoRI and pos.1477bp HpaI (see Figure 1).

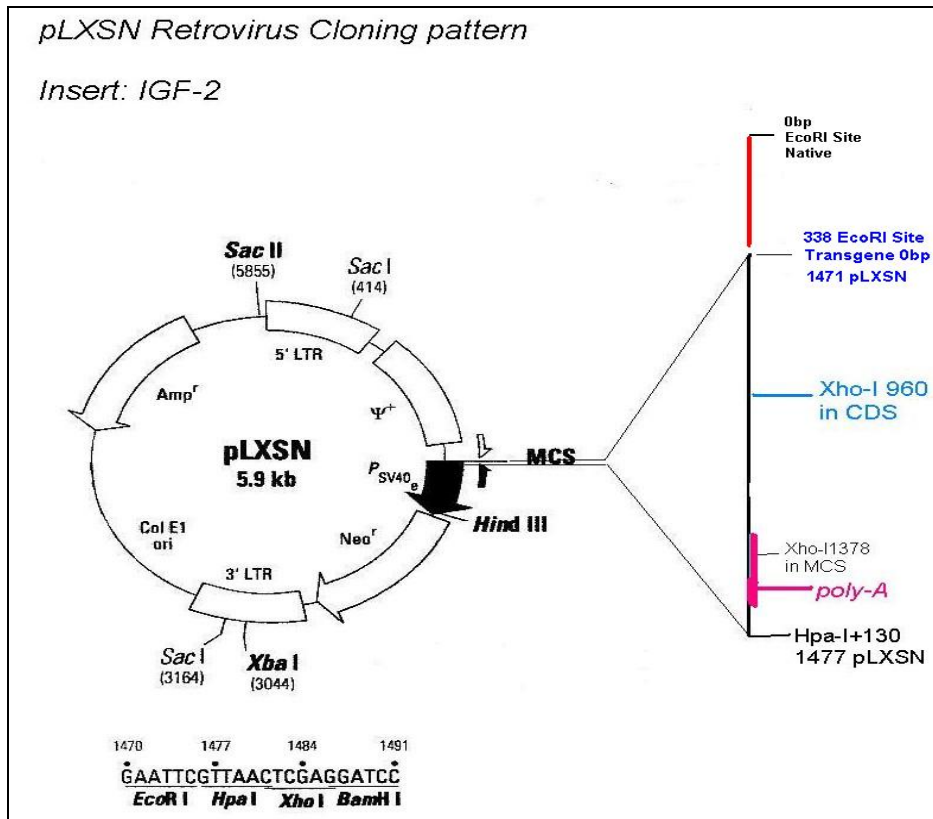


Figure 1: cloning pattern for IGF2 sequence integration into pLXSN vector

2.2.2.Human-AKT1

The AKT1 Insert was delivered in the pOTB7 vector as was IGF2 and it was processed in analogy to the IGF2 insert. The AKT1 coding sequence was digested with Eco-R1 restriction endonuclease at the 5' end and with the Hpa-I enzyme at the 3' end. The resulting fragment length counted 2870 basepairs. Afterwards the DNA was processed as described for the IGF2 template above.

pLXSN Retrovirus Cloning pattern

Insert: AKT-1

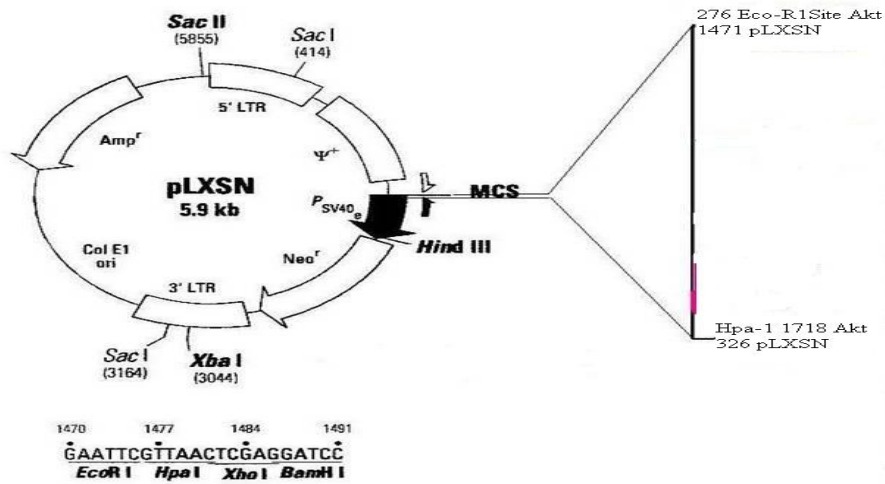


Figure 2, AKT1 cloning pattern sequence integration into pLXSN vector

2.2.3. Human-Angiopoetin 1 (ANG1)

The human Angiopoetin-1 DNA was obtained integrated into the pDNR-Lib vector and the coding sequence was extracted with SFI-1 at the 5' ending and with EcoR1 at the 3' end. The resulting sequence was 1201 basepairs of length and was further processed in analogy to the IGF2 template described above.

pLXSN Retrovirus Cloning pattern

Insert: Angiopoetin-1

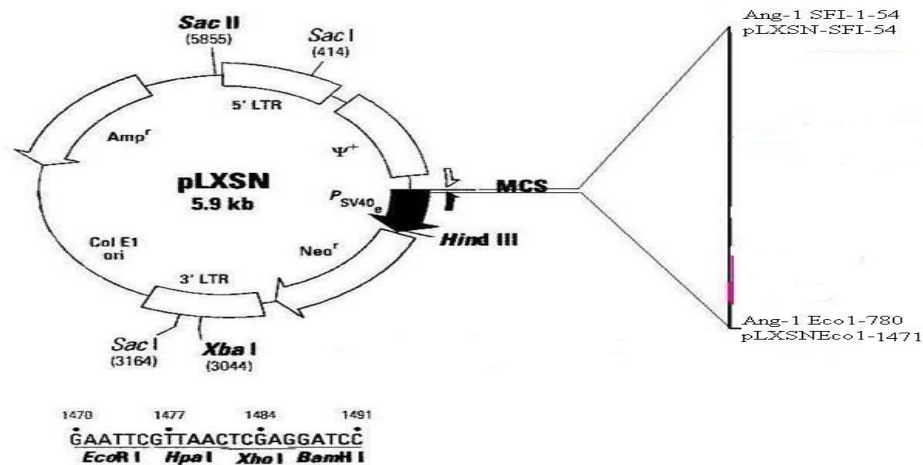


Figure 3, Angiopoetin-1 cloning pattern

2.2.4. Human-PLGF

The PLGF template was cut out from the pOTB7 vector with just one endonuclease, EcoR1, resulting in two DNA parts of 1004 bp and 2555 bp. The smaller one contained the coding sequence and was processed as explained for the IGF2 DNA. One important difference resulted in the fact that when only one enzyme is used, the ligation results have to be checked for the correct orientation. We performed this check with a specialized primer set that was designed to fit only the correctly orientated base pair sequence. The template which led to an amplification product of the correct length in the PCR was further processed and integrated into the producer cells.

pLXSN Retrovirus Cloning pattern

Insert: PLGF

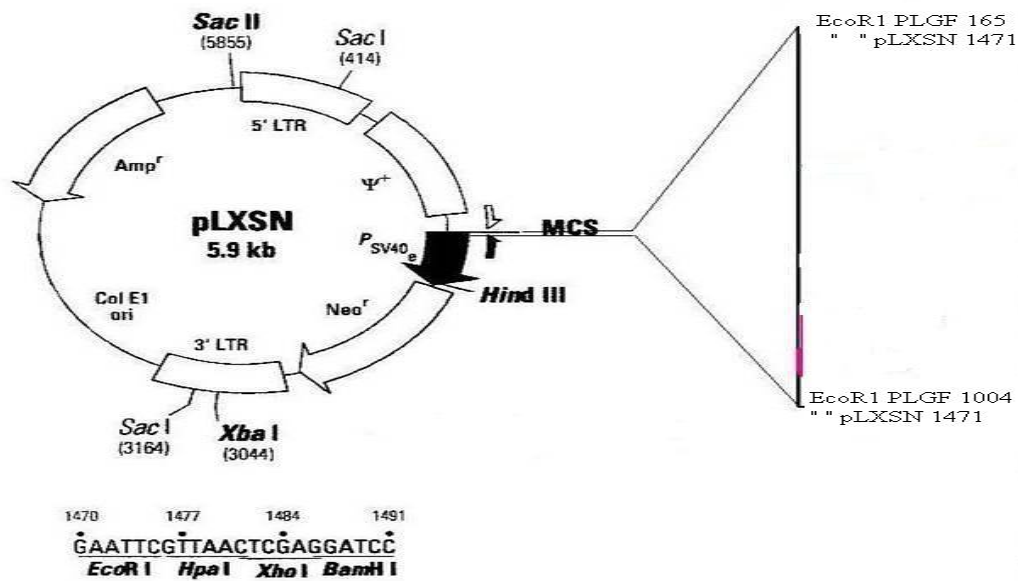


Figure 4, pLGF cloning pattern

2.2.5. Summary of inserted sequences.

The MGC numbers and details of our target genes are shown in the table below:

Gene:	MGC Nr.:	Definition:
hIGF2	8683 BC000531 ID 2964584	Homo sapiens insulin-like growth factor 2 (somatomedin A)
hAKT1	8686 BC000479 ID2964603	Homo sapiens v-akt murine thymoma viral oncogene homolog 1
hAngiopoetin-1	6694163 BC029406 ID4805448	Homo sapiens angiopoietin 1
hPLGF	14095 BC007789 ID3629125	Homo sapiens placental growth factor, vascular endothelial growth factor-related protein

Table 3: mRNA Clones used for analysis assays

2.3. Ligation procedure

In the course of my investigations, a reliable and easily reproducible ligation protocol was established. First, the CDS was obtained, by digesting the delivered plasmid with two different digesting enzymes at once or in two steps, depending on the digestion buffer because some are suitable for both enzymes or some are not. After 1 hour of incubation time, the corresponding fragments were gained by cutting out from a 1.5 % Agarose Gel after 1 hour of electrophoresis time at 80 Volt. Afterwards the resulting fragments were dissolved in high salt lysis buffer and the DNA was obtained with the help of a PCR Clean up / Gel Extraction Kit (Qiagen Inc., Cat. No.: 28104)

Having extracted and purified the CDS from the delivering vector, the target vector was cut and purified by the same treatment as the CDS. For the ligation of AKT1 and PLGF, only one restriction enzyme could be used, so that the vector had to be dephosphorylated before the ligation procedure. With this step it was assured that the opened vector ends were not religated to themselves without the desired CDS integration. The dephosphorylation was achieved by incubating in Shrimp alkaline phosphatase for exactly 15 minutes at 37° C and following heat inactivation of the enzyme at 65°C for 15 minutes. Purification of the opened vector was carried out with a PCR Clean-up Kit (Qiagen Inc., s.above).

The purified CDS and the digested vector were ligated with T4 Ligase for 18 hours at 16°C. Complete ligation was confirmed by gel electrophoresis and successful plasmid retransformation into *E. coli* DH5 α , (Invitrogen Inc., s.above). After the selection procedure with Ampicillin different *E. coli* clones were taken and the retransformation efficiency was measured. A high proliferating and expressing clone was cultured to gain the desired retroviral vector-plasmid encoding the CDS Insert with the gene of interest. The reliability of the ligation procedure was improved by identifying and carefully monitoring of some critical steps in the procedure:

1. Great care should be taken when digesting the desired DNA. If the DNA has to be ligated after digestion, even more accurate working is necessary to avoid damaging the DNA. The opened ends of the DNA double strands are very sensitive and can easily be damaged by the restriction nucleases if the buffer quality, concentration or composition is insufficient. Therefore, the buffer, keeping in mind that it must be suitable for both enzymes, must be well shaken and not used since more than 2 months, even when frozen, because the buffering qualities degrade. Mostly due to suspending and refreezing cycles. Often the included salt is precipitated and needs to be resuspended. Otherwise the buffer can decrease the enzyme activity or induce star activity of the endonuclease (the restriction enzymes cut the DNA at irregular sites, producing a useless DNA puzzle).
2. Even more attention must be given to the dephosphorylation procedure, because it is very sensitive but decisive for a mono-enzyme assay ligation. The assay duration time must be determined and controlled exactly, the amounts of buffer and enzymes must be measured more accurate than in the ligation assay. And very decisive is, that the assay is performed with the recommended conditions, first of all the exact temperature. The Ligation procedure is not as sensitive for the environmental parameters as is the dephosphorylation step.
3. The extraction and purification of the DNA fragments:
The following points were each tested and adjusted for optimum performance in the ligation assay: DNA-Amount, DNA-loss while processing, saline-buffer quality, elution-process, different elution methods.
Very important is to use either Crystal violet as staining substance to prevent damaging and intercalation of the DNA by Ethidium bromide or using a parallel lane running next to the marked one without staining buffer. So there is no

intercalation and DNA degradation by the staining buffer and the DNA is cut out of the agarose gel at exactly the same running length as the marking lane.

4. In the ligation assay itself, -temperature, assay-duration and buffer quality must be analyzed and optimized by testing different versions prior to performing ligation.
5. An obligate check after ligation by Gel-electrophoresis before using the DNA templates in the amplification assay. Complete and closed plasmids don't move in the electric field because of their circular structure. Next the Plasmids were cut with other enzymes, and if successful, longer fragments with the included insert must be detectable.
6. Analyze of the retransformation efficiency before using ligated plasmids to insure a reliable amount of DNA. If the plasmid size measures over 7.5 kbp, it reduces the retransformation efficiency!

2.4. Producer and Target cell transfection

2.4.1. PT67 Producer Cells

Because of the fact that the target virus includes elements of leukemia viruses and is of retrovirus origin, it could infect human cells and potentially harm them. Since the inserts we investigated may have proto-oncogenic activity, such infections could lead to neoplasia. To prevent such a complication, the vector system we used is designed in a way that the virus cannot replicate and amplify by itself after having infected a human cell. This safety mechanism is reached with the safety mechanism of the virus lacking its essential genes for the virus envelope (env-gene, 10A1 viral envelope gene sequence) and the coating information. These genetic codes are only included in the PT67 packaging cell line, which provides the virus with all the necessary information to form infectious coated virus particles.

The PT67 cells were transfected with the pLXSN plasmids containing the coding sequence of the gene of interest with the help of a detergent to increase the transmission through the cell membrane (Lipofectamin 2000, Invitrogen, Cat. No. 11668-019). Afterwards it was cultured and amplified to receive coated infectious virus. These Producer Cells were then selected for incorporated retroviral virus with the help of 800 µg/ml G-418 (Geneticindisulfate) cytotoxic agent. The neomycin resistance gene included in the pLXSN vector protected those producer cells translating the viral genetic information from the apoptotic effects of the G-418.

The target cells were then cultivated with supernatant removed from the producer cells after 18 hours of incubation, growth factors were added and the target cells grew within this medium for 8 hours. 48 hours after this procedure, the cells were selected for (G-418) resistance with 400 µg/ml Geneticidin. The vector expression was screened first by g-DNA PCR. Afterwards, c-DNA PCR and c-DNA Real-Time-PCR (Taqman) were performed to verify the integration, transduction and translation of the virus in the target cells.

2.4.2. Determination of the Virustiter produced by the PT67 Producer cells:

The success of infection by viral particles depends for the main part on the amount of particles interacting with the target cells. To determine the amount of infectious virus particles that were produced by the PT67-Insert positive cells, we developed a standardized titer-analysis protocol:

3T3 Fibroblasts were cultured in 6-Well Plates, then transfected with different dilutions of 150µl filtered PT67 supernatant in steps of $E \cdot 10^{-1}$ dilutions per well. After an incubation period of 2 days, the selection cytotoxic agent G-418 was added and after another 4 days, the cells that did not include a vector coded resistance were all apoptotic. Then the remaining cells were counted in the last dilution step that was containing any living cells and leading to the specific viral dilution titer.

2.5. The cells that were used in our assays

2.5.1. Escherichia coli DH5α

Escherichia coli DH5α, subcloning efficiency, Invitrogen Cat.No.18265-017

2.5.2. PT67 Producer Cells

PT67 Producer Cells (Clontech K1060-D), sold as part of the pLXSN Retro-Pack^o Retrovirus Expression Kit [51].

2.5.3. Cord blood derived Endothelial Progenitor cells: CD34+ CBEC

Cord blood mononuclear cells were isolated from the cord blood of newborn children from the gynecological department of our hospital following an approved protocol. The cells were separated with Ficoll density separation and purified with magnetic-activated cell sorting (MACS) with the help of the direct CD34+ Progenitor Cell Isolation Kit (Miltenyl Biotec, Cat.No. 130-046-702).

2.5.4. HUVECs

Human umbilical Vein Endothelial Cells were gained out of cord blood veins of newborn children from the gynecological department of our hospital.

2.5.5. Human umbilical vein stromal precursor cells (HVSC)

HVSC 1216, 1219 and 1220 were gained out of cord blood veins of newborn children from the gynecological department of our hospital.

2.5.6. Human diploid fibroblasts

Human diploid fibroblasts were obtained from Cellsystems (generous gift from Dr. Peter Frost, Cellsystems, St. Katharinen)

2.5.7. 3T3 Fibroblasts

These cells were purchased mouse embryonic fibroblast cells and were only used for the determination of the IGF2 viral titer.

2.6. Cell cultivation

2.6.1. PT67 Virus Producer cells

The PT67 Virus Producer cells were cultured in α Dulbecco's-Modified Eagle Medium (Cambrex Cat. No.: 12-604F) supplemented with 10% FCS, Sodium-Pyruvat, L-Glutamin, and Streptomycin plus Penicillin.

2.6.2. CD34+Endothelial Progenitor Cells

The CBEC were isolated from initial colony forming units of cord blood cell colonies. The cells were separated and analyzed with the help of RT-PCR gene expression array. The cells did produce many HUVEC like markers as vWF, CD 31, VEGF-Receptor and Tie-1. These cells were expanded and could be generated despite a very low CFU-EC frequency. We were able to gain 10×10^6 cells out of 1×10^6 cells. The cells were cultured in EBM-2 Endothelial cell medium including 2% FCS, cytokines and growth factors supplied with the single quot kit (CC-3162 Cambrex- Clonetics). The cells were sown at a density of 5×10^4 cells on a 100 mm dish (Nunc Corporation, Cat. No. 150679), splitted and passaged when they reached a level of 70-80% confluency. The medium, 8 ml per plate, was changed every 3 days.

2.6.3. HUVECs:

The human umbilical vein endothelial cells were treated in the same way as the CD34+ CBEC.

2.6.4. HVSC

The human umbilical vein stromal cells were cultured from the subvascular layer of umbilical cord veins from newborns in AlphaMEM (Gibco), supplemented with 10% FCS, antibiotics and growth factors FGF-2 (10 ng/ml, R&D Systems) and PDGF-B (10 ng/ml, R&D Systems). A detailed description of the procedure to isolate and expand these cells, as well as detailed phenotype of these cells, is given by Kaltz et al. (58).

2.6.5. Human diploid Fibroblasts

The human fibroblasts were cultured by analogy to the PT67 Producer Cells in a-Dulbecco-MEM until setting them together with the CD34+-CBEC into the coculture assay, in which they were treated with the EBM-2 endothelial cell medium.

2.7. Coculture

The coculture model was used as first described by Bishop et al. [53]. Endothelial cells were plated with mesenchymal stem cells or human diploid fibroblasts at densities of 1×10^4 cells per dish of 60mm for the endothelial cells and the same for the fibroblasts. If seeded on 8 Well LabTek^o glass dishes (Nunc Corporation, Cat. No. 177402) (coated with 0.1% gelatine for better attachment), the cells were given into the assay at densities of 3×10^3 cells per dish for each cell type. We observed that the Lab-Tek dishes have a great advantage because they are easier to count, easier to photograph and need less amounts of cell culture media, implicating lower costs.

The cells were cultured in EBM-2 endothelial cell medium as described above. After 5-7 days the culture reached confluency and began to grow in multiple layers. Within these layers, tubuli-like structures of endothelial cells formed and grew until day 14. The culture was fixed and immunohistochemically stained.

2.8. Cell Analysis

2.8.1. Cell growth

Cells were separated from the dishes with trypsin to loosen the Collagen connection to the dish surface, the trypsin-enzyme-activity was stopped with EBM-2 Medium and the suspended cells were counted in a Neubauer counting chamber.

2.8.2 Cell morphology under IGF2 and TGFB1 stimulation

We checked if the parental, untreated cells changed their morphology under treatment with external IGF2 or TGFB1, each added into the cell culture media. This assay was performed to check if the cellular morphology we observed resulted from the stimulation or rather from the selection process. We monitored cellular morphology after 1, 2, and 4 weeks of initial seeding using a phase contrast microscope.

The cellular morphology was analyzed by measuring the average diameter of the cells with ImageJ from the NIH (Image J, National Institute of health, <http://rsb.info.nih.gov/ij/features.html>) and counting the morphological altered cells in the culture dishes compared to the untreated and only empty vector containing cell controls.

2.8.3. Survival

2.8.3.1. Cell survival under cytotoxic influence

The cells were cultured in EBM-2 Medium with all nutrients and growth factors. As cytotoxic agent Geneticindisulfate (G-418) was added in different concentrations per assay, consisting of 2 dishes per concentration (400 µg/ml and 1600 µg/ml). Cell culture was administered as under normal circumstances, medium was changed every 3 days, cells were splitted if necessary. Apoptosis was evaluated via counting of the cells in 5 defined fields per dish, each measuring 9 mm². Every day cell population was counted in the same areas.

2.8.3.2. Cell survival under nutrient restraint and growth factor restraint

Cell culture and counting was performed as described above, except the fact that the cells were cultured in Medium with strong reduction of nutrients and growth factors (pure D-MEM). All the additionally included nutrients in EBM-2 like L-Glutamine, L-Pyruvat, a diversity of amino peptides, fetal calve serum etc. were left out.

2.8.3.3 Cell survival after UV-irradiation

To stimulate apoptosis, growing cells were exposed to ultraviolet light. Despite that, the cells were cultured as under normal circumstances. The cell culture dishes were irradiated with doses of 0 J/m², 5 J/m², 15 J/m², and 45 J/m² of UV-b (wavelength 302 nm) applied in a UV-Radiation chamber supplied with Sankyo UV-Lamps (Sankyo, Cat. No.: G8T5E). After irradiation medium was changed and 2 dishes per dose were cultivated for 2 weeks and the apoptotic cells were counted as described above.

2.8.4. Stimulation

2.8.4.1. IGF2

The assay was performed with external IGF2 stimulation onto untreated parental and empty vector cells. The stimulant was added at levels of 0 ng/ml, 25 ng/ml, 100 ng/ml and 500 ng/ml. It was added to the EBM-2 Medium, after having left both IGF-1 and Insulin out of the single quot growth factor kit so that no interference with these growth factors occurred.

The cells were processed and counted as in the survival assays, afterwards the data was analyzed with the SPSS statistic software.

2.8.4.2. External TGFB1 stimulation

The stimulation assay was performed as described before. The Medium contained 0 ng/ml, 25 ng/ml and 100 ng/ml TGFB1 by leaving IGF1, IGF2 and Insulin out of the EBM-2 Medium. Analyze was also performed as described above.

2.9. Coculture Analyze

2.9.1. Fixation and Immunohisto-staining

The wells in which the coculture was grown were covered with Glycinealcohol to fix the cells and afterwards blocked with a blocking solution mainly consisting of PBS and BSA. Next the primary antibodies were added and incubated. After that, the secondary marker- antibody to stain the primary antibody was added. This antibody was conjugated with alkaline phosphatase. Substrate for this enzyme was Fast Red (Sigma-Aldrich, Prod. No. F4523), staining the structures marked with the conglomerate of primary and secondary antibodies with an intense red color. To analyze the stained structures, the wells were examined under the microscope and photographed.

2.9.2. Tubuli-analyze

The formed structures, if tubuli-like or not, were counted under the microscope and measured for thickness, length and crossings in the pictures taken with ImageJ from the NIH (40).

The results of the measured distances are presented directly from Image J in a box with the following output:

	Mean	Min	Max
1	167.175	113.875	209.121
2	185.45	144.744	197.568

The best way to analyze the lengths is to use the segmented line selections tool. With that it is very easy to get the exact length of the examined line. An example of a measurement is shown below:

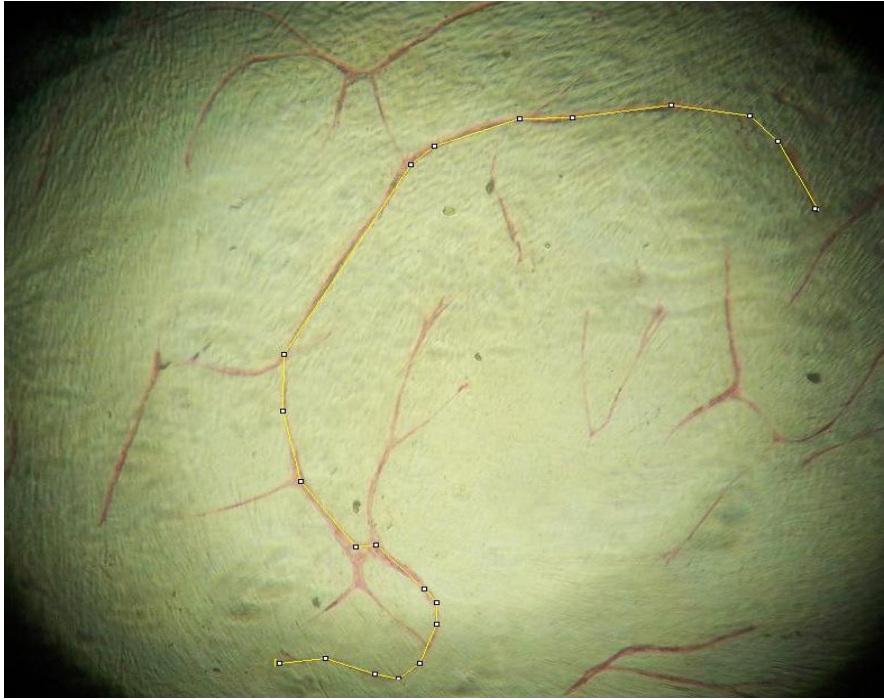


Figure 5: Example from tubuli measurement with Image J

2.10. Statistic software analyze of the data sets

Because of the reduced number of individual counts used in mostly every scientific experiment, statistic test have to be used to receive a result that can be stated as proved with significant accuracy. This accuracy is defined by the degree of errors accepted, named the level of significance α and the power β . The statistics were performed with SPSS Version 15 (27), most of the statistic tasks were to identify significant differences between cell population counts, e.g. the number of cells that had survived the ultraviolet irradiation treatment. Therefore a two-sided statistical assay was used with the hypothesis that the cell count differs in number versus the assumption that it didn't differ significantly (26).

To interpret the results gained in the experiments, the experimental values were first checked for parametric scattering, to find out whether the data distribution fit a Gauss-curve. Most of our experimental values did not fulfill this presupposition. Thus, to compare populations of data points, we mainly used the Kolmogorov-Smirnov-Test (28). Subsequently, the data was divided into bound and unbound value categories and tested for significant differences with the help of standard statistical tests. For most of the data in this study the non-parametric tests like the Mann-Whitney-U-Test, the Wilcoxon-Test and the Fisher-Exact-Test were used. So, in the end, the desired p-value can be obtained and the results can be compared and interpreted.

III. Results

3.1. Verification of the genetic alteration of the cells

3.1.1. Confirmation of transfection

After the plasmid was cloned and amplified, it was sequenced by GATC Biolabs (21) and the obtained sequence was aligned (MacMolly Alignment-tool, pDRAW Alignment) with the original sequence from the Mammalian Genome Collection (MGC-8683, Image ID 2964584, BC000531). The first assays did not deliver the correct ligation products, but after the optimization of the ligation technique, the correct orientation and length of the inserted plasmid was confirmed. The plasmids from the other growth factors were analyzed in the same way (AKT1, ANG1, and PLGF). For IGF2 a part of the 5'-sequence from the delivering vector pOTB7 was cut out with the coding sequence of IGF2, a piece of 118 bp, and this piece was also cloned into the pLXSN plasmid. Therefore the integrated coding sequence of IGF2 had a small extra part of DNA before the 5' beginning end. Because of that circumstance, we had the possibility to distinguish the genomic DNA of the cloned IGF2 from the native cellular form of IGF2 by designing a primer for the PCR that also contained this linked sequence. Because this part of the delivering vector was positioned before the start codon of the IGF2 protein, it was not translated in the process of producing a working protein. This has been proven by the fact that we were able to detect significant amounts of functional protein in our transgene cells with the help of the Immuno sorbent assay, binding an antibody onto the completely transcribed, translated and processed protein of IGF2.

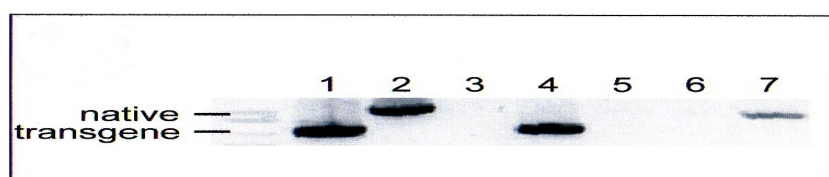


Figure 6: IGF2 native vs. transgene form in the PCR-gel electrophoresis for NB1591-94

- Lanes: 1= producer cells with IGF2 Insert after transfection
2= untreated producer cells native IGF2
3= negative control for transgene IGF2 in untreated producer cells
4= CBEC NB 1591-94 after transfection with IGF2 transgene plasmid
5= negative control in untreated CBEC NB 1591-94 for transgene IGF2
6= empty lane
7= untreated CBEC NB 1591-94 with proof of native IGF2

3.1.2. Producer cells

3.1.2.1: Gene verification in the producer cells with PCR

The gene transfection to the PT67 producer cell line was controlled via genomic DNA PCR, which could reliably proof the insertion of all cloned plasmids (IGF2, AKT, PLGF, Ang1) into the producing and packaging PT67 cell line.

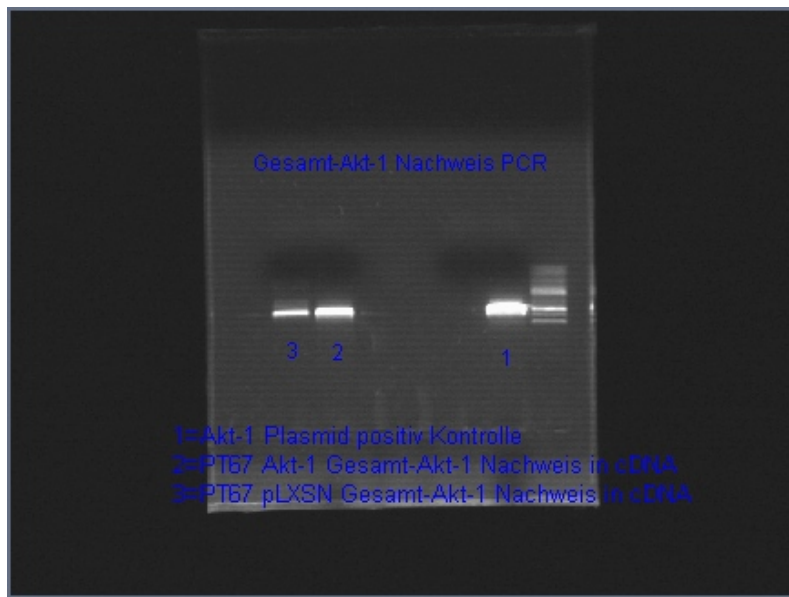
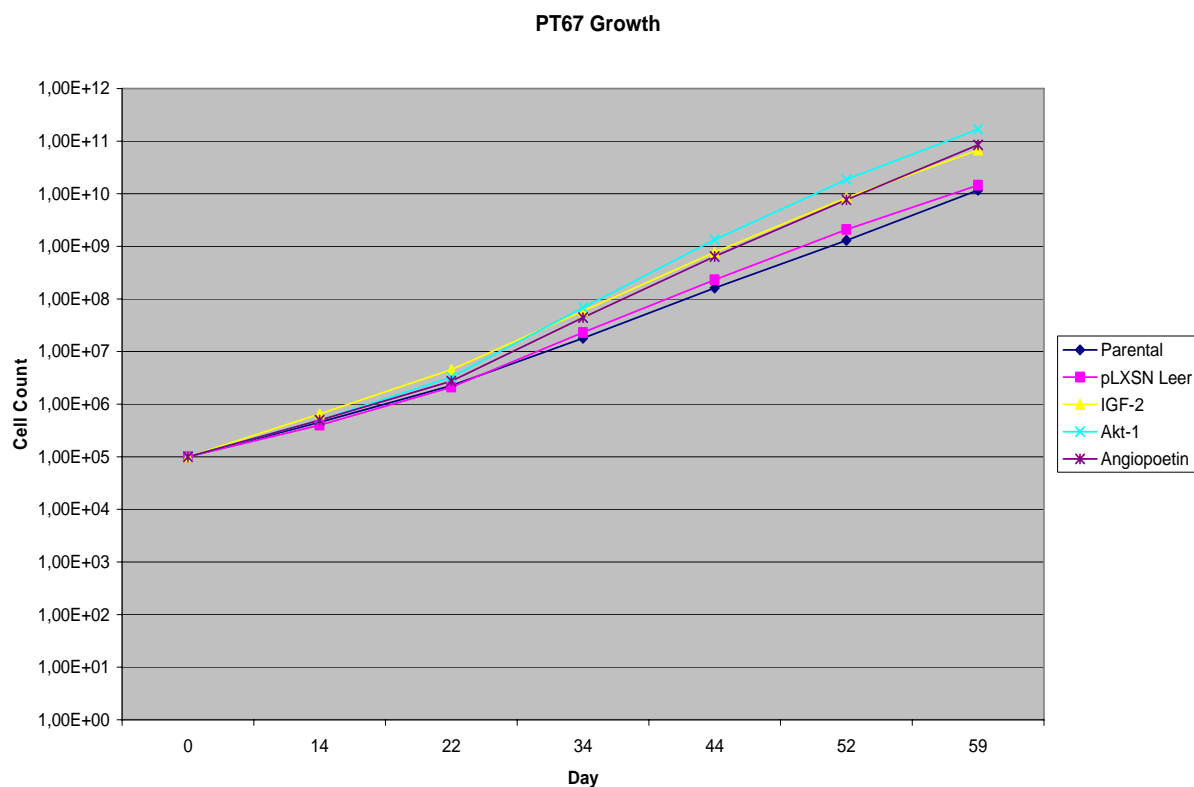


Figure 7: PT67- PCR proof of Integration of plasmid e.g. for AKT1

3.1.2.2. Growth of the producer cells after retroviral transfection

A growth curve of the Producer cells was recorded to figure out differences between the cell duplication rates depending on the gene they had been transfected with.

They differed significantly with AKT1 having the greatest duplication rate, followed by Angiopoetin and lastly IGF2.



P-Values with Wilcoxon and Fisher-Exact-Testing for significant difference of PT67 Growth curve comparison for different inserts

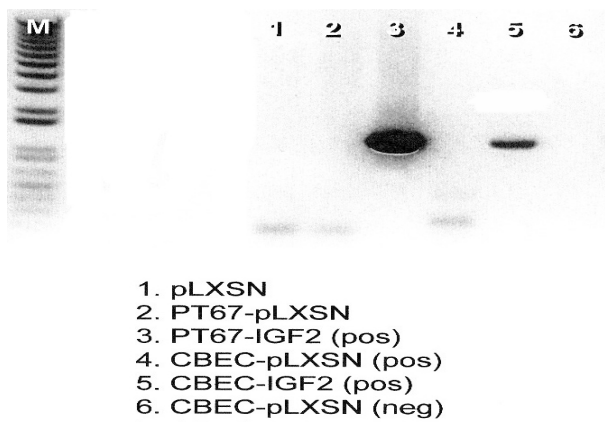
Analysis	P-values
AKT1 vs plxsn	0,016
igf2 vs parental	0,031
igf2 vs plxsn	0,031
igf2 vs AKT1	0,688
igf2 vs angiopoetin	0,219

Table 4: statistic and growth curve results from PT-67 Growth Curve comparison

3.1.3. Target cells

3.1.3.1: Proof of the vector integration into the DNA of the target cells

Afterwards, the supernatant gained from the producer cell colonies, containing the infectious virus particles was used to transfect the target cord blood endothelial CD34⁺-precursor cells, the HUVECs and the mesenchymal stem cells. The insertion of the viral genetic information into the native genome of the target cells could be proved, as performed for the producer cells, by gDNA PCR from the cells, extracted after different growing times.



1. pLXSN
2. PT67-pLXSN
3. PT67-IGF2 (pos)
4. CBEC-pLXSN (pos)
5. CBEC-IGF2 (pos)
6. CBEC-pLXSN (neg)

Figure 8: PCR of genomic-DNA from the Target cells

3.1.3.2. Proof of IGF2 transcription in the transfected target cells

3.1.3.2.1: mRNA / cDNA Proof with PCR and Realtime PCR

To verify the transcription and translation of the virus genetic information by the host cell, cDNA Real-Time Taqman PCR's were performed to gain information about the amount of growing factor mRNA that was produced by the infected cells. All growth factor plasmids could be verified to be integrated into the target cell and significant amounts of mRNA were produced. The amounts differed significantly, shown in example for the IGF2 assay in Figure 9:

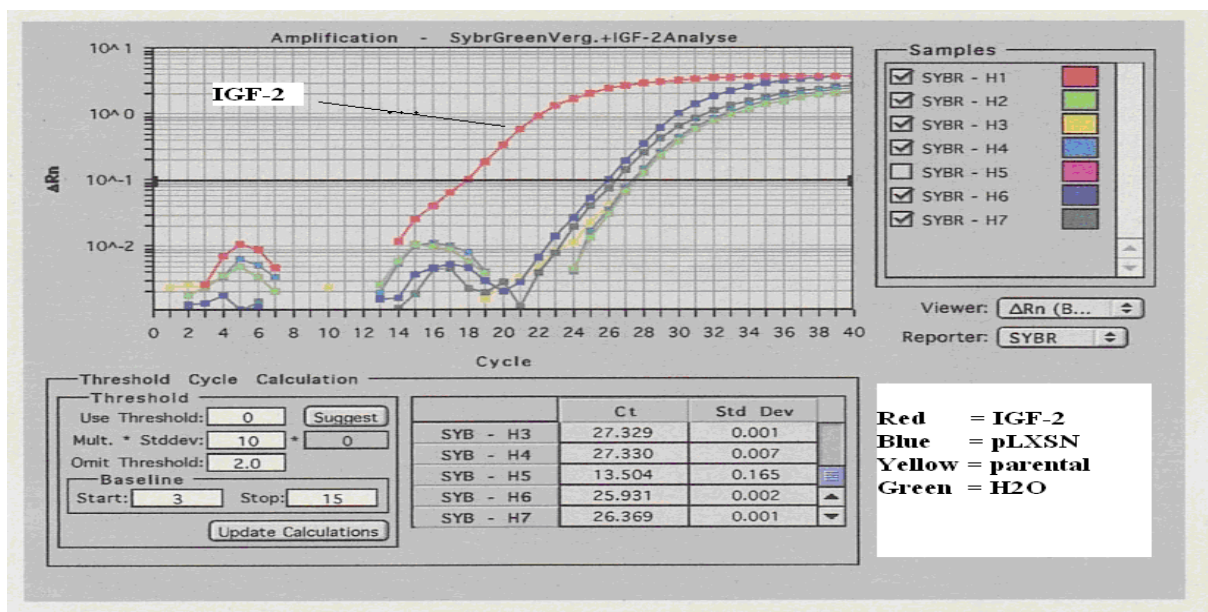


Figure 9: example of a Taqman[®] Real-Time PCR curve obtained from a IGF2 cDNA assay

1.	1. NB1591-94	1. NB1166-67	1. NB1683	1. Mean
1. IGF2	2. 1423	2. 324	2. 1323	2. 1023,3
1. Parental	3. 0,9	3. 9,1	3. 2,9	3. 4,3
1. pLXSN	4. 1,03	4. 16	4. 6,5	4. 7,84

Table 5: Relative Quantity of cDNA copies of the cells (ddCT-Method compared to normalizer (H₂O))

For the IGF2 growth factor sequence, a nearly 235 times higher concentration could be detected compared to the parental cells, furthermore compared to the control group with the empty pLXSN vector the cells contained approximately 130 times more IGF2 cDNA.

3.1.3.2.2. Proof of transcription of AKT1 and ANG1

As performed for the IGF2 protein, AKT1 and ANG1 were proven to be transcribed into mRNA via the vector coded information with the help of PCR and RT-PCR assays. As shown in the following picture, the PCR could proof the correct translation. As used for the IGF2 Insert, a short sequence of the delivering vector was cloned into the plasmid and could now be used as sense primer for the PCR reaction to distinguish the native from the artificial cDNA extracted from the target cells.

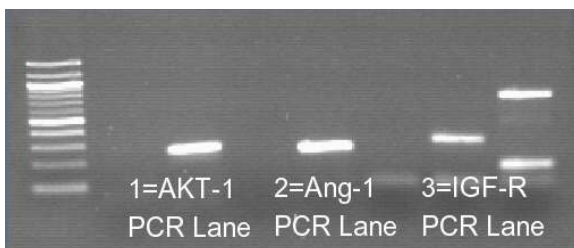


Figure 10: Electrophoresis of PCR-Products from AKT1, ANG1 and IGF-receptor Primer

In the Realtime-PCR the inserted vector coded genetic information could be determined. The levels found were not as high as for the IGF2 sequence, but were obviously transcribed in the cells.

	1. NB1166-67	2. NB1166-67	NB1166-67
	IGF2	AKT1	Angiopoetin
1. Insert	324	220	195
2. Parental	9,1	4,2	2,2
3. pLXSN	16	7,4	3,1

Table 6: Relative Quantity of cDNA copies of the cells (ddCT-Method compared to normalizer (H₂O))

3.1.3.3. Proof of protein translation by the target cells with ELISA

As final step in the verification of transgenic expression, the IGF2 Peptide could be shown to be processed into a working protein, resulting from the fact that we were able to detect a significant higher amount of IGF2 Protein in the transgenic cells with the help of an Elisa examination. The parental control cells had only spare amounts of IGF2 in their cytoplasm. For the NB 1591-94 cell line, the average amount (of 3 templates each) of IGF2 Protein in the Immunosorbent assay was 4.7ng/ml and for NB 1683, it counted 5.9 ng/ml. The increase of IGF2 Protein concentration in the genetically altered cells was at least 9-11 times compared to the untreated parental control (n=12 different templates plus controls in 2 repeated Elisa's, $p \leq 0.05$, Fisher-Exact + Wilcoxon Test for significant difference in paired samples).

We examined the cell lysates as well as the cell supernatants, but in repeated ELISA checks, we were not able to detect a significant amount of IGF2 Protein in the supernatant.

Interestingly, the possible extraction step of the commercial ELISA Kit did decrease the quality of the results. The data was comparable but clearly scattering a lot more. From thereon, we used the non-extraction protocol.

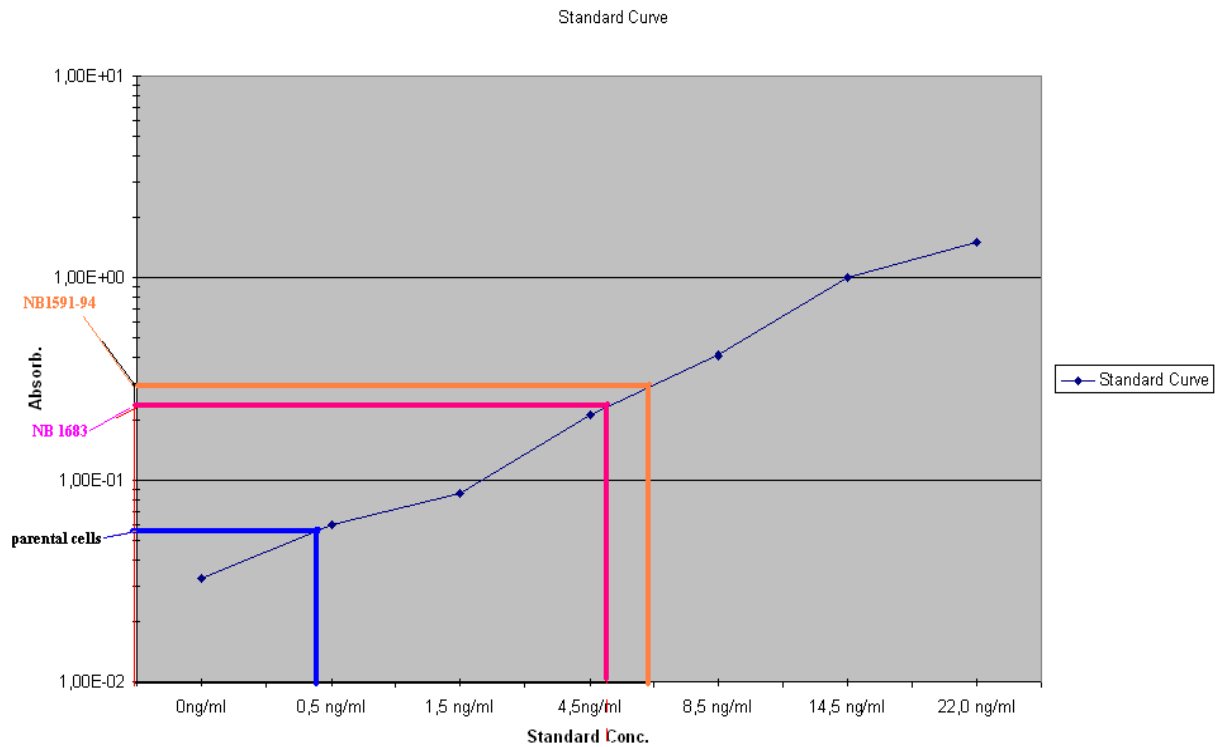


Figure 11: Elisa: Light-Absorption vs. Concentration of template IGF2 (NB1591-94 and NB 1683)

We also performed several Western Blot assay to detect the IGF2 protein, but we were not able to detect the IGF2 protein due to technical problems (see discussion).

We tried normal Western blot techniques as well as a special dot blot, but none of them could reliably detect the IGF2 protein complex.

3.1.3.4. Determination of the viral titer

With the help of the titer-assay we were able to determine the range of the amount of viral infectious particles that were produced by our Packaging Cell Line PT67. We detected a viral titer of 4×10^6 .

3.2. Consequences of the genetic alteration of the target cells

3.2.1. Growth

To analyze the effects of the viral transmitted genetic changes we first examined the growth behavior of the cells in the normal cell culture environment. The resulting growth curves are shown in the appendix.

It becomes clear, that the IGF2 overexpressing endothelial-like cells did not growth faster but slower. That effect puzzled us at first and we changed the further process of the experiments to elucidate the reason for this unexpected behavior (s. Discussion).

The cells transfected with AKT1 had a clearly better growing capability. Indeed, they didn't exceed the parental, untreated cells (see discussion).

Furthermore, the Angiopoetin overexpressing cells did grow a bit faster than the IGF2 cells, but stopped their growing early and went apoptotic.

The statistic analysis for the different cell lines and inserts is shown in the box below.

Statistical growth curve analysis for significant differences between different Inserts with P-Values from Wilcoxon and Fisher-Exact-Testing		
Cell line	Analysis	P-value
NB 1683	IGF2 vs. plxsn	0,655
NB 1683	IGF2 vs. parental	0,001
NB 1594	IGF2 vs. plxsn	0,014
NB 1594	Igf vs. parental	0,001
NB 1164-65	igf2 vs parental	0,001
NB 1164-65	igf2 vs plxsn	0,248
NB 1166-67	igf2 vs parental	0,003
NB 1166-67	igf2 vs plxsn	0,005
NB 1166-67	igf2 vs AKT1	0,004
NB 1166-67	igf2 vs angiopoetin	0,95
NB 1166-67	akt vs parental	0,05
NB 1166-67	Akt vs. pLXSN	0,02

Table 7: statistics of the different growth curves from the overexpressing cell lines

3.2.2. Cell survival

We suspected the IGF2 treated cells to be slowed down in their growth behavior because of a down regulated cell cycle. Gray et al. (24) have shown that an IGF2 over stimulation leads to a significant increase in p21 tumor suppressor gene expression. And therefore slows down the cell cycle (s. Discussion) implementing a better DNA repair. We suggested an increased cell repair and survival ability of the IGF2 overexpressing cells. We applied several types of apoptotic and oncogenic stress factors to the cells to test their surviving and repairing abilities.

3.2.2.1. Cytotoxic stress

First the cells were confronted with G-418 Geneticidin cytotoxic agent, where the IGF2 positive cells had a slight advantage in the survival capacities compared to the empty vector cells, but adjusted to cell numbers and cell passages, the advantage showed no statistic significance.

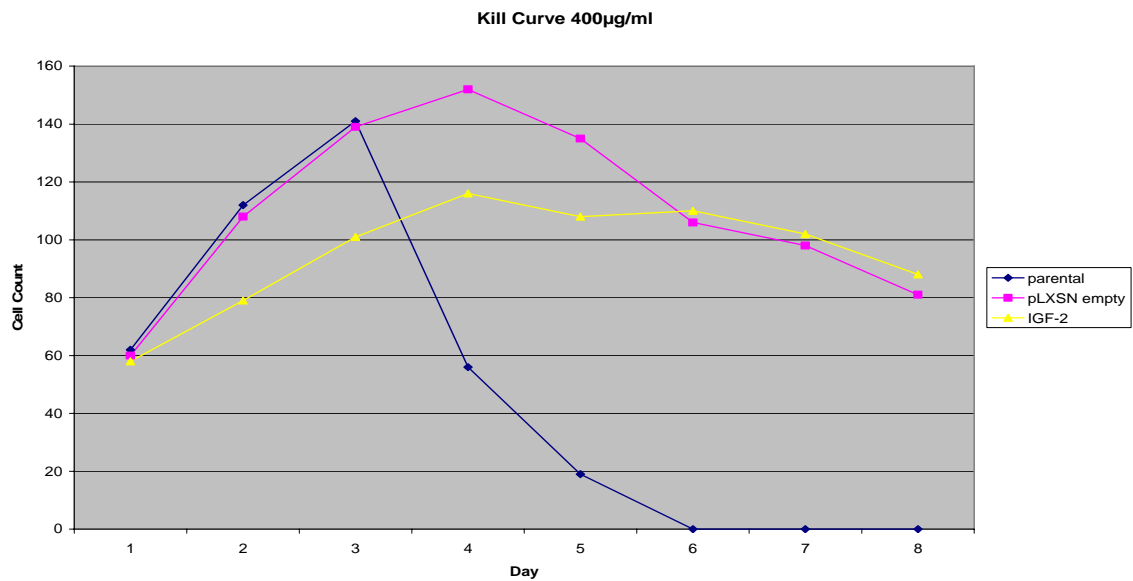


Figure 12: G-418 Kill Curve 400µg/ml



Figure 13, G-418 Kill Curve with 1600µg/ml

P-Values from paired sample test for G418 kill curve			
Cell Line	Type	P-Values	Test
NB 1591-94 g418 Kill curve 1600µg	IGF2 vs. Parental	0,092	Paired samples Test
NB 1591-94 g418 Kill curve 1600µg	igf2 vs. Plxsn	0,293	Paired samples Test
NB 1591-94 g418 Kill curve 400µg	IGF2 vs. Parental	0,109	Paired samples Test
NB 1591-94 g418 Kill curve 400µg	igf2 vs. Plxsn	0,234	Paired samples Test

Table 8, statistics with p-values of the kill curves for the different insert types

3.2.2.2: Growth factor withdrawal

Under growth factor restraint, we could observe that the IGF2 expressing cells had a survival advantage in the culture assay. Like the parental cells, CBEC-IGF2 showed growth arrest but they tended to survive the growth factor restriction better than the parental cells. However, a statistically significant difference could not be found. The growth factor depletion led to decreased growth in all cell cultures.

P-Values for growth factor withdrawal survival time			
Cell line	Assay	p-values	Test
NB 1591-94 growth factor restraint	igf2 vs. Plxsn	0,242	T-Test for paired samples
NB 1591-94 growth factor restraint	igf2 vs. Parental	0,797	T-Test for paired samples

Table 9: statistics for growth factor withdrawal assay

3.2.2.3. Cell survival under FCS withdrawal

Similar results were obtained with cultures in serum-free media (D-MEM without any further additions). Again, although the IGF2 pos. cells survived a bit longer than the untreated parental and the pLXSN cells, the statistical comparisons did not show a statistically relevant significance between the groups.

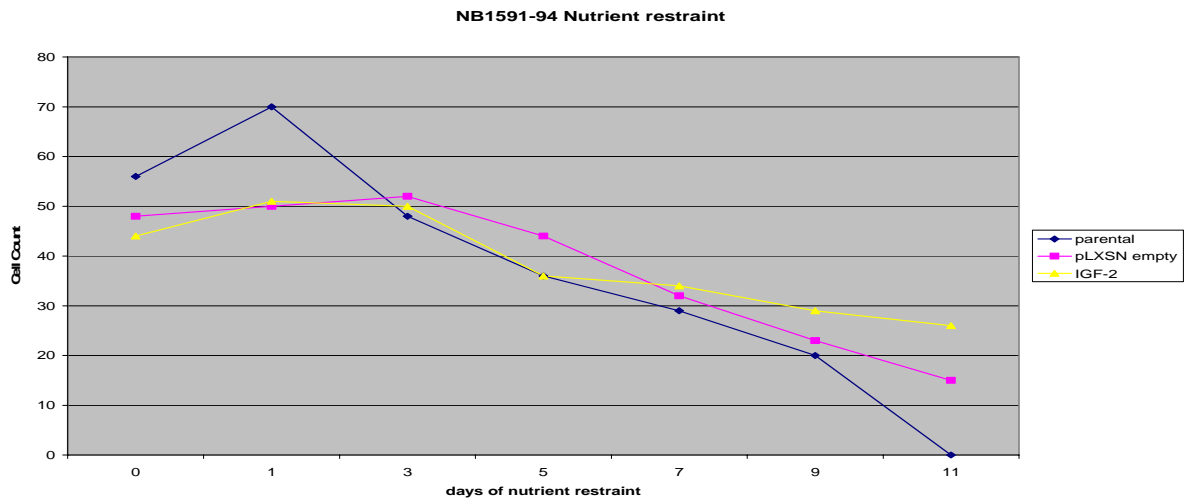


Figure 14: growth curve for NB 1591-94 FCS withdrawal

P-value for nutrient withdrawal survival time			
Cell line	Type	P-values	Test
NB 1591-94 nutrient restraint	igf2 vs. plxsn	0,22	T-Test for paired samples
NB 1591-94 nutrient restraint	plxsn vs. parental	0,657	T-Test for paired samples
NB 1591-94 nutrient restraint	igf2 vs. parental	0,345	T-Test for paired samples

Table 10: p-values of nutrient withdrawal assay

Interestingly, although all cultures showed a growth arrest, the parental CBEC and the pLXSN cells formed networks of tubular like structures, as previously described by Peters et al. (27). In contrast, the IGF2 over expressing cells did not form any kind of tubular network. In 3 assays of 2 cultures per template/insert, we repeatedly could observe this networking by the CBEC, always without the IGF2 pos. cells forming any kind of tubular structure. The corresponding pictures are shown in the appendix.

3.2.2.4. Cell survival under ultraviolet irradiation

Cell- and DNA damage causes cell death, particularly apoptosis. Ultraviolet irradiation is a strong inducer of such damage. After the application of different doses of UV-irradiation, the cells were cultured and repeatedly counted as described (s. Materials & Methods). The IGF2 over expressing cells showed a significant survival advantage. As for the conditions of growth factor withdrawal, CBEC-IGF2 stopped their growing or duplicating activity. But, CBEC-IGF2 tolerated higher doses of UV-irradiation to induce cell death than the parental CBEC and empty vector CBEC. The IGF2 pos. cells clearly had a better survival capacity in all of the tested cell lines, bearing higher UV-light doses and surviving longer time periods after application of identical radiation doses.

P-Values for UV survival time			
Cell Line	Type	P-Values	Test
NB1164-UV-Survival	igf2 vs plxsn	0,063	Wilcoxon, Fischer-Exact
NB1164-UV-Survival	igf2 vs parental	0,016	"Wilcoxon, Fischer-Exact
NB 1166-UV-Survival	igf2 vs parental	0,018	Wilcoxon, Fischer-Exact
NB 1166-UV-Survival	igf2 vs plxsn	0,018	Wilcoxon, Fischer-Exact
NB 1166-UV-Survival	igf2 vs akt	0,016	Wilcoxon, Fischer-Exact
NB 1166-UV-Survival	akt vs plxsn	0,018	Wilcoxon, Fischer-Exact
NB 1591-94 UV survival	igf2 vs. Parental	0,028	Wilcoxon, Fischer-Exact
NB 1591-94 UV survival	igf2 vs plxsn	0,016	Wilcoxon, Fischer-Exact
NB 1683 UV survival	igf2 vs. Parental	0,018	Wilcoxon, Fischer-Exact
NB 1683 UV survival	igf2 vs plxsn	0,034	Wilcoxon, Fischer-Exact

Table 11: p-Values of the ultraviolet survival assays

The corresponding apoptosis curves of the assays are shown in the appendix.

3.3 Cell stimulation

To further investigate the influences of the different intracellular cascade pathways and their activation on cell growth, function and morphology, we stimulated the untreated endothelial precursor cells with different growth factors in different amounts of them.

3.3.1. IGF2 stimulation

The analysis of the cell morphology showed clearly that the IGF2 positive cells were changed. The comparison of the altered cells with the untreated parental cells showed, that the slower

growing IGF2 pos. cells were 2-2.5 times larger in the mean and their morphology was changed the way that they looked more like spindle cells than like flattened endothelial cells. In addition, the cytoplasm showed increased vacuolisation and the nucleus was larger than the ones from the parental cells, as well as it had more and larger nucleoli. By stimulating the parental cells with external IGF2 (s. chapter Material & Methods) a similar change in the morphology could be recognized with the cells also becoming large and plump. In a small assay we compared the average diameter of the parental control cells with the diameter of the parental cells, stimulated with 50ng/ml external IGF2 after an incubation period of 2 weeks. Always the greatest size of the cell body was measured with the help of Image J, counted in pixel at a given zoom factor of the photographs. The treated cells were significantly larger than the control group ($p\text{-value} \leq 0.003$). These results suggest that IGF2 stimulation may induce cellular senescence of CBEC. Photographic examples of the cell morphology are shown below.

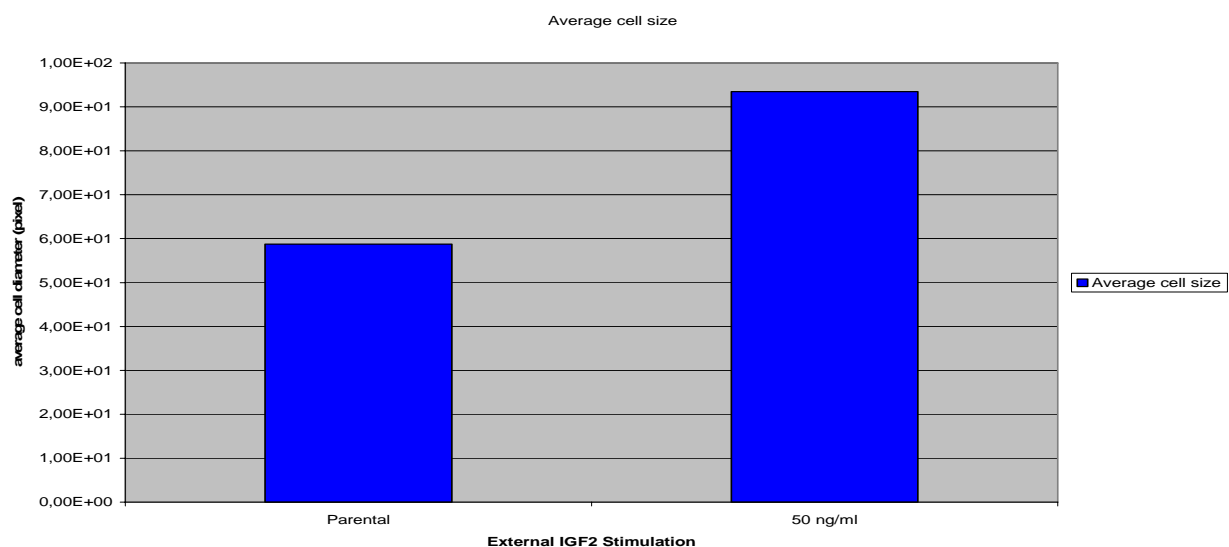


Figure 15: Comparison of average cell size for 50ng/ml IGF2 stimulation vs. parental untreated cells



Figure 16: picture of untreated parental endothelial cells after 2 weeks incubation

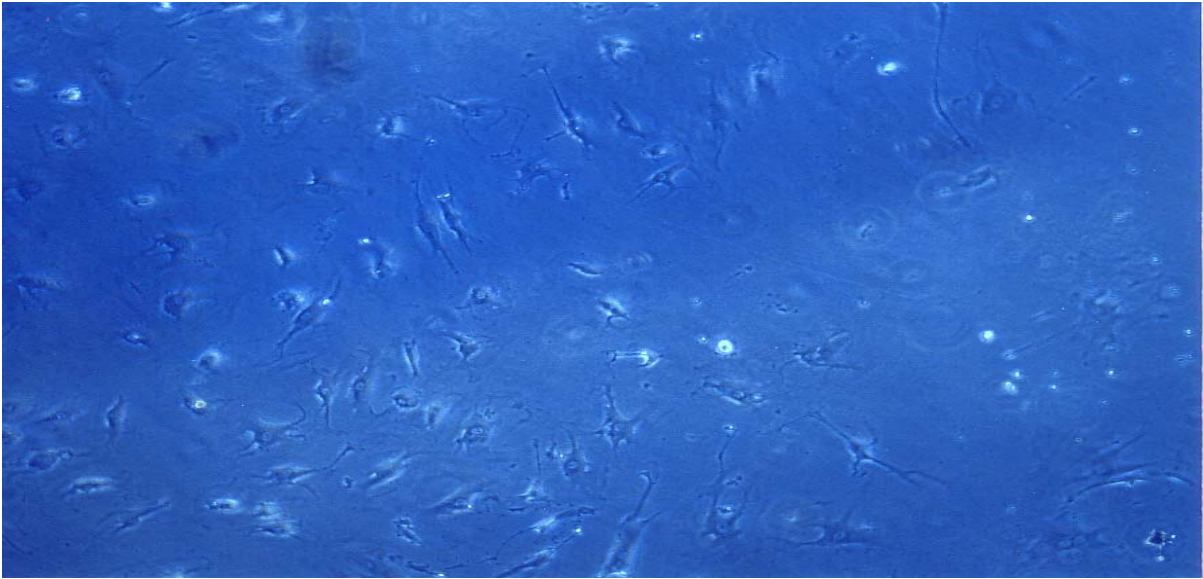


Figure 17: Picture of IGF2 treated cells and their morphology after 2 weeks

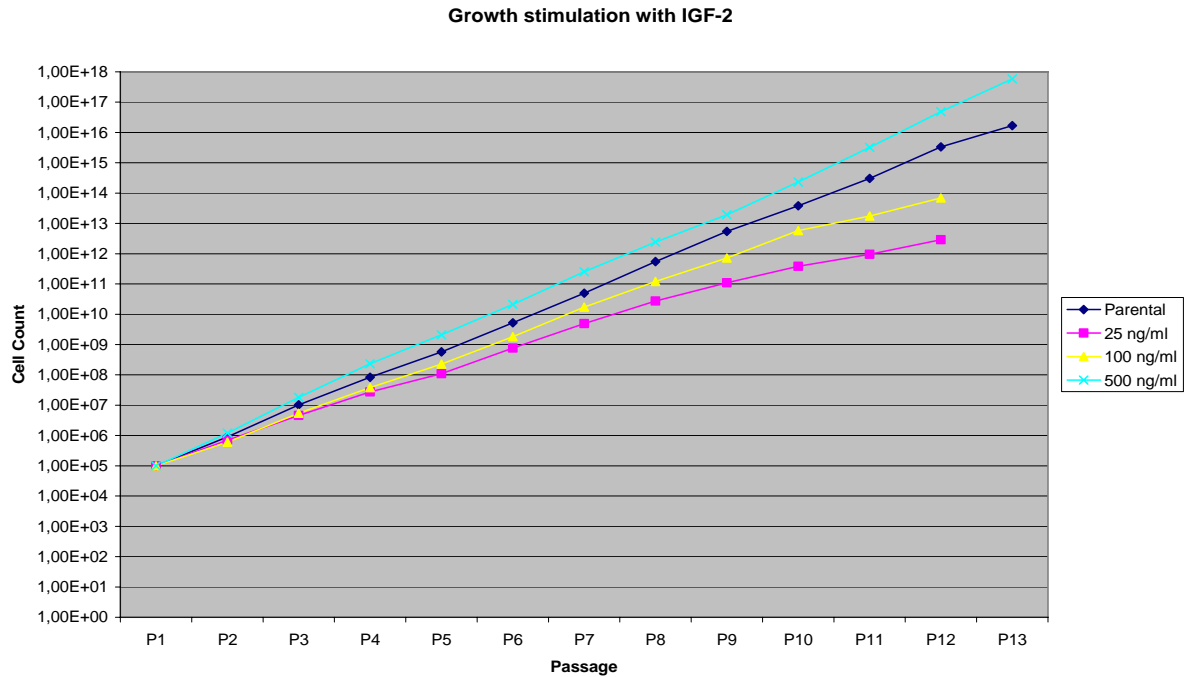


Figure 18: Growth curve of external IGF2 stimulation of NB1591-94

P-Values for external cell stimulation of CBEC with IGF2			
Cell Line	Assay	p-values	Test
NB 1166-67 IGF2 Stimulation	25ng vs. Parental	0,063	Wilcoxon, Fischer-Exact
NB 1166-67 IGF2 Stimulation	25ng vs. 500ng	0,031	Wilcoxon, Fischer-Exact
NB 1683 IGF2 Stimulation	25ng vs. 500ng	0,008	FISCHER-EXACT
NB 1683 IGF2 Stimulation	25ng vs. Parental	0,063	FISCHER-EXACT
NB 1591-94 IGF2 Stimulation	25ng vs. Parental	0,01	FISCHER-EXACT
NB 1591-94 IGF2 Stimulation	25ng vs. 500ng	0,01	FISCHER-EXACT

Table 12: statistics for external IGF2 Stimulation

With IGF2 concentrations of 100ng/ml and 500ng/ml, the repeatedly published effects (see discussion chapter 4.1 to 4.2) of growth stimulation via IGF2 were detectable with a high statistic significance of $p \leq 0.01$.

3.3.2. TGFB1 Stimulation

At low IGF2 concentrations, we observed a slower proliferation. It was shown previously, that IGF2 at low concentrations may induce TGFB1 expression (59). Hence we stimulated untreated parental control CBEC with external TGFB1 to compare the effects of those two growth factors because of the main participation of TGFB1 in the downstream cascade of IGF2 (s. discussion). A slight change in the look of the TGFB1 stimulated cells was

observable, but the cells did not reach the specific spindle-shaped morphology of the IGF2 stimulated cells. Nevertheless, a significant decrease in proliferation was observable. Thus, TGFB1 can mimic the antiproliferative effect of low IGF2 concentrations, but not its effect on morphology.

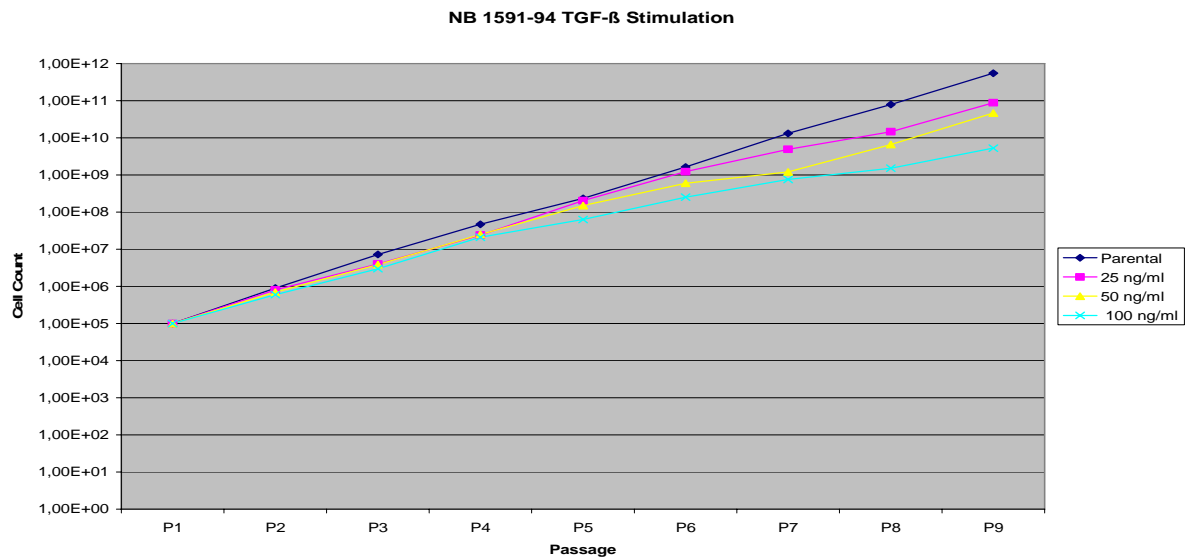


Figure 19: Growth Curve of external TGF-B1 Stimulation of NB1591-94

P-Values			
Cell Line	Assay	p-values	Test
NB 1591-94 TGFb Stimulation	25ng vs. Parental	0,008	FISCHER-EXACT
NB 1591-94 TGFb Stimulation	25ng vs. 100ng	0,008	FISCHER-EXACT
NB 1591-94 TGFb Stimulation	100ng vs. Parental	0,004	FISCHER-EXACT
NB 1591-94 TGFb Stimulation	25ng vs. 50ng	0,07	FISCHER-EXACT

Table 13: statistics for external TGFB1 stimulation of NB 1591-94

3.4. A coculture assay of vessel formation

Coculture of fibroblasts and endothelial cells have been described to result in formation of three-dimensional vessel-like tubuli (22, 53). In contrast to the Matrigel tubuli assay, the tubuli formed in cocultures are only formed in the presence of true endothelial cells, but not by hematopoietic EBC (60). In this coculture tubuli formation assay, several parameters could be observed and statistically analyzed to elucidate the differentiation capabilities of the cells.

3.4.1. Cell growth and formation of a multilayer cell compound

If used with the cells described in the original publication first describing this assay (22), namely human diploid fibroblasts and HUVECs, the formation of the necessary cell sandwich layer could reproducibly be achieved after a short period of establishing and adjusting the protocol for our needs. Also, when HUVEC were replaced by CBEC, the desired multilayer cell sandwich architecture was also reproducibly formed.

When the fibroblast were replaced by Umbilical Vein Stromal Cells (UVSC), despite being the progenitor cells for fibroblasts, in 3 following assays of 3 cultures each, the UVSC reached confluency, but did not continue their growth to form the desired multilayer. We therefore did not investigate any further with replacing the fibroblasts. Also the UVSC did not form any kind of tubular structure in coculture with either HUVEC or CBEC.

3.4.2. Tubuli formation

In all control fibroblast/HUVEC cocultures, tubular vessel-like structures were formed. The formation of tubuli depended most on the age and number of passages of the cells. Tubular structures were rather formed by younger cells, used early after the retroviral selection procedure. Therefore the data was analyzed by adjusting for the cell passage. Only cells with corresponding passage numbers were compared in one graphic or analysis, by dividing the data into groups of young (3-5 passages), middle (6-9 passages) and old (over 9) cells. Finally it became clear that only the cells up to passage 7 were comparable with the HUVECs and therefore the statistic data analysis was only performed with the data from the younger cells.

In cocultures of fibroblasts and CBEC, rather than the formation of tubular structures, the formation of cell clusters was observed. This tendency was even stronger when we used CBEC-IGF2. The formation of cell clusters depended on age/passage of the cells and was decreased when using cells early after isolation. These cluster like structures were expressing the typical surface markers also found on the tubular structures, e.g. PECAM-1(CD-146), CD-31, von Willebrandt-Factor. But, on the other hand, the IGF2 overexpressing cells did produce a lot more Clusters than their corresponding parental or empty vector controls. Even when the results were separated and analyzed for the age/passage number, the IGF2 cells did show a clear tendency to grow in clusters rather than forming tubular structures.

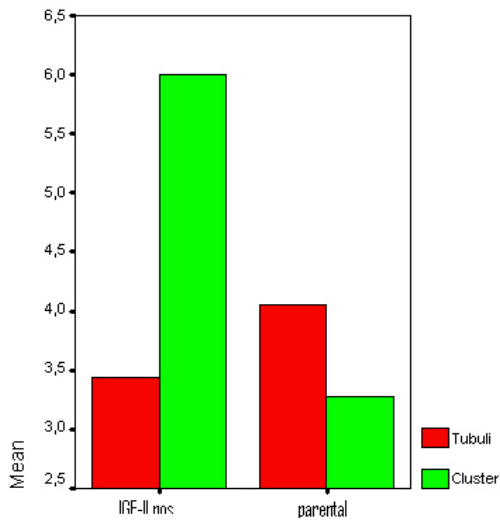


Figure 20: Tubuli vs. Cluster-formation depending on Insert IGFII vs. parental $p=0.019$

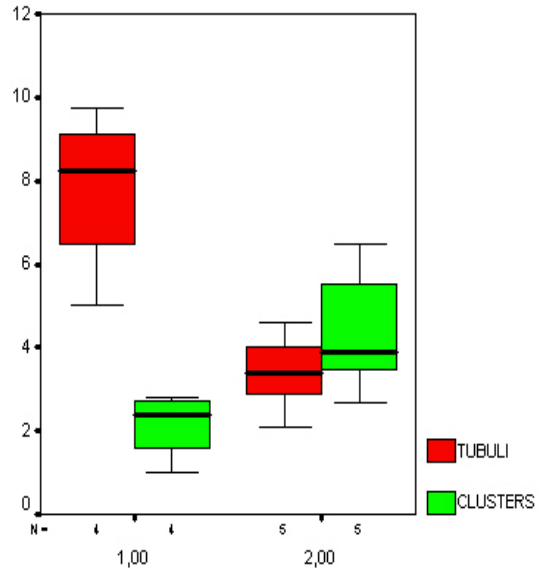


Figure 21: Mean cluster formation of parental CBEC vs. HUVEC

The statistic analysis of the data showed a significant tendency even of the parental CBEC to form cluster-like structures if compared with the HUVECs ($p < 0.001$, Mann-Whitney & Wilcoxon test). Furthermore, the IGF2 pos. cells did produce significantly more clusters than the pLXSN control CBEC of the same age ($p = 0.018$, Mann-Whitney & Wilcoxon test).

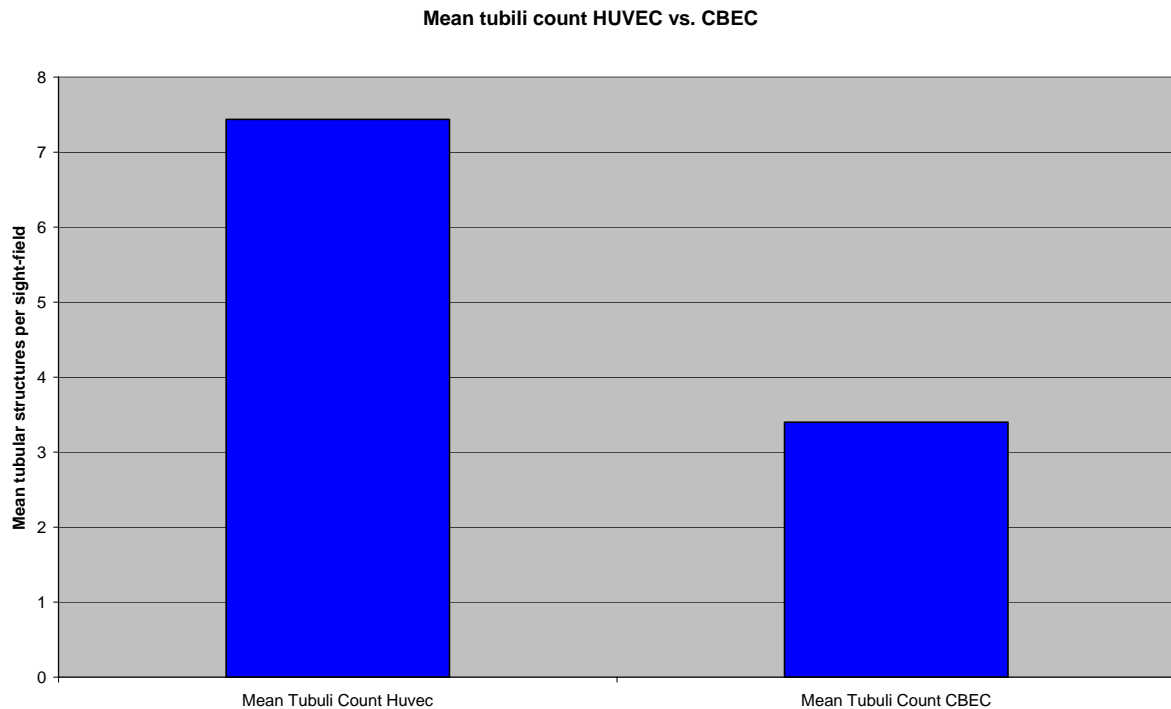


Figure 22: Mean Tubular structure count in HUVEC vs. CBEC

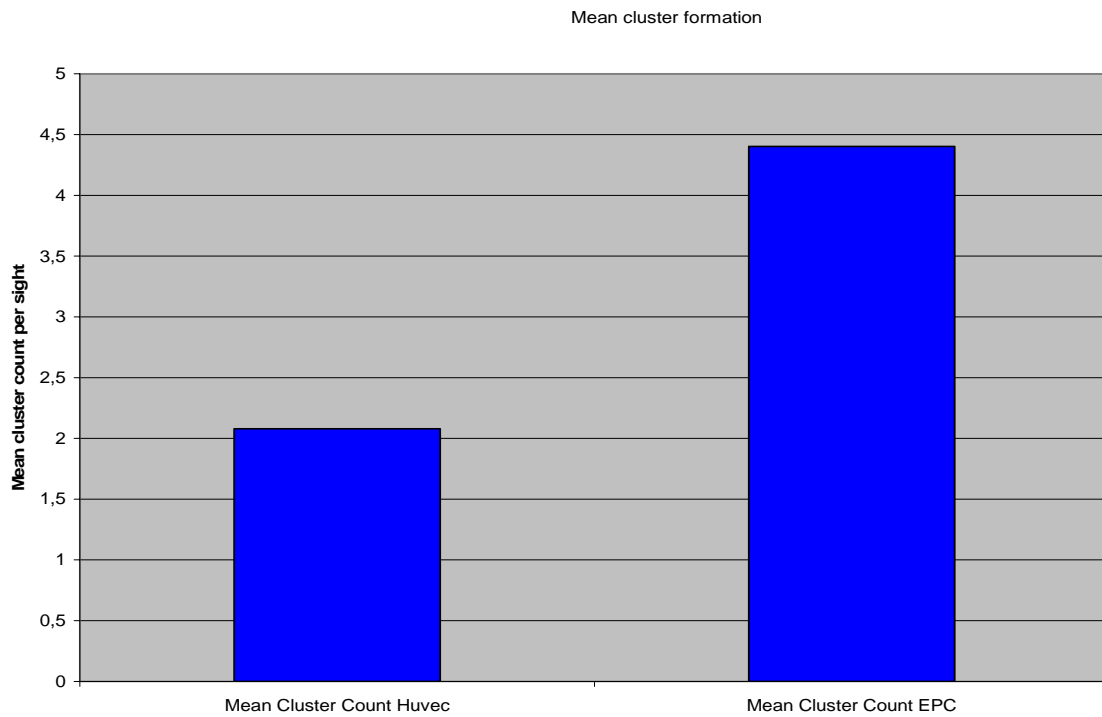


Figure 23: Mean cluster count in HUVEC vs. CBEC

When the absolute tubular structure count was examined, the CBEC produced less tubuli than the HUVEC, with the parental forming the most out of the CBEC, followed by the empty vector CBEC-pLXSN. CBEC-IGF2 did, instead of increasing the formation of tubular structures, form significantly less tubular structures in our assays.

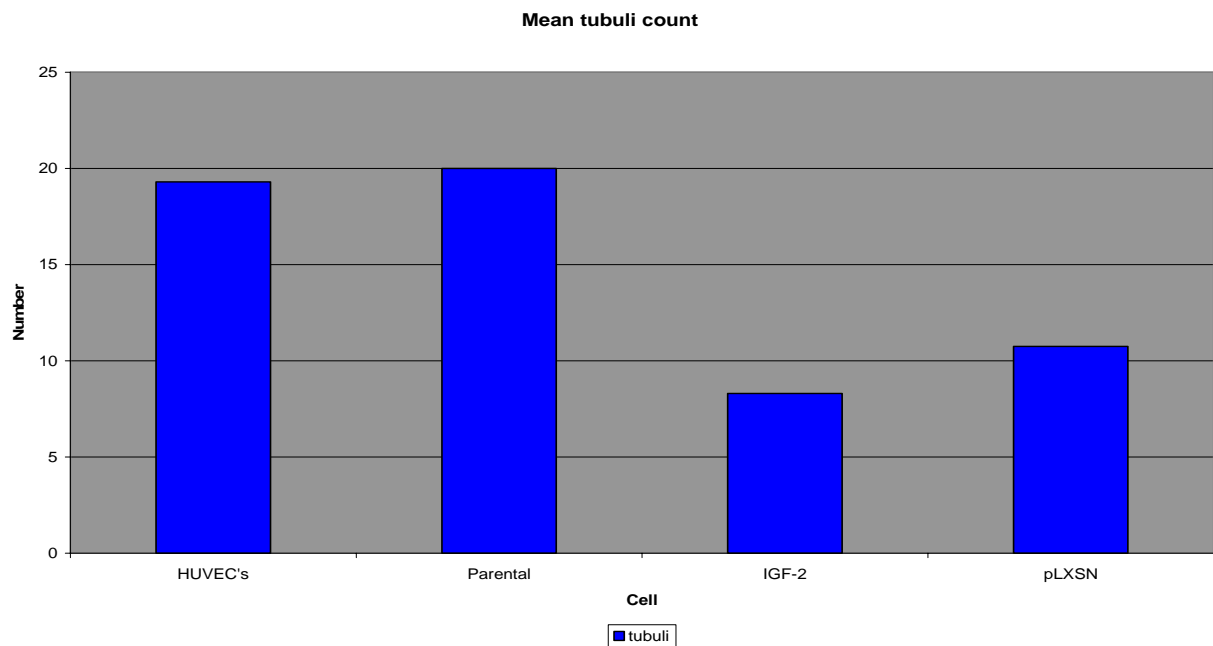


Figure 24: Mean of tubular structures for all assays:

P-Values		
Coculture summary	Comparison	P-Value
Coculture NB 1591-94 and Huvec Tubuli Count	Normalverteilung erfüllt.	0,862
Coculture NB 1591-94 and Huvec Tubuli Count	IGF2 Vs. Parental	0,001
Coculture NB 1591-94 and Huvec Tubuli Count	IGF2 vs. pLXSN	0,014
Coculture NB 1591-94 and Huvec Tubuli Count	IGF2 vs. HUVEC	0,001
Coculture NB 1591-94 and Huvec Tubuli Count	HUVEC vs. Parental	0,049

Table 14: Statistics for number of tubular structures depending on cell type or insert in NB 1591-94

3.4.3. Tubuli quality parameters: Length, Thickness, Crossing/Sprouting

3.4.3.1. Length

Figure 25 shows, that the HUVEC produced the longest tubular structures in the comparison, followed by the parental CBEC, whereas the IGF2 pos. CBEC showed the shortest tubuli. All of those comparisons showed significant differences in these parameters between the CBEC-IGF2 and the empty vector cells.

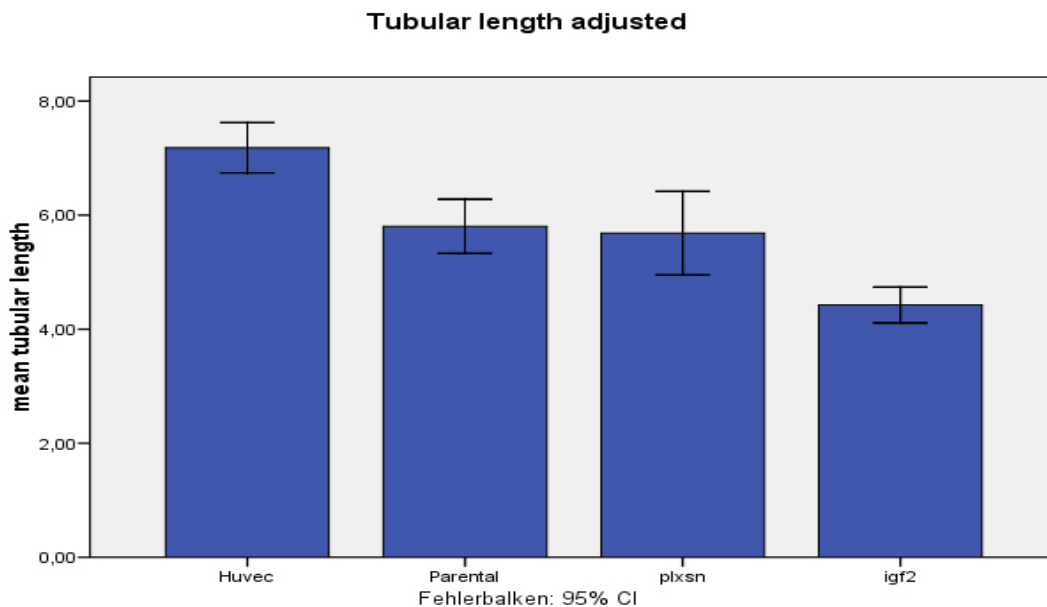


Figure 25: Mean tubuli length depending on insert for NB 1591-94

P-Values			
Cell line+assay	Comparison	p-values	Test
Coculture-NB1591-94-Length	IGF2 vs. Huvec	0,001	T-Test
Coculture-NB1591-94-Length	IGF2 vs. Parental	0,001	T-Test
Coculture-NB1591-94-Length	IGF2 vs. pLXSN	0,003	T-Test

Table 15: Statistics for tubular length depending on insert

Also a statistic significant difference was found between the HUVEC and all of the CBEC, showing a clear advantage for the HUVEC in formation of long tubular structures.

3.4.3.2. Thickness

As described by Bishop et al., (53), the tubular thickness increased at the end of the culturing period and the formation of the tubular network was accompanied by lengthening, thickening and anastomosis of the cellular tubuli structures. Therefore we measured another parameter to analyze the quality of the formed tubular structures, namely the thickness. Whereas the HUVEC showed longer tubuli, the CBEC had in general thicker tubuli than the other cells. Again, however, CBEC-IGF2 showed the weakest activity, resulting in the thinnest tubular structures.

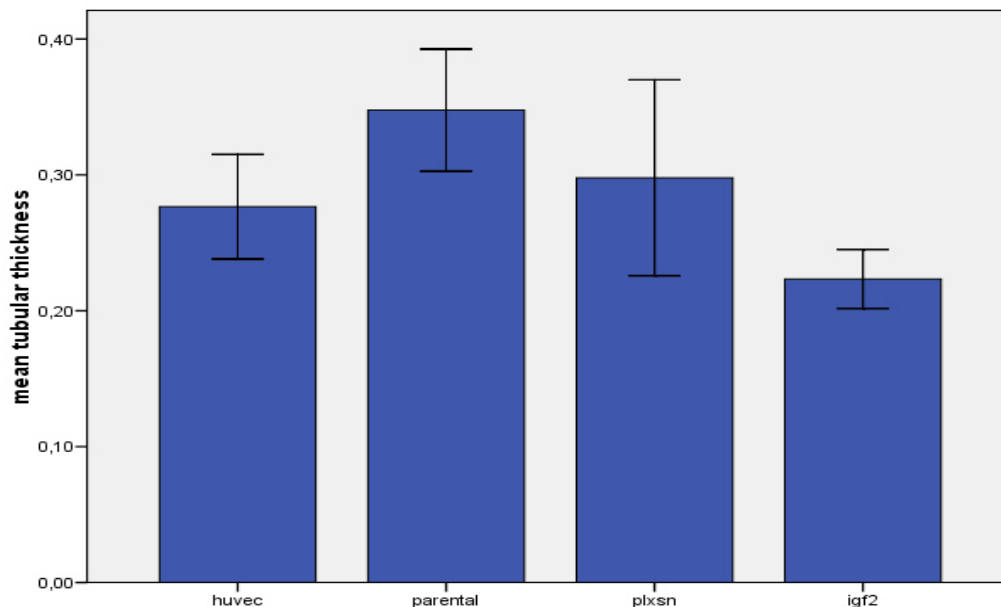


Figure 26: Mean tubular thickness

P-Values			
Cell line- assay	Insert	p-value	Test
Coculture-NB1591-94-Thickness	IGF2 vs. HUVEC	0,018	T-Test
Coculture-NB1591-94-Thickness	IGF2 vs. Parental	0,001	T-Test
Coculture-NB1591-94-Thickness	IGF2 vs. pLXSN	0,037	T-Test
Coculture-NB1591-94-Thickness	Parental vs. HUVEC	0,021	T-Test

Table 16: Statistics for tubular thickness

3.4.3.3. Crossings/Sprouting

The crossings were counted as points of communication between tubuli, forming a tubular network. In control fibroblast/HUVEC cocultures, we found more crossings and more complex networks than the CBEC, with significant advantage to the parental CBEC $p \leq 0.034$. In comparison to transfected CBEC, the parental CBEC were forming the most crossings and therefore were showing the strongest neovascular activity of our CBEC in all of our assays.

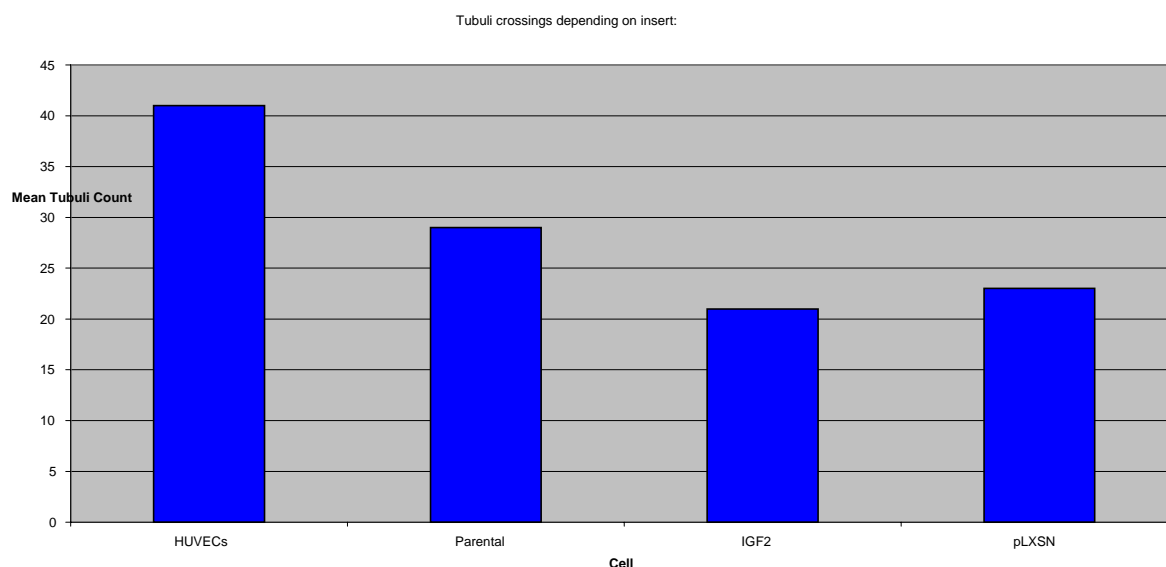


Figure 27: Amount of tubular crossings of the different cells for NB1591-94

3.4.3.4. AKT1 in the Coculture assay

We had just two assays with CBEC-AKT1 cell lines to perform a reliable statistic analyze, but in those cocultures we performed, the AKT1 overexpressing cells did form only a few cluster like structures and did form more tubular structures than the IGF2 positive cells. But nevertheless they formed less tubuli than the HUVEC and even less than the parental controls.

3.4.3.5. Cooperation project with the cardiology department to transplant the CBEC:

During the project cooperation with the department of cardiology we were able to transplant the genetically alternated cells into a myocardial infarction model in immunodeficient rats. Myocardial ischemia was provoked by interruption of the blood flow in the left anterior derived coronary artery (LAD) of 6-8 week old male athymic nude rats. After thirty minutes

of absolute ischemia, the ligation was released and reperfusion was started and 1×10^6 CBEC were injected. To measure the cardiac performance before and after the infarction, echocardiographic examinations were performed to determine the left ventricular ejection fraction (LVEF) of the hearts. The results showed that CBEC transplantation was able to increase the LVEF of infarcted hearts significantly from 44% in the control group to 52% at two weeks in the CBEC group ($p < 0.05$). The overexpression of IGF2 in the CBEC increased the LVEF up to 54% ($p < 0.05$). Immunohistological analysis of the post-mortal hearts proved that the transplanted human CBEC took part in neo-vasculogenesis and increased vessel density and the number of vessel-like structures (52).

IV Discussion

4. Main findings summary:

We started our study to explore the restorative angio- and vasculopoetic capabilities of endothelial progenitor cells and ways to improve their possibilities.

To achieve this, we integrated different growth factors into the target cells via retroviral transfection. Our main subject was the IGF2 protein and its effects on the cells.

We found out that the overexpression of IGF2 led to a reduced cell growth but on the other hand to an improved survival ability of the cells. The overexpression of AKT1 resulted in a better growing capability and better survival of the cells compared to the untreated parental controls. To compare the vasculopoetic potential we established the coculture assay from Bishop et al. (53) and compared the growth of the transfected cells with parental untreated CBEC and untreated HUVECs. It became obvious that the HUVECs formed the most tubular like structures, whereas the IGF2 overexpressing cells did form the less. The IGF2 positive cells produced rather cluster like structures than tubuli and the few tubuli were shorter and thinner than the ones produced by the other cells, first of all the HUVECs. We claim that the overexpression of IGF2 leads to an increased cell survival and augmented repair capabilities, but on the other hand to a reduced cell growth and decreased differentiation capacities.

4.1. Receptor growth cascades

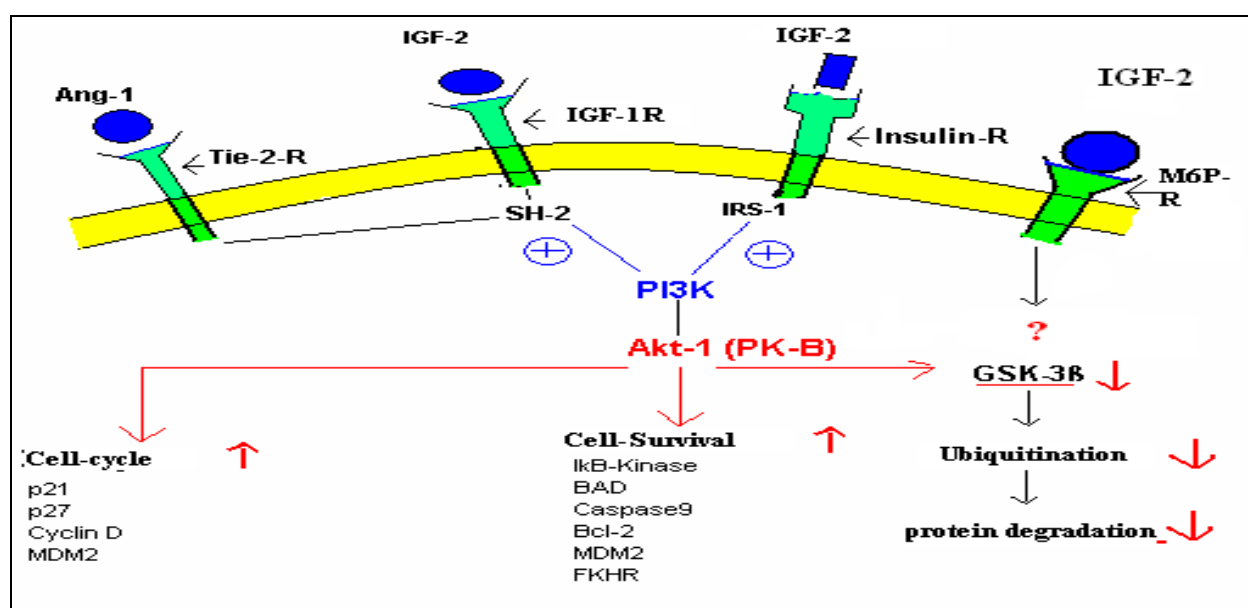


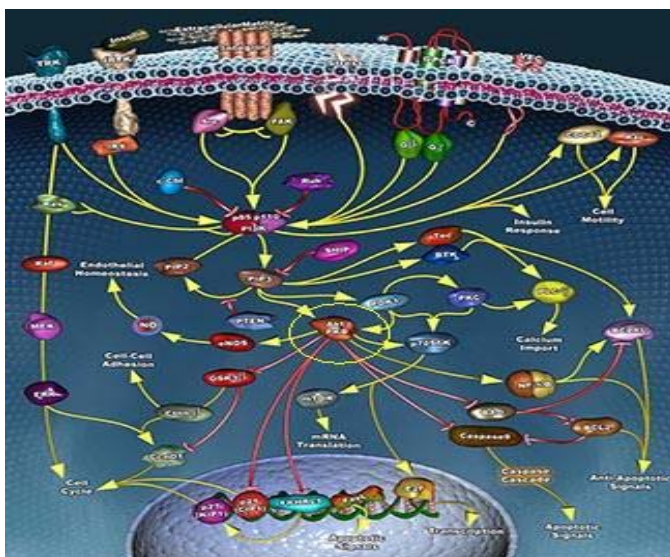
Figure 28: Overview of the intracellular pathway of the growth factors we used in our assays

With the idea of improving the growth and the vasculopoetic potential of our CBEC, we integrated different growth factors with the help of a retroviral transfection system into our target cells. We expected an improved cell duplication rate and with the help of this, an improved tissue engineering ability of our endothelial progenitor cells.

To understand the effects of the different growth factors we integrated into our CBEC, it is important to elucidate the essentials of the intracellular pathways of our growth factors and their potential receptors. Unfortunately, the exact pathways of the IGF2-Mannose-6-phosphat-receptor weren't clear as we started the study and aren't identified in all aspects yet. An overview of the pathways involved in the effects of the growth factors we used is shown in the figure 28.

4.1.1. Effects of AKT1 (Protein-kinase-B) activation

The AKT1 Proteinkinase: Being the downstream target of most growth factors, the Proteinkinase B or AKT1 is activated via phosphorylation through the Phosphoinositide-3-Kinase. Figure 29 shows the complexity of the intracellular streams in which AKT1 (marked in yellow) is involved. To avoid becoming too complicated by going in detail to deep, the following summary describes the main effects:



After its activation that is followed the receptor binding of e.g. Insulin or other growth factors like IGF-1 it will itself activate a lot of proteins by phosphorylating them at a catalytic activation site. These downstream effects are, e.g. the activation of the cell cycle by slowing down the expression of tumor suppressor proteins such as p53 or down regulation of cyclin-dependant kinase inhibitors such as p21

Figure 29: Intracellular AKT1 involved cell cascades

or either direct activation of cell cycle promoting kinases such as the cyclin-dependant kinases, first of all CyclinD, which is mainly responsible for the mitotic activity of the cell (26). The next target is the cell's survival capability; it is increased by stimulation of protooncogenic genes (36, 37, 38, 39).

4.1.2. Insulin-receptor and its activation effects

The Insulin-receptor achieves its effects by activating the Insulin-receptor-substrat-1-protein (IRS1) that is linked to the intracellular domain of its transmembraneous receptor. This IRS1 phosphorylates the Phosphoinositide-3-Kinase and triggers its activity. Then the next step is the activation of AKT1 that is explained above. The main target proteins for the stimulated AKT1 are:

- SH-PTP2: Mediating the fast responding Insulin effects.
- PI3-Kinase: Phosphatidylinositol-3-Kinase (PI-3K), converting Phosphatidylinositol bisphosphat (PIP₂) to Phosphatidylinositol-tris-phosphat (PIP₃). PIP₃ is mainly responsible for the initiation of the exocytose of Glucose Transporter (GLUT-4) molecules that import blood glucose into the body cells (17).
- SOS-GRB: The son-of-sevenless (sos) / growth-factor-bound (grb) complex is activated by hormone binding and the target protein of this protein complex is the rat sarcoma (RAS) protooncogenic protein, initiating a powerful serin phosphorylation cascade after its activation. RAS activates RAF (RAS activated factor), phosphorylating MEK (mitogen expressed kinase), resulting in MAP (mitogenig activated protein)-Kinase activation. The active MAP-Kinase regulates numerous protein activities and diverse gene expression profiles, which lead to fundamental changes in the cell metabolism to achieve anabolic and growing effects. Those enzymes being synthesized on the RAS stimulus are responsible for the long-time anabolic effects of the insulin, as well as its influence on cell proliferation, cell survival and cell differentiation (19).

4.1.3. The IGF1 Receptor

The IGF1R is stimulating the PI3-Kinase and MAP-Kinase pathways like the Insulin-Receptor does. That's the reason why the effect of their activation is mainly alike (17).

4.1.4. Mannose-6-phosphate receptors and Insulin-like Growth factor-2-receptor

We know two different forms of Mannose-6-Phosphate-receptors: The cation-dependent form (approximately 46kDalton) and the cation-independent form (approximately 300kDa). They both are, until now, the only members of the p-type lectin family. Interesting for our study is only the cation-independent isoform, because it is also the IGF2 protein receptor. It is a multifunctional receptor which was first discovered concerning its role in the intracellular transport processes, mainly delivering newly synthesized proteins from the trans-Golgi network to the lysosomes (48). It's isolated lacking or defect results in a specific lysosomal disease, the I-cell disease (49). The structure of the IGF2-receptor on the cell surface is different from the other growth factor receptors. It has only a short cytosolic tail that lacks any intrinsic kinase activity (47).

The IGF2/M6P-receptor binds IGF2 at the cell surface and internalizes it for degradation to prevent increased levels of growth factor (50).

But despite the designated degradation, the IGF2-protein-ligand plus receptor complex fulfills other complex tasks. It is capable of activating the inactive latent form of TGF β 1 that is then able to induce the p21 expression (46, 59). This leads to an upregulation of the CIP/KIP family of cyclin dependant kinase inhibitors (e.g. p21, p27, p57kip2) and results in a p53 independent way of inhibiting the cell cycle (26). Furthermore a cell cycle arrest can result from the induction of histone-deacetylase-inhibitor proteins which is also promoted by the IGF2-M6P-complex (26).

IGF2 can work as a growth stimulating factor, when binding to its other receptors, the Insulin- and the IGF1-receptor, but normally it works as a growth repressor when binding to the normal M6P-receptor. Furthermore it has much lower binding capacities to the IR and IGF1 receptors.

Therefore the IGF2-M6P-ligand-receptor complex has antioncogenic effects when IGF2 is used in physiological doses. The loss of the M6P-IGF2-receptor function has earlier been clearly shown to result in promotion of oncogenesis (41, 42, 43, 44, 45).

But in fetal development, the IGF2 is expressed in such high doses, that its receptor binding effects to the stimulating receptors such as Insulin-receptor is overwhelming. Last but not least the growth factor threshold theory (see below) demonstrates another point how to explain the complex diversity of effects that are caused and promoted by the IGF2-M6P-receptor and growth factor complex.

4.2. Method verification

4.2.1. Affirmation of the viral construct

With the help of the 118bp sequence of the delivering vector pOTB7 that was linked to the DNA of the IGF2 gene (s. materials and methods 2.1.1) we could clearly discriminate the native from the transgenic form of the IGF2 gDNA. Because the extra base pairs were located downstream of the Poly-A stop codon, we didn't fear any interference in the transcription process of the inserted genes. The DNA Replication itself wasn't affected neither, because high amounts of the replicated IGF2 gDNA could be extracted from the transfected cells. The problem that we couldn't detect the working protein in the cell's supernatant is explained below (4.2.3.4).

4.2.2. Producer cells

In each step the integration of the intended plasmid DNA was confirmed with the help of gDNA PCR before further experiments were started.

The analysis of the growth curve of the producer cells is difficult, because of the artificially altered nature of these cells. They have been changed to perform a powerful replication and encoding of the desired vector based on the NIH/3T3 cells. But despite this fact, the cells showed a reaction to the integrated growth factor DNA. The genetic information was not only replicated but also transcribed and processed by the packaging cells. The growth of the cells was clearly increased by the integration of AKT1 into the cells with a significant p-value of $p \leq 0,016$ compared to the empty vector cells. Interestingly these cells were not slowed down by the expression of IGF2. We could not further elucidate on the reason of this phenomenon. One could assume that the slowing effects IGF2 were antagonized by the growing stimulation of the 3T3 cells themselves. Or maybe the concentration of IGF2 in the cells exceeded the growth factor threshold step (s. below) and reached an amount that stimulated all receptors, first of all the Insulin- and IGF-1-receptors.

We didn't perform further investigations on this circumstance because this cell type was not of interest for our study and even more important, because of the high security classification of those cells (S2-level), expressing high levels of infectious human oncogenic virus particles.

4.2.3. Target cells

The proof of the vector integration into the genomic DNA of the target cells was carried out the same way as it was performed for the producer cells. All plasmids could be detected by their specific bands in the PCR-Product gel electrophoresis. Amplified with the corresponding primer sets they could clearly be identified in the genomic DNA of the target endothelial cord blood cells.

4.2.3.1. Proof of IGF2 Transcription (mRNA/cDNA) in the transfected target cells with PCR and RT-PCR

The next step was to follow the process of cellular protein synthesis downstream, that meant proving the genomic DNA to be transcribed into a functional mRNA copy. After elution and processing of the mRNA into cDNA, we could proof the presence of the desired transgene growth factor DNA specific by the corresponding primer pair. Afterwards, to analyze the amount of Insert DNA that was produced by the target CBEC we performed a RT-PCR with new primers. Because of the assay of the RT-PCR cycles, new primers had to be used and the resulting DNA strand must not be longer than 200 basepairs to ensure fast and accurate amplification by the Taq-Polymerase. The results were encouraging as IGF2 was expressed nearly 240 times stronger in the transgenic cells compared to the parental CBEC. The genetic alteration of the target cells was considered as effective and reliable, because comparable results were gained from all the cell lines. Unfortunately this did not result in the desired stimulation of the cellular growth behavior as we hoped it to be (s. 4.3.1.).

4.2.3.2. Proof of transcription of AKT1 and ANG1

AKT1 and ANG1 were also analyzed to compare the transgenic growth factor mRNA to the native cells. Because we examined these growth factors not as intensive as IGF2, we transfected only several cultures of one cell line. The results should lead to other studies in the future. The genetic transfection process could reliably and reproducibly be established as for the IGF2 insert. The target cells showed significantly increased amounts of AKT1 and Ang1 mRNA in the cytoplasm. AKT1 was approximately 50 times higher, ANG1 even a hundred times higher.

Interestingly all the empty vector cells showed higher amounts of the analyzed growth factors. This might be the consequence of the empty vector DNA or it could be a result of the transfection process. However, it was not statistically significant and we therefore did not further investigate on this fact.

4.2.3.3. Proof of protein translation by the target cells

To complete the cellular protein synthesis cascade analysis, we had to perform a search for the complete, working protein in the cytoplasm of the target cells as well as in the supernatant that was produced by the CBEC. For our study, we had to use a commercially available ELISA-IGF2 Detection test for in-vivo-use, no in vitro test system was available at that time . The test did recommend a specific protein extraction step to minimize side effects caused by other proteins. The ELISA could also be carried out without this step and in the pretest phase we compared the results as it was recommended. Repeatedly, this step did clearly decrease the performance of the test, resulting in minor protein amounts and a lower test sensitivity. Furthermore, the test did neither produce any false positive values, even without the extra cleaning step. Therefore, the final analyzes were carried out without it.

We were finally able to detect 9-11 times higher concentrations of IGF2 protein in the overexpressing CBEC than in the untreated control cells. But this is definitely less than the cDNA results implemented. Why the amounts of mRNA and working protein differed is not clear. First of all there may be bias faults in the tests itself. Also the protein production out of the translated mRNA is regulated and controlled by the cell so that the cell might downregulate its IGF2 processing and amount.

Unfortunately we were not able to detect the protein in the Western Blot, most likely because of methodical problems. IGF2 has a very problematic molecule size of 7,5 kD which is difficult to detect with normal methods because it is too small for normal detection. We therefore tried the dot-blot technique (54), but disappointingly without reliable results. The detection limit for our Western blot assay was about 2ng for the amount but, more important, approximately 10kDa for the protein size. Because the ELISA showed good and reproducible results, we did not continue developing a functional western blot for the CBEC-IGF2 assay.

4.2.3.4. IGF2 supernatant Elisa

We examined the cell lysates as well as the cell supernatants, but in repeated ELISA checks, we did not detect a significant amount of IGF2 Protein in the cell supernatant. The reason for this is not clear. It maybe due to a missing exclusion sequence in the coding sequence so that the IGF2 protein is not excluded out of the cells. Interestingly, the M6P-receptor as IGF2 receptor is situated mostly in the cytoplasm of the cells and perhaps all protein is absorbed and degraded before exclusion. We could not clearly prove the reason for the fact that the IGF2 protein was not secreted by the cells. The coding sequence of the protein was cut out of the delivering vector in one piece and no part was missing in the full line DNA sequencing. Maybe the exclusion processing information was not integrated in the delivered CDS. The alignment database search for the CDS and the DNA sequencing products did not elucidate the nature of the problem, because the part of the gene responsible for externalization was not identifiable in our DNA sequence.

4.3. Consequences of the genetic alteration

4.3.1. Growth

With the results shown before, it becomes clear, that the IGF2 overexpressing cells did not grow faster, as intended when the study was designed, but slower. That effect puzzled us at first and we changed the further process of the experiments to elucidate the reason for this unexpected behavior. In this chapter the following chapters will be summarized: cell growth, external IGF2 stimulation, IGF2 translation proof and some Coculture aspects, to explain the contradicting IGF2 Growth factor effects that we observed in our assays.

First of all, in all growth curve assays, as well as in the Coculture assays, the IGF2 overexpressing endothelial cells did all grow slower than the untreated control cells of the same origin and cell line. This effect contradicts the in vitro effects that were in example observed by Bar et al. (56, 57) in stimulating cell cultures and that were considered when the study was planned. The assumption was that IGF2 should, as IGF1 does, stimulate the Insulin-receptor and the IGF1-receptor. This should have lead to an increased cell growth by the IGF2 overexpression instead of a decrease of those parameters. We could prove this effect by externally stimulating our untreated endothelial cord blood cells with different amounts of IGF2 protein. The assay and the effects are shown in chapter 4.3.1.1. But interestingly the IGF2 overexpressing cells did survive longer in the cellular growth assays than their empty vector controls. In most assays the cell growth curves were ended because the pLXSN empty

vector or the parental cells went apoptotic, but there were always IGF2 positive cells left. They had duplicated less so one can guess that their telomeres were eventually still long enough, but with all the facts gathered about the cells, it is rather another prove of their increased ability to survive. There may be various reasons for this fact and probably all of them may summarize to the observed effects:

4.3.1.2. Growth factor threshold theory

As shown and explained by Zandstra et al. (31), growth factors that are overexpressed or added to cellular stem cell colonies do have a critical level of concentration that their effects depend on. If the ligand to receptor interaction is lower than a certain amount, the cellular response can decisively change. In our case, this might be one aspect of the changing from proliferation to growth restriction. The most important part of this alteration would probably take the fact that, IGF2 binds to very different receptors. First of all in physiological concentrations minor to 50ng/μl, it binds to the Mannose-6-phosphat-receptor, exactly the cation-independent isoform (50) to which it has the highest affinity (for further information on this receptor see corresponding chapter). The effects of an activation of this receptor are very different to the ones of the IGF1- and Insulin-receptors. It slows down the cell cycle by expressing TGFB1 and CREG and this explains the peculiar effects of IGF2 stimulation with lower intracellular concentrations.

Receptor	Relative affinity for hormone		
	insulin	IGF1	IGF2
IR-A	1	0.002	0.3
IR-B	1	0.002	0.03
IGF1R	0.01	1	0.3
IGF2R	<0.002	<0,002	1
IGF1R / IR-A	0.1	1	0.5
IGF1R / IR-B	< 0.01	1	0.15

Table 17: Receptor affinities of IGF2 (35)

When added to a cell culture of responsive cells in very high concentrations over 100ng/ml, the binding of IGF2 is less specific and more of it can bind to the IGF1-receptor and further more to the Insulin-receptor, which both stimulate cell growth and proliferation. This fact is one explanation, why, as our study was planned, most reports of IGF2 effects showed a clear growth stimulation, e.g. the findings of Zhang et al. (41), because they were observed while IGF2 was added externally into the cell cultures in very high doses and often combined with other growth factors such as SCF (stem cell factor (a c-kit ligand)).

4.3.1.3. Possible transfection process induced cell damage

One important point of limitation for all our findings is that all the cells had to be selected for positive transfection with the help of the G-418 selection process. This part of the cell culture might have had an impact on the cell's growth capabilities and viability. As the growth curves show, the empty vector cells had reduced growth potential when compared to the native parental cells. In most cultures, they were still significantly better than the IGF2 cells, but there might be a slight damage, produced by the g-418 selection process. Therefore we compared all the results in the statistical analyze of the altered cells with the untreated native ones as well as with the empty vector cells that underwent the same selection process, to get reliable statistic data. In detail the empty vector cells performed poorer than the parental untreated cells in nearly any assay that was linked to the cell viability in any circumstance and the most common reason is the assumption of a selection induced cell damage.

4.3.1.4. Cell Growth for AKT and Angiopoetin-1

The overexpression of Angiopoetin-1 did reduce the proliferation of the cells as shown in the growth curve in the Appendix. The cells did grow a little bit faster than the IGF2 cells but died a lot earlier than all the other cells. Statistically there was no significant difference in the growth behavior between the Angiopoetin and the IGF2 overexpressing cells ($p\text{-value} \leq 0.95$). So those results were rather disappointing, but the AKT1 overexpressing cells performed much better. They had the best growing capacity of all cells that underwent the selection process, with highly significant growing advantage versus the IGF2 overexpressing cells ($p\text{-value} \leq 0.005$). But despite their very good growth compared to the other transfected and Geneticin-selected cells, they did not reach the growth of the untreated parental cells. This fact strengthens the assumption that the Geneticin selection process did affect the cells and their capability to grow. But the assays cannot be performed without it and therefore all analyzes always had to be compared to the empty vector cells (pLXSN), to which the AKT1 cells had highly significant advantage in the cell growth ($p\text{-value} \leq 0.02$). Further experiments with the established AKT1 overexpressing cells were performed in the Coculture assays.

4.3.2. Cell survival

4.3.2.1. Cytotoxic stress

First the cells were confronted with G-418 Geneticin cytotoxic agent, which represents their integrated, vector coded resistance for the selection process. Therefore the results of this test are not absolutely valuable, because the effects of genetic alteration by the integrated growth factor genes could interfere with the ones from the plasmid resistance code. But it was used for a first evaluation of the assay and later on for a comparison with further tests. In the corresponding growth curve there was a slight advantage of the IGF2 overexpressing cells first of all in the high dose assay with 1600 μ g/ml, but in the statistical analysis with the SPSS software, there was no significance in this difference. Even with two more assays we could not prove a significant difference, mostly because of the small cell number that survived the assay.

4.3.2.2. Cell survival under Growth factor restraint

Under the lack of the growth factor mix, that was normally added to the cell culture with the EBM-Media, the cells were clearly affected in their growth and survival. We assumed that the overexpression of the internal IGF2 protein would clearly increase the capability of these cells to survive the lack of other growth factors. And they did, but despite the fact that the IGF2 cells did reduce their population less than the other cell lines, this effect could not be proven to be statistically significant. This might be caused by the fact that the IGF2 pos. cells have in all cell cultures a very slow growing behavior and therefore the differences are harder to detect. Furthermore, we guess that the effect of the IGF2 as single growth factor in the very strong mix of stimulating factors in the EBM Media is too small to make a significant difference when compared to the lack of the other powerful growth factors such as VEGF, Insulin, IGF1 and others. The endothelial progenitor cells were probably too much depending on the correct growth factor substitution to be able to grow with IGF2 alone.

4.3.2.3. Cell survival under nutrient restraint

The statistic surviving analysis of the nutrient restraint was desperately not significant as the other stress assays described so far. But we found another very interesting aspect of the IGF2

overexpression: The parental and empty vector cells did form network structures when cultured under nutrient restraint as previously shown by Peters et al. (27). Interestingly, the IGF2 pos. cells did not form any kind of network structure. In 3 repeated culture assays, we could clearly prove this effect. It is very hard to say why these cells did not show this reaction. Interestingly, the IGF2 pos. cells did also form less tubular structures in the Coculture assay and the reason might be an IGF2 induced reduction of the capability to differentiate. The cellular program seems to be pushed into the direction of self-renewal rather than differentiation.

4.3.2.4. Cell survival under ultraviolet irradiation

To analyze the cell survival time that we have examined for the IGF2 pos. CBEC in our assay, it is helpful to explain the way the UV-Irradiation damages the cells. The ultraviolet irradiation is especially dangerous for the cell because of the wavelength of its light waves. It interferes with the molecular ring of the Thymine-basepairs of the DNA and their molecular structure absorbs the energy of the light wave. Because of the wave characteristics of the light, it deploys its energy to structures that have approximately the dimensions of the amplitude of its wave. This effect is called harmonic resonance. What happens is that the Thymine molecules are activated and one molecule links to another by bridging. The effect is the so called bulky DNA with Two pairs of Thymine molecules linked together. If the DNA is replicated or transcribed, the DNA-Polymerase is not capable of reading over these molecules and has to stop. The replication and transcription cannot be continued. These defects can be repaired by the nucleotide excision repair system, which cuts out those linked basepairs. But if the amount of damages exceeds the repairing capabilities of the cell, they cause severe cell damage by stopping the transcription and reproduction of the DNA, leading to multiple mutations and ending in apoptosis (32, 33).

The ability to survive damages like this is mainly depending on the antiapoptotic and repairing abilities as well as the speed of proliferation of the cell. If the cell's doubling rate is low, it has more time to repair those damages and the cell may survive longer. This is one aspect why the overexpression of IGF2 should lead to a longer surviving period compared to the native untreated cells.

And that was exactly what our repeated assays have shown. The IGF2 overexpressing cells had highly significant statistical results for an increased surviving ability compared to all empty vector and parental cells.

Interestingly the AKT1 pos. cells, expressing a highly oncogenic gene, had also improved surviving abilities in this assay. The reason is probably the increased level of antiapoptotic proteins in the cell that is caused by the AKT1 activation (s. above), but they did not exceed the IGF2 pos. cells.

Our theory about the IGF2 overexpression effects had its next prove: IGF2 overexpression improves the cell survival after ultraviolet irradiation.

4.3.3. Cell stimulation

4.3.3.1. External IGF2 stimulation

The stimulation of the untreated parental cells with externally added IGF2 protein into the cell culture media led to the typical morphological changes as the cells became greater and decisively dysmorphic. The effect we observed with our genetically altered cells was proven to be IGF2 induced. Even more important, we could prove that the effects of the IGF2 growth factor stimulation depended on the amount of IGF2 that the cells were exposed to. As we assumed concerning to the growth factor threshold theory (see 4.3.1.2), the cells reduced their duplication and growth at concentrations lower than 100ng/ml. At concentrations of 25ng/ml, the cells grew slowest. This amount of growth factor, as we later found out in the ELISA tests, is at the same level of IGF2 amount that we achieved with our genetic overexpression. Because of these correlations and the amount of the IGF2 protein in the ELISA, we stated that this amount of IGF2 was either stimulating the IGF2-receptor more than the IGF1-receptor or it was lower than the stem cell growth factor threshold, or maybe both.

4.3.3.2. TGFB1 Stimulation

As explained in chapter 4.1.3.1, the IGF2-M6P-receptor has TGFB1 as some of its main downstream targets. We therefore checked if parental cells were changed in comparable ways to the IGF2 stimulation / overexpression when they were incubated with high levels of external TGF β growth factor.

The cells reduced their growth comparable to the IGF2 overexpressing cells. The higher the concentration of TGFB1, the slower the cells grew (with high statistic significance $p \leq 0.05$). But the cells did not alter their look in the specific way the IGF2 overexpressing cells did. So we can state that TGFB1 might be one of the main factors concerning the growth

reduction caused by an IGF2 overexpression, but there must be more factors participating in the altering of the cells. This could be a very interesting subject for future studies.

4.4. Coculture

4.4.1. Cell growth and building of a multilayer cell compound

As explained in the results chapter, we were, after having established a functional protocol for the Coculture assay, reliably able to gain the desired multilayer cell structure with the original cells (HUVEC&Fibroblasts) as well as with our CBEC. Remarkably, this so called sandwich layer showed to be essential for the formation of the desired tubular endothelial structures, mainly because of its decisive function for the cell interaction with mutual paracrine stimulation of the different cell types. A photograph of this multilayer cell architecture is shown in the appendix.

Interestingly, we did not receive any multilayer cell compound in the assay with our Human vein stromal precursor cells (HVSC). These cells, despite being the progenitor cells of the fibroblast cells did not form any sandwich layer. And as explained above, no tubular structures were produced by the HUVEC that were embedded into the HVSC. The HVSC were not stimulated to differentiate into fibroblasts or equally functioning cells neither. Nor were they producing any kind of tubular structures when incubated with fibroblasts. So we couldn't gain any conclusion whether the HVSC are able to differentiate into fibroblast in such an assay, nor could we analyze their cell interactions. Even the AKT1 overexpressing HVSC that we had cultivated didn't work in this assay.

4.4.2. Tubuli formation

The tendency of the IGF2 overexpressing cells to develop cluster like structures rather than tubular ones was obvious as shown in the results chapter. It might be caused by the suggested fact that the IGF2 overexpression did reduce the CBEC's ability to differentiate as well as their ability to grow. As shown above, these cells also did not form any tubular network when put under nutrient restraint as did the corresponding empty vector cells (see 4.3.2.3). In conclusion it seems likely that the cells were clearly inhibited in their tendency to differentiate into functional cells. But after all, they did form some tubular structures that were comparable to the other cell lines and were analyzable.

Furthermore, the CBEC did all produce less tubuli than the HUVECs. This might be a consequence of their cell nature. Importantly the empty vector cells did perform poorer than the untreated parental control cells of the same age, which might be a result of the retroviral selection process with high doses of toxic substance such as Geneticin (G-418) as it became obvious in many other assay before (see above, e.g. cell growth).

4.4.3. Tubuli quality parameters: Length, Thickness, Crossing/Sprouting

4.4.3.1. Length

First of all, the average length of the tubular structures is even a better marker of the vasculopoetic potential of the investigated cells than the number of the produced tubular structures. This fact isn't caused by a biological effect, but by statistic usefulness. The pictures of the culture dishes are better to analyze for their length with a program such as ImageJ (40) rather than the fewer numbers of tubular structures that are just counted per view. Next reason is that the statistical data quality is much better because the observer gains a higher amount of data and the data sets are more detailed, what makes it easier for the statistical analysis to check them for significant differences.

But nevertheless, the results of the cell comparison for the length of the tubular structures showed exactly the same results as the tubular quantity comparison: The HUVEC forming the longest structures, followed by the parental CBEC, then the empty vector cells and our IGF2 pos. cells producing the smallest tubuli ($p < 0,05$).

4.4.3.2. Thickness

Interestingly, this testing was the only one in which not the HUVECs performed best. The parental CBEC did produce the thickest tubular structures. But very important to mention is, that the thickness is no reliable marker of the vasculopoetic potential and should not be used or interpreted alone. It is very difficult to measure the exact wide and the differences are so minimal that all data gained by this method has to be used very careful. The structures are nearly lines and therefore their length is essential for the testing. The width has very high probability for a wrong measurement or even more likely a statistical bias with estimated differences that are not truly there.

4.4.3.3. Crossings/Sprouting

Much better to compare the vasculopoetic activity of the Coculture partner cells is their ability to build a real tubular network with crossings. This is a true physiological feature of the vasculopoetic process and represents a great part of the ability to maybe develop real vessels out of the tubular structure network in vivo. And as in the other assays, the HUVEC did lead the comparison of the number of crossings formed in our Coculture assays and the IGF2 pos. cells had the least of all.

4.4.3.4. Coculture summary

The tubuli formed by CBEC were less and shorter than the ones formed by the HUVEC. In the group of the CBEC, the parental, untreated cells had the highest activity in all parameters, whereas the pLXSN and IGF2 cells did produce significantly less tubular structures and even more important, shorter and thinner ones. Only the tendency of the IGF2 pos. cells to form cluster like structures rather than tubular like ones was obvious and significant.

V Conclusion and summary

As a summary we can state that the integration of growth factor DNA Codons into retroviral vectors is a very reliable way to transport and integrate genetic information into human cells. To establish a stable transfection system for altering human stem cells is, with some expertise and training, a fast and reliable way to modify the desired properties of the target cells. But if the effects of the integrated DNA information aren't clearly identified yet or contradictory, care must be taken, because the effects can turn the study upside down, leading into a different direction than initially planned.

The intracellular interactions and consequences are so complex, that they are hard to predict. Also a slight but important restriction has to be mentioned: We could clearly prove that the retroviral transfection process did affect the target cells. Probably the selection processes as well as the integration of a retrovirus into the cells itself did reduce the abilities of the cells to duplicate and grow. In the statistic analyzes, this effect has always to be controlled as a confounding parameter.

When we put all our facts about IGF2 overexpression together in some words, the conclusion is that retroviral induced IGF2 overexpression in endothelial progenitor cells slows down their cell cycle as shown above, which leads to less proliferation. On the other hand it improves the surviving abilities of the cells, for example by increasing the DNA repair systems and probably the cell cycle control mechanisms which in the end lead to a better cell survival when the cells are confronted to stress situations or long time incubation.

Furthermore, the IGF2 overexpressing cells are rather forced into the direction of self renewal than into differentiation. This effect has clearly been proved by the nutrient restraint assay and even more obvious in the Coculture assays, where the IGF2 pos. cells did gather in clusters, rather than differentiating into tubular vessel-like structures. To elucidate this phenomenon, more investigations on the nature of this effect and the cellular differentiation markers would be necessary to prove the mechanisms on the level of the cellular protein and gene expression profiles. This effect might be useful for the application when long-term maintenance of the cells is desired rather than differentiation. External IGF2 addition or, even more elegant, the retroviral transduction with IGF2 including a gene profile with an activation codon to be expressed or repressed depending on the presence of the desired activation substance could be an approach for longer periods of stem cell conservation or cultivation.

The findings for AKT1 were promising and did clearly prove the theoretic effects of an overstimulation with best growing and surviving abilities, but one has to keep in mind that

the cell with ultimate growing, renewing and surviving capabilities is a tumor cell! The task is, whether those cells keep their function and differentiation or not. Care must be taken with such powerful oncogenic factors and even more important their clinical use in vivo when we talk about stem cell therapeutics.

The Coculture assay is a promising and very interesting way to examine the vasculopoetic potential and behavior of vessel forming cell partners. It is reliable and after some adjustments, very useful and cheap. It should lead to further studies and applications concerning re- or neovascularisation and, as it was developed, tumor inhibition by restriction of neovascularisation.

Finally the examined CD34+ Endothelial Progenitor Cells have without a doubt a great feasibility for the use in clinical routine as candidates for a therapeutic revascularization if the existing problems with the reduced cell duplication rates are solved. First of all if cells from patients, suffering from cardiovascular diseases, typically aged fifty years and more, are used to regain peripheral or myocardial vascular and structural organ function. More studies on this chapter of regenerative medicine promise interesting and hopefully useful results.

Last to be mentioned is an explanation about my project: The core of this project was to establish and produce retroviral transduced IGF2 overexpressing CBEC for the transplantation into a rat model in a cooperating project with the “Deutsches Herzzentrum” Munich. This project is depicted in the results chapter. The cooperation did not perform well as the IGF2 positive cells did grow slow and contradicted the initial plan of the study to increase the growth of the CBEC. But because of this circumstance, our time and resources were too few to elucidate all interesting parts of the aspects we discovered with our IGF2 and AKT1 overexpression.

VI Appendix

6.1. Typical cell appearance:

Altered look of IGF2 positive cells:

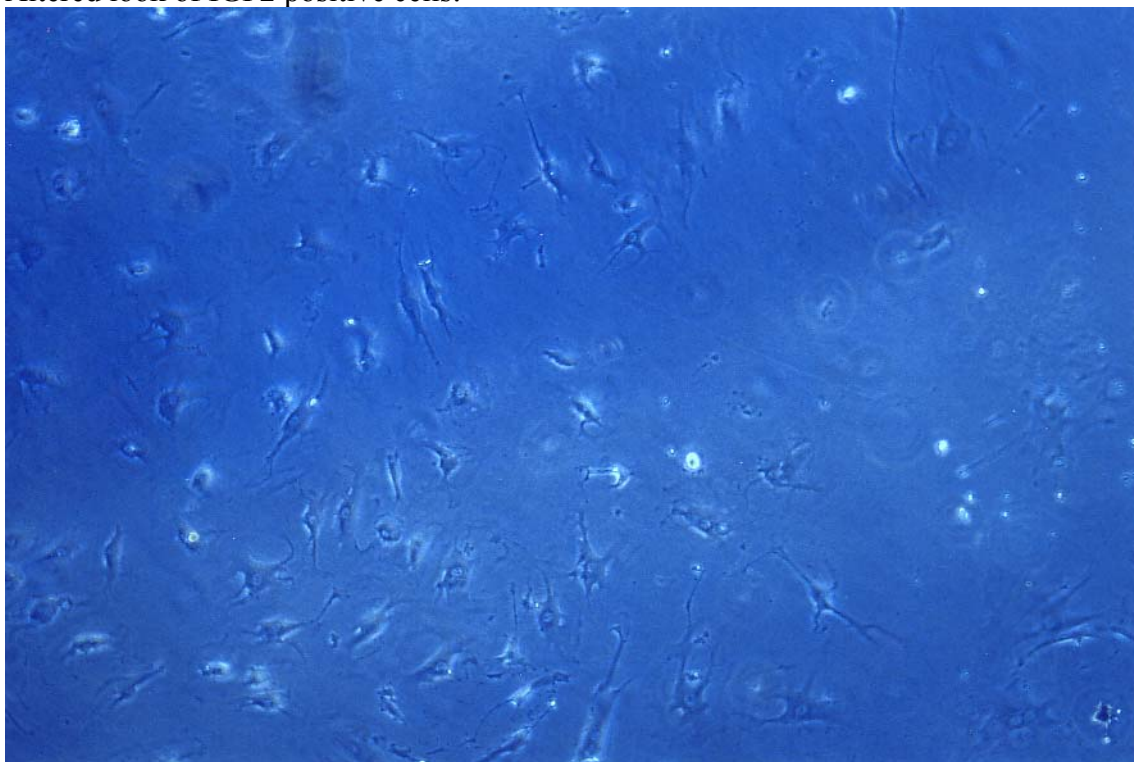


Figure 30: NB1591-94 IGF2 positive cells after 3 weeks of incubation with their typical appearance

Parental CBEC with the typical CBEC look, being of the same passage count/ age as No.1 above:

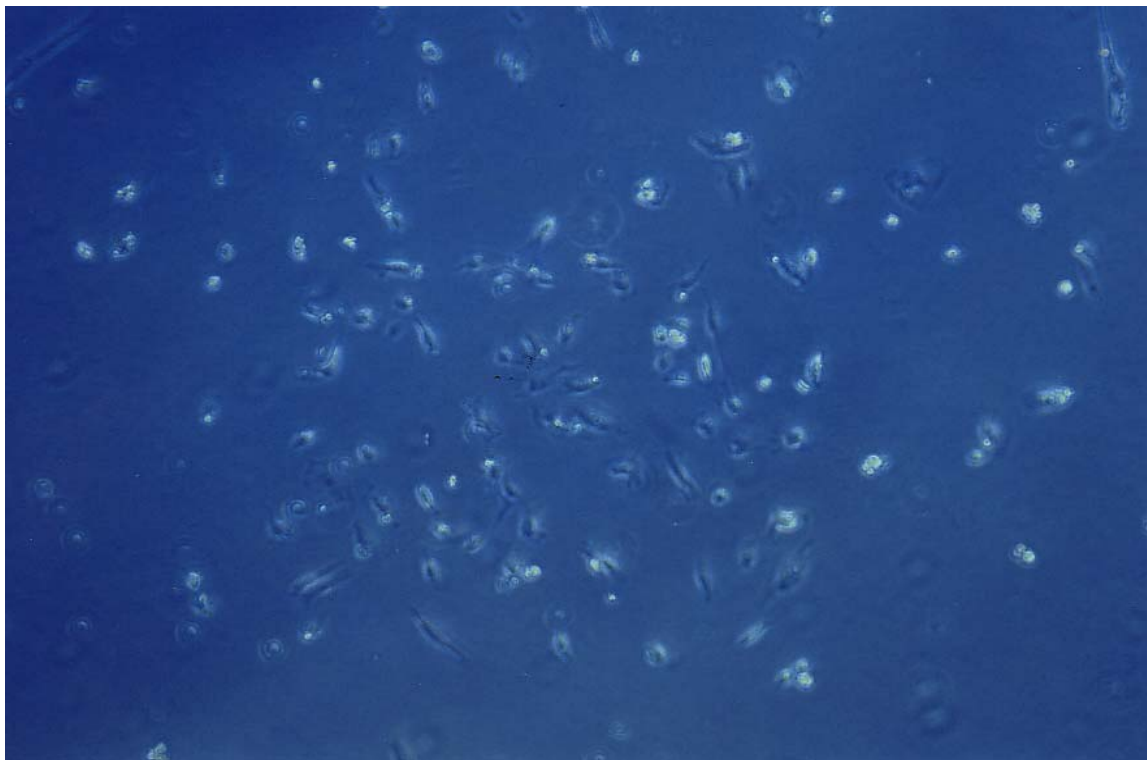


Figure 31: NB1591-94 parental untreated cells after 3 weeks of incubation time

6.2. Growth curves of the different cell lines:

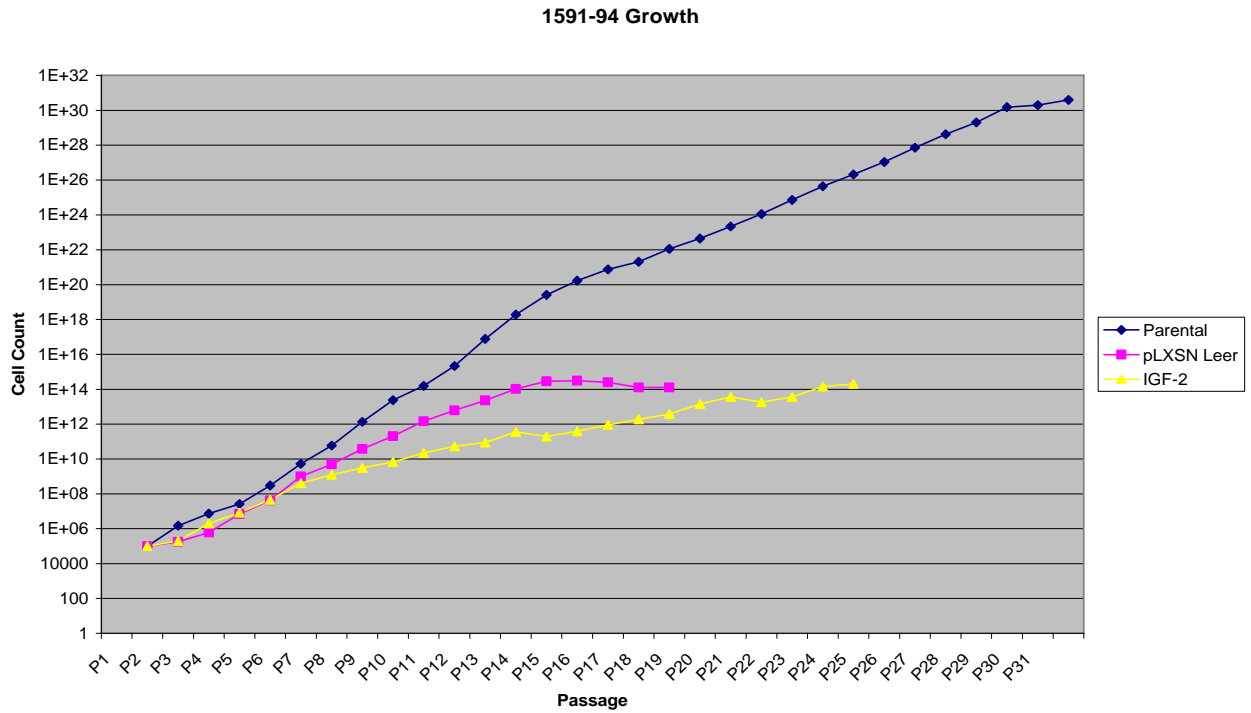


Figure 32: Growth curve for CBEC NB1591-94

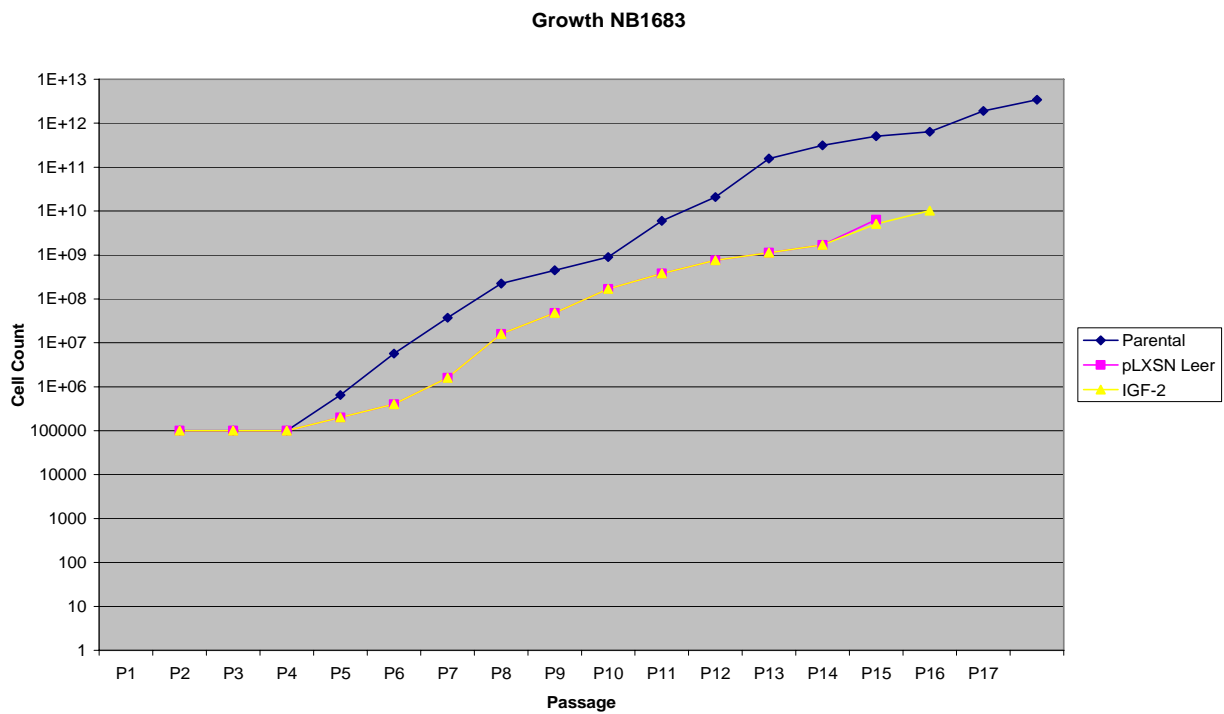


Figure 33: Growth curve for CBEC NB1683

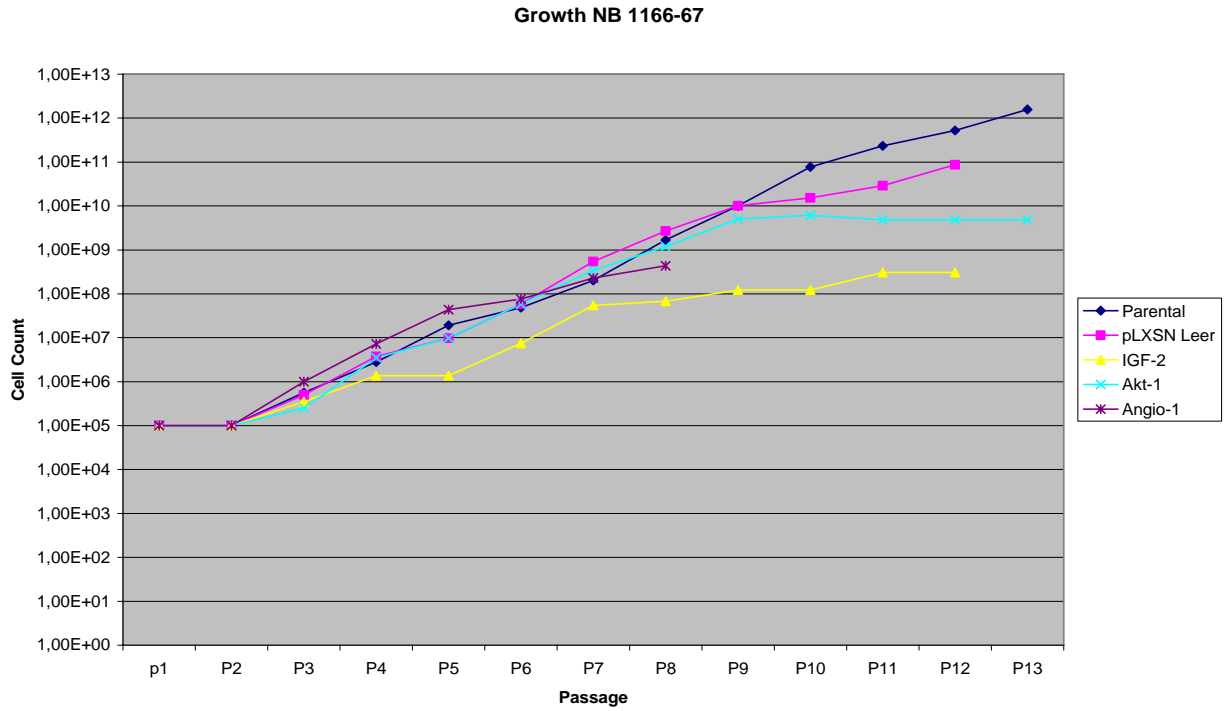


Figure 34: Growth curve for CBEC NB1166-67

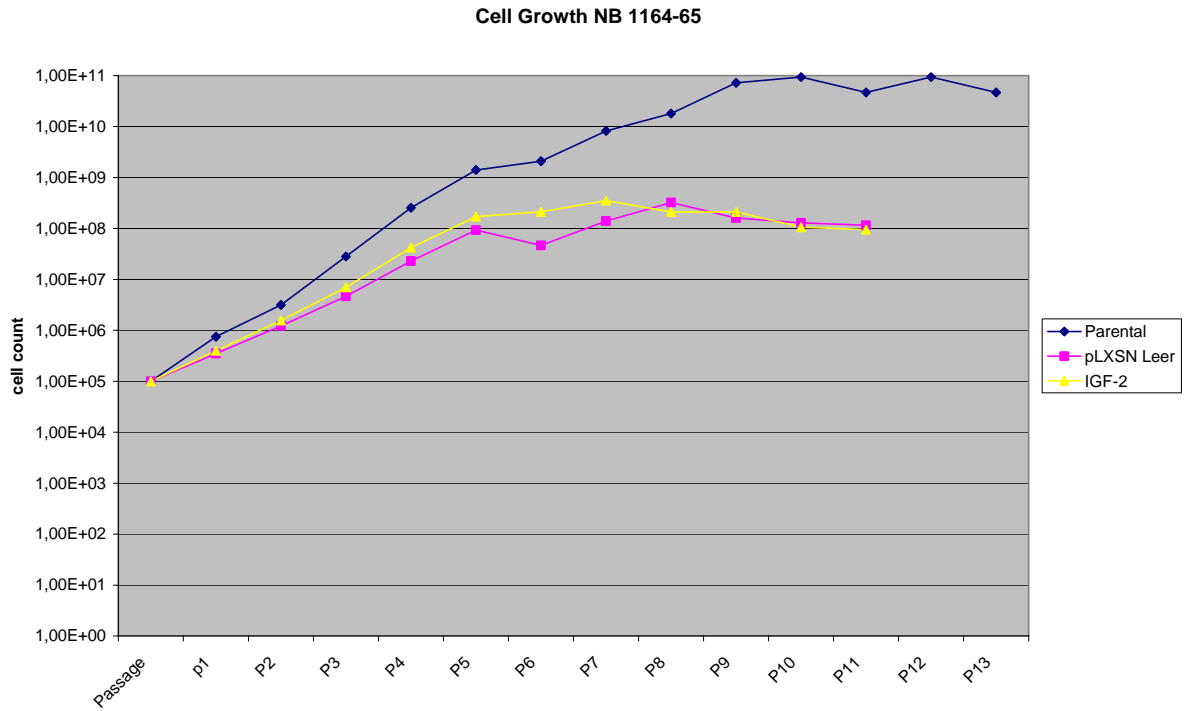


Figure 35: Growth curve for CBEC NB1164-65

6.3. Network formation of CBEC:

Picture tubular network structures formed under nutrient restraint by parental CBEC:

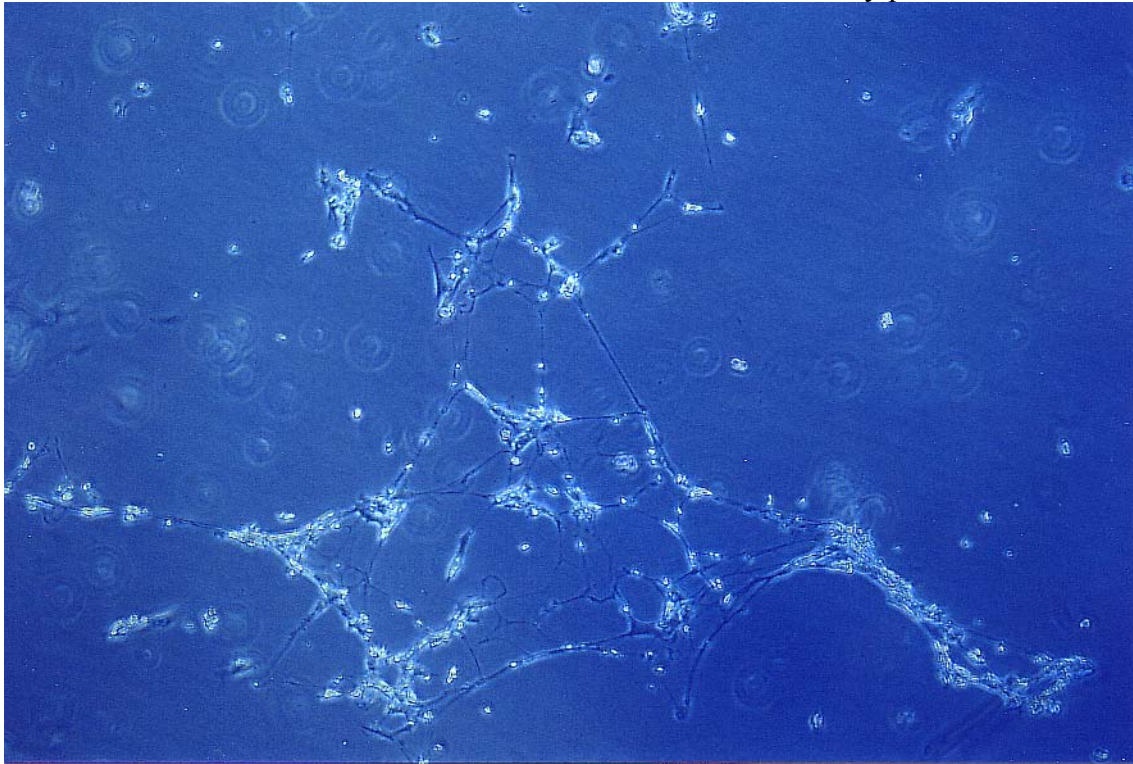


Figure 36: CBEC untreated forming tubular network under nutrient withdrawal

Picture Network structures formed under nutrient restraint by empty vector cells:

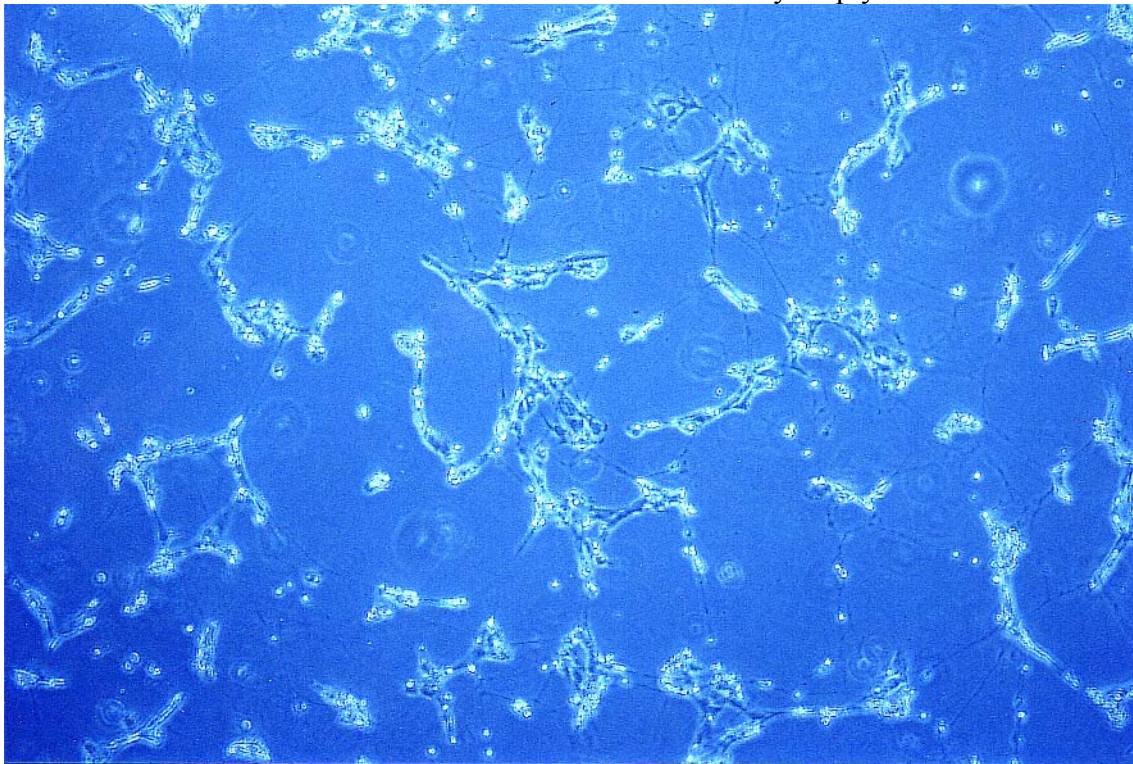


Figure 37: CBEC- pLXSN empty vector forming tubular network under nutrient withdrawal

6.4. UV-Apoptosis assay:

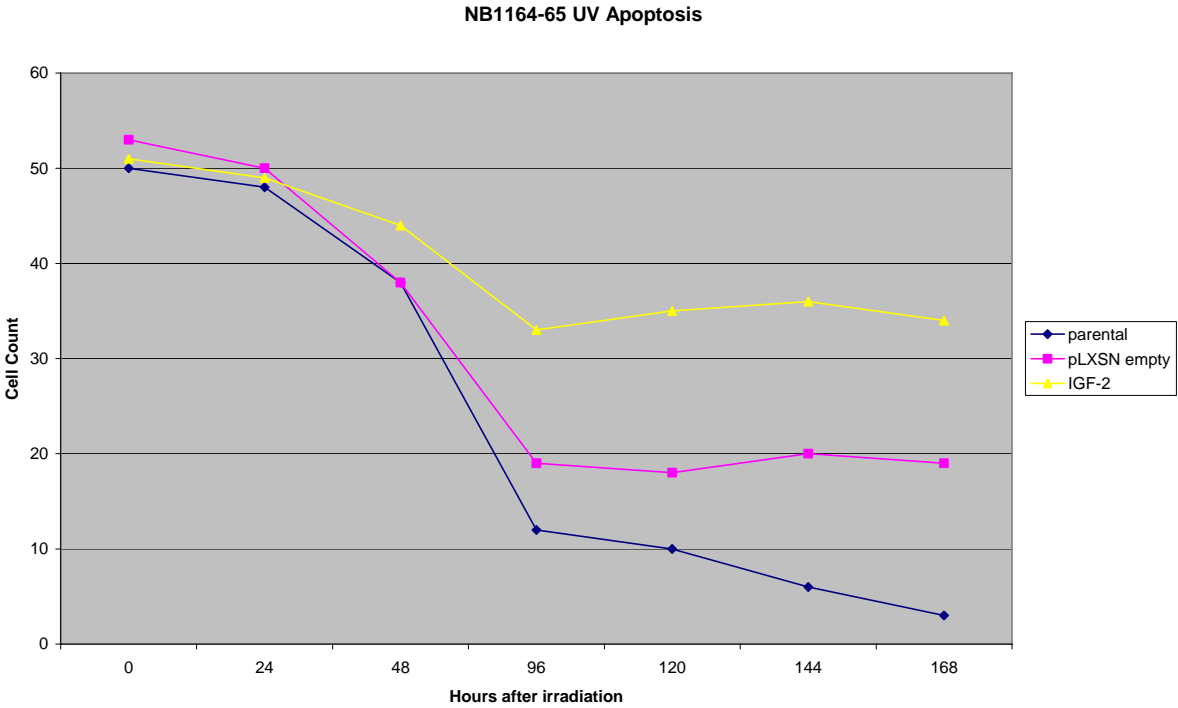


Figure 38: CBEC NB 1164-65 Apoptosis Assay with ultraviolet irradiation

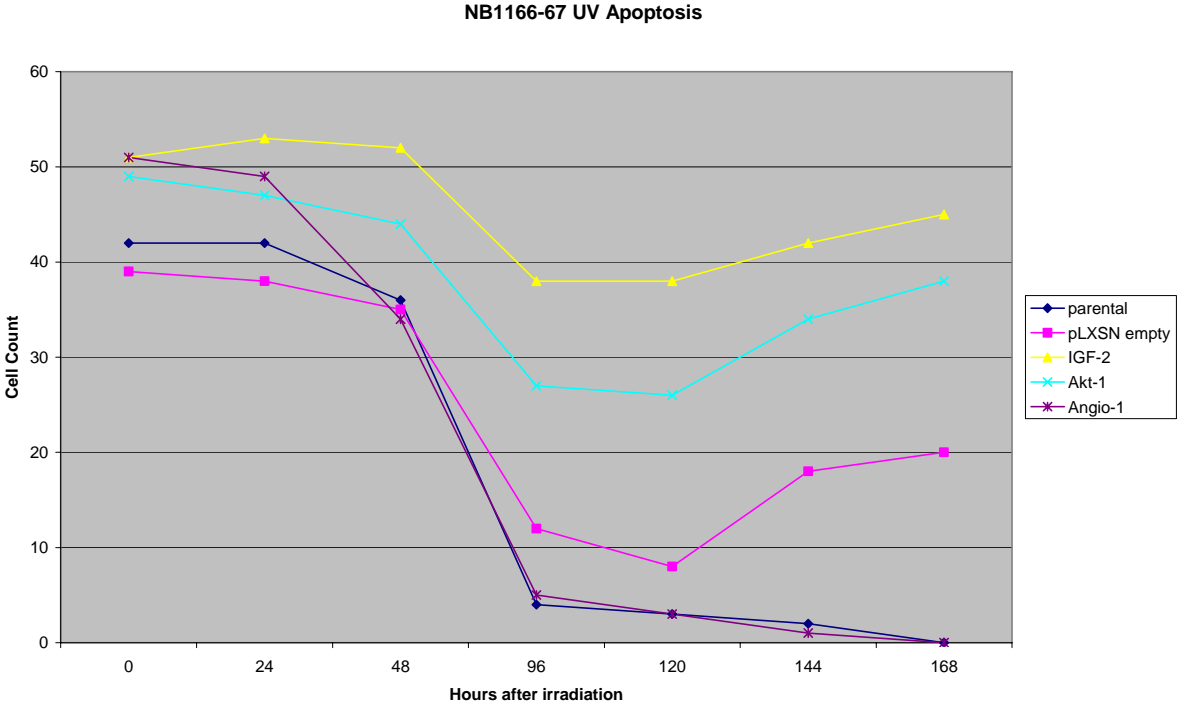


Figure 39: CBEC NB 1166-67 Apoptosis Assay with ultraviolet irradiation

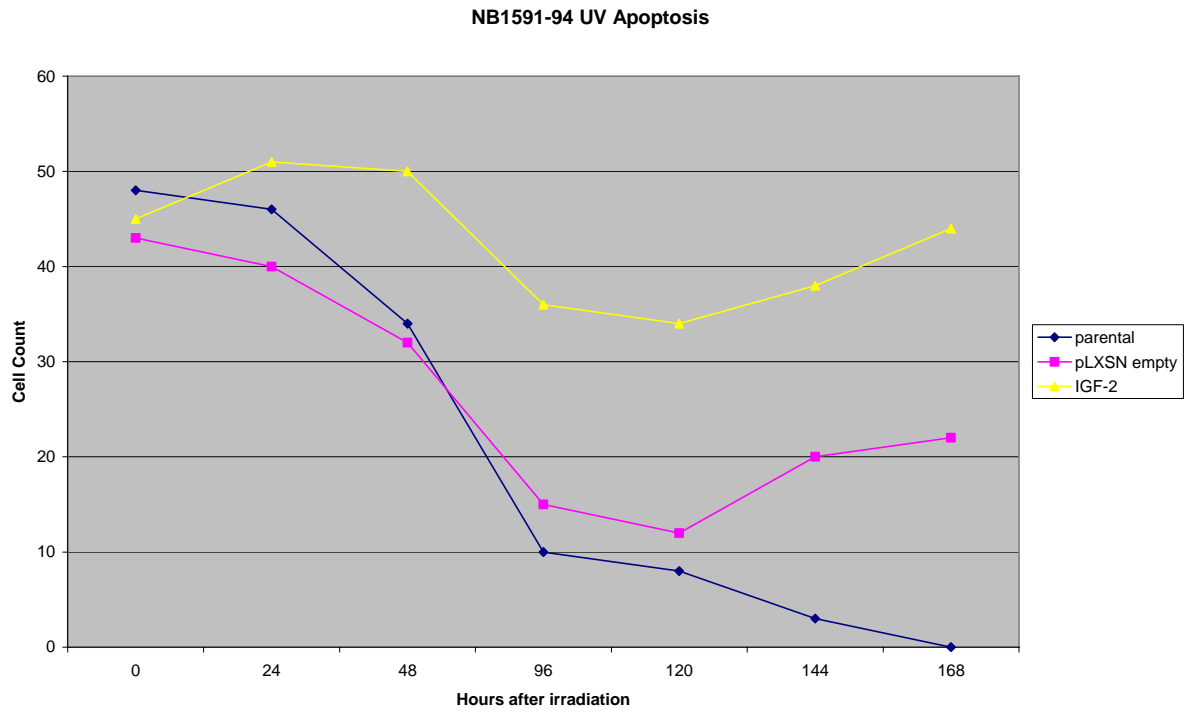


Figure 40: CBEC NB 1591-94 Apoptosis Assay with ultraviolet irradiation

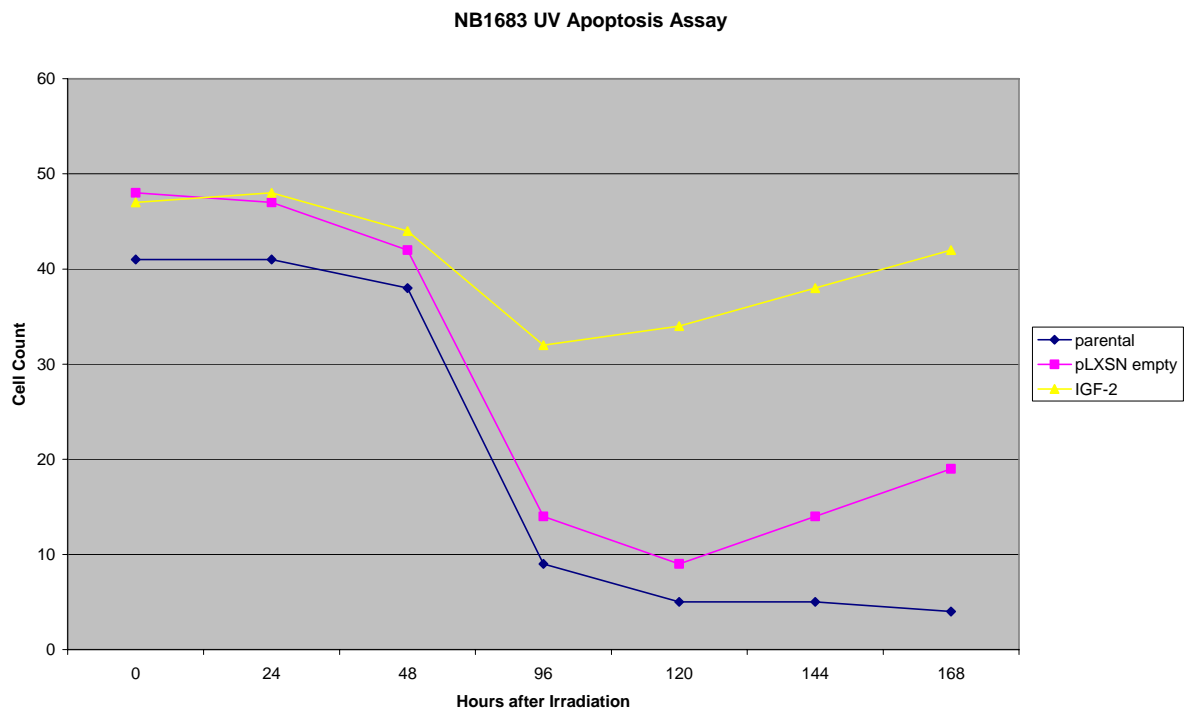


Figure 41: CBEC NB 1683 Apoptosis Assay with ultraviolet irradiation

6.5. Growth curves of the external IGF2 stimulation:

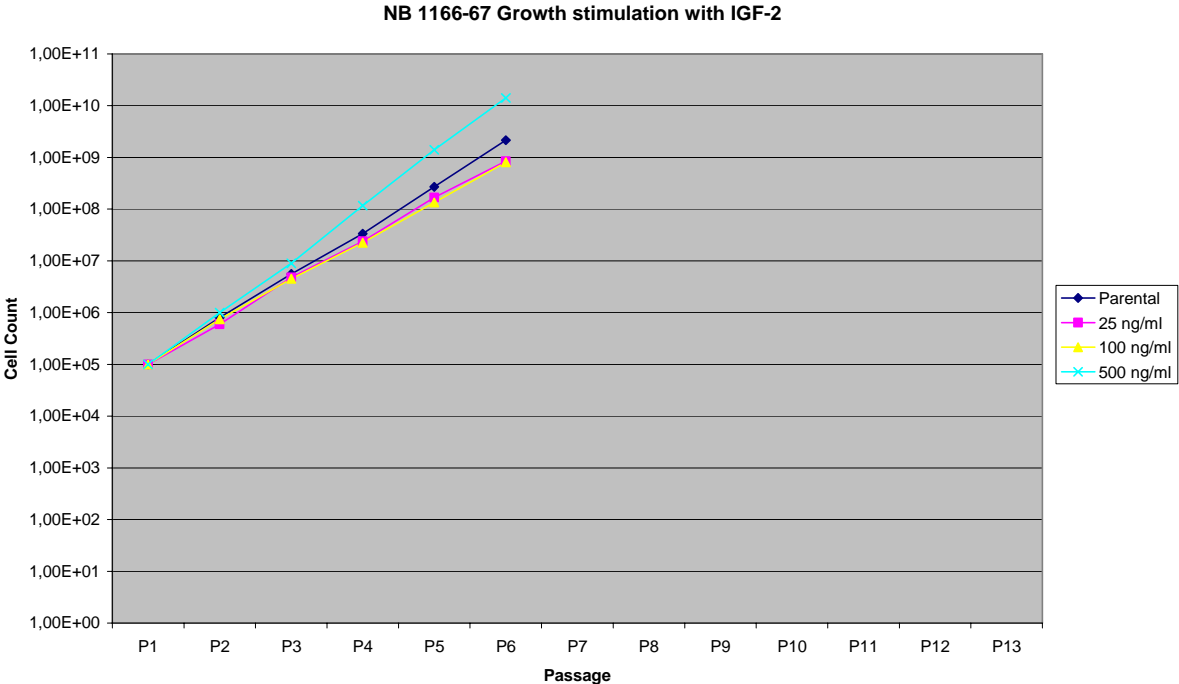


Figure 42: CBEC NB 1166-67 Growth stimulation assay with external IGF2 in different amounts

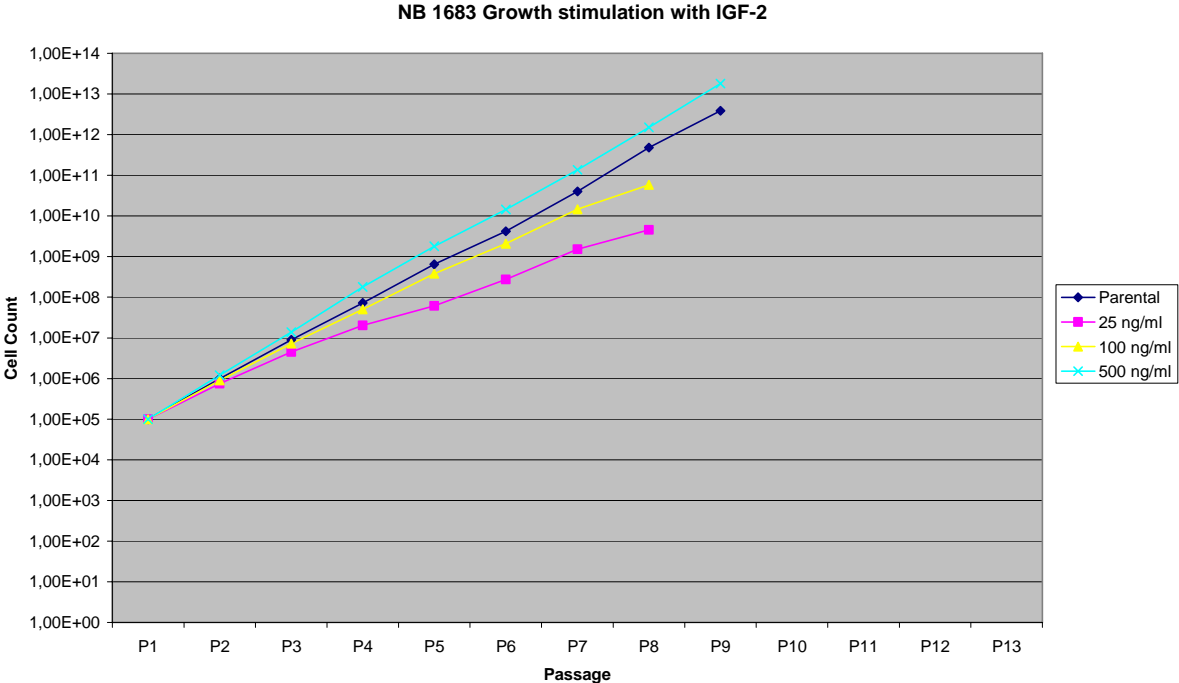


Figure 43: CBEC NB 1683 Growth stimulation assay with external IGF2 in different amounts

6.6. Coculture cell sandwich layer:

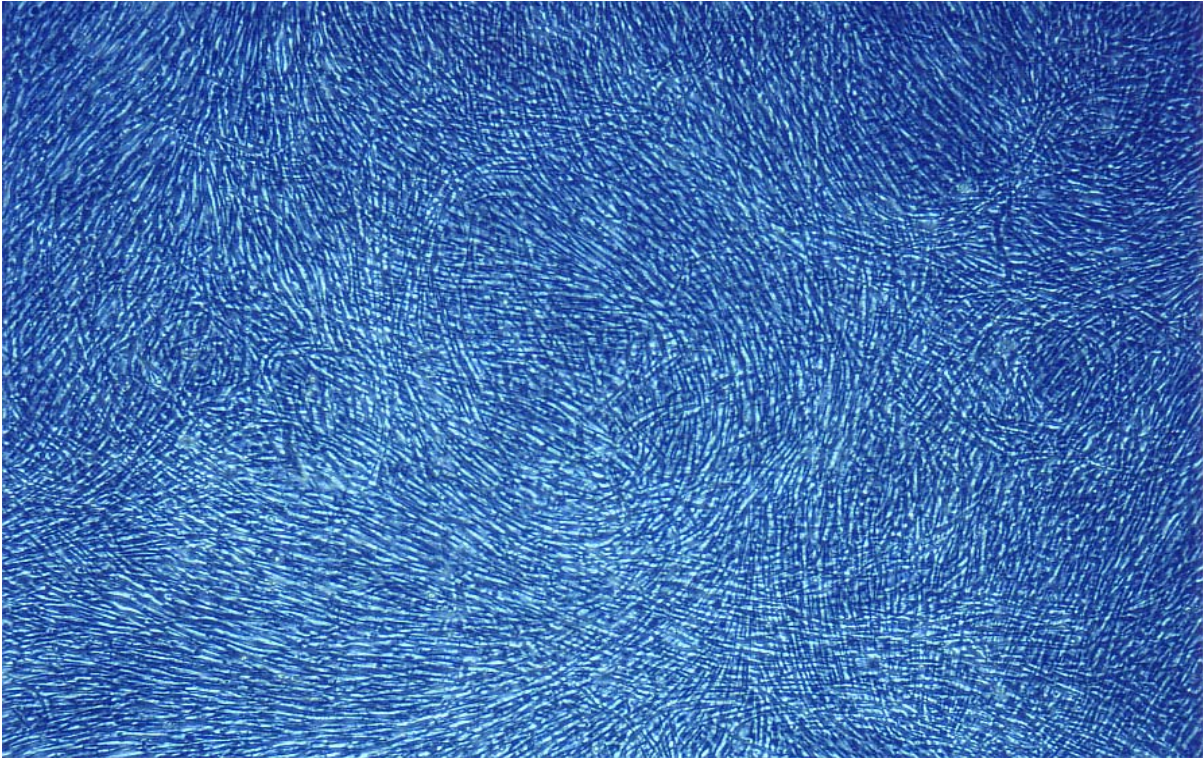


Figure 44: Coculture cell sandwich layer with HUVEC and fibroblasts after 1 week incubation

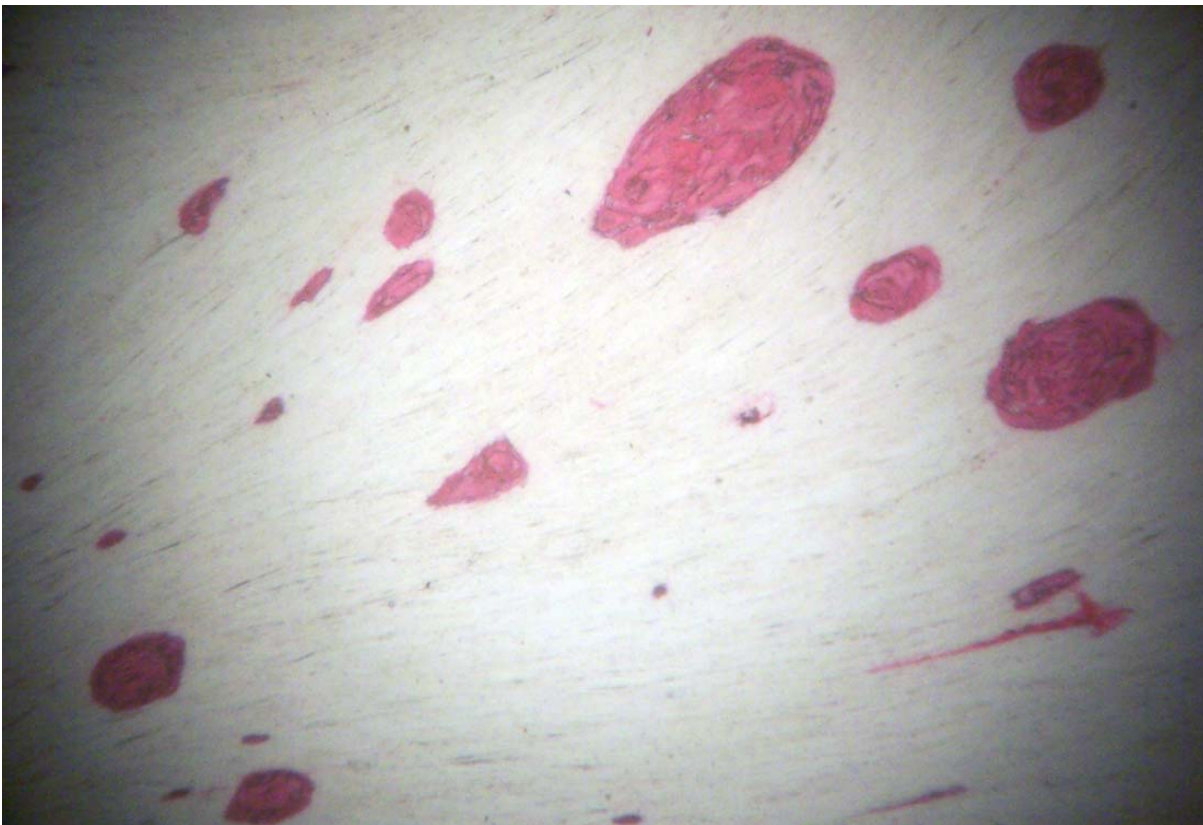


Figure 45: Cluster formed in Coculture by incubation of IGF2 overexpressing CBEC with fibroblasts



Figure 46: Typical Tubular structures built by HUVEC in the Coculture assay

VII Thanks

First of all I'd like to thank my wife, who always supported me and never criticized neither me nor the work, even as it took so much from our time and from my energy. The only consequence for her was to give me even more of her own energy, raising me up again every time.

Next I thank my parents, who supported me for all of my life unquestioned and absolutely reliable, reinforcing every decision I made without criticizing, even knowing that it could mean a hard time for their son.

My Sister and my brother-in-law, thank you for all your nice words, your support and your understanding. The words you wrote in my lab-book led me through a lot of dark hours when everything seemed to brake into pieces.

Katja, who made this whole work possible by working, explaining and supporting much more than she had to, spending lots of extra-hours in the laboratory and always taking care of our cells.

Robert, our head of the project, who always believed in what we did and never led me down, even when things went absolutely wrong, always supporting, always having a nice word and bringing up new resources and new thoughts. Following my opinion, one could not wish for a better lab chief.

All the other ladies in the laboratory thank you for all your help and support.

My emergency room team of the Hospital Munich-Pasing, starting my career, teaching me, showing me what medicine is about, what it takes to be a good physician and opening the gates to my medical future.

Many thanks to all of you,

Lest we forget!

VIII Literature

- 6) Aicher A, Heeschen C, Mildner-Rihm C, Urbich C, Ihling C, Technau-Ihling K, Zeiher AM, Dimmeler S.; „Essential role of endothelial nitric oxide synthase for mobilization of stem and progenitor cells.”
Nature Medicine 2003;9:1370-1376.
- 56) Bar, Richard S., Boes M., Drake BI, Booth BA, Henley SA; “Insulin, insulin-like growth factors, and vascular endothelium.”
American Journal of Medicine, 1988, Nov.29 ; 85 S:59-70
- 57) Bar RS, Siddle K, Dolash S, Boes M, Dake B.; „Actions of insulin and insulinlike growth factors I and II in cultured microvessel endothelial cells from bovine adipose tissue.” Metabolism. 1988 Aug;37(8):714-20.
- 53) Bishop Eileen T, Bell Graham T., Bloor Stephen, Broom I.J., Hendry Neil, Wheatley Denys N.; “An in vitro model of angiogenesis: Basic features.”
Angiogenesis 3;335-344, 1999
- 7) Conway EM, Collen D, Carmeliet P.; “Molecular mechanisms of blood vessel growth.” Cardiovascular Research 2001; 49, 507-21.
- 46) Dennis. P. A . and Rifkin. D. B.; „Cellular activation of latent transforming growth factor beta requires binding to the cation-independent mannose 6-phosphatelinulin-like growth factor type II receptor.” Proclamation National Academy Science. USA 88, 580-584.
- 41) De Souza. A. T., Hankins. G. R., Washington. M. K., Orton T. Co and Jirtle, R. L.; „M6P and IIGF2Receptor gene is mutated in human hepatocellular carcinomas with loss of heterozygosity. Nature Genetics 1995, 11,447-449.
- 42) De Souza. A. T., Hankins, G. R., Washington. M. K., Fine. R., Orton, T. C. and Jirtle. R. L. „Frequent loss of heterozygosity on 6q at the mannose 6-phosphatelinulin-like growth factor II receptor locus in human hepatocellular tumors.” Oncogene 1995, 10,1725-1729.
- 23) DNA Extraction Protocol (Stand 04.12.2006):
http://www.riedlab.nci.nih.gov/publications/2437.2337DNA_Prep_Adherent_cells.pdf
- 24) Dulbecco's-Media composition (Stand 03.08.2004):
<http://www.c-c-pro.com/Navigation/FI%FCmedien.html>
- 45) Duyang, H ., Shiwaku. H., Hagiwara. H ., Miura, K., Abe. T., Kato. Y., Ohtani, H., Shiiba. K., Souza. R. F., Meltzer. S. J. and Horii. A.; „The insulin-like growth factor II receptor gene is mutated in genetically un.stable cancers of the endometrium. stomach. and colorectum. Cal}cer Res. 57,1851-1854 (1997).
- 25) EBM-Media composition, Lonza Biosciences, PhD Mancestri, M. (Stand 30.06.2005):
http://www.lonzabioscience.com/Lonza_CatNav.asp?oid=510&prodoid=Endo-2media&noCK=Y

- 22) Donovan D., Brown N.J., Bishop E.T., Lewis C.E. ; « Comparison of three in vitro angiogenesis assays with capillaries formed in vivo. » *Angiogenesis* 4, 113-121, 2001
- 2) Ertl, G., “Störung der koronaren Mikrozirkulation“ out of Fölsch, Kochsiek, Schmidt, Pathophysiologie, Springerverlag, 03/2000, ISBN3-540-65782-7
- 21) GATC biolabs: <http://www.gatc.de>
- 10) Gehling UM, Ergun S, Schumacher U, Wagener C, Pantel K, Otte M, Schuch G, Schafhausen P, Mende T, Kilic N, Kluge K, Schäfer B, Hossfeld DK, Fiedler W. “In vitro differentiation of endothelial cells from AC133-positive progenitor cells”. *Blood*. 2000;95:3106-12.
- 3) Gefei Zeng, Sarah M. Taylor, Janet R. McColm, Nicholas C. Kappas, Joseph B. Kearney, Lucy H. Williams, Mary E. Hartnett, and Victoria L. Bautch; „Orientation of endothelial cell division is regulated by VEGF signaling during blood vessel formation“; *Blood*. 2007 February 15; 109(4): 1345–1352.
- 50) Ghosh Pradipta, Dahms Nancy M., Kornfeld Stuart; “Mannose-6-phosphat receptor: New twists in the tale.” *Nature*, March 2003, Volume 4; DOI:10.1038nrm1050
- 26) Gray Steven G., Yakovleva Tatiana, Hartmann Wolfgang et al. “IGFII enhances Trichostatin A-induced TGFβ1 and p21 Expression in Hep3b Cells.” *Experimental Cell Research*, 253, page 618-628(1999)
- 27) Statistics: Harms Volker Statistics-Book: Biomathematik, Statistik und Dokumentation, Harmsverlag, Kiel, 7. Auflage 1998 And: SPSS statistic software 2008 Version 15, SPSS Inc. Chicago, Illinois 60606
- 40) Image J, National Institute of health, <http://rsb.info.nih.gov/ij/features.html>
- 28) Ishibe M., Rosier RN., Puzas JF., “Activation of osteoblast insulin-like growth factor-II/cation-independent mannose-6-phosphate receptors by specific phosphorylated sugars and antibodies induce insulin-like growth factor-II effects.“ *Endocrinological Research*, 1991;17(3-4):357-66
- 12) Kawamoto A, Gwon HC, Iwaguro H, Yamaguchi JI, Uchida S, Masuda H, Silver M, Ma H, Kearney M, Isner JM, Asahara T.; “Therapeutic potential of ex vivo expanded endothelial progenitor cells for myocardial ischemia.” *Circulation*. 2001;103:634-637
- 58) Kaltz N., Funari A., Hippauf S., Delorme B, Noël D, Riminucci M, Jacobs VR, Häupl T, Jorgensen C, Charbord P, Peschel C, Bianco P, Oostendorp RA.; “In vivo osteoprogenitor potency of human stromal cells from different tissues does not correlate with expression of POU5F1 or its pseudogenes, *Stem Cells*. 2008 Sep;26(9):2419-24
- 18) Kemenes, Igo; *Biochemie Script der Vorlesung; Bunte Reihe*, 2000, page: 13,14,66,67
- 52) Knoelder Martina, Sitz Wiebke, Stein Andreas, Schurmann Maren, Seidl Stefan, Rümmler Marc, Peschel Christian, Oostendorp Robert, Ott Ilka ; “Overexpression Of

- Insulin-like Growth Factor-II In Expanded Endothelial Progenitor Cells Improves Left Ventricular Function In Experimental Myocardial Infarction.“ *Circulation* 2008 ;118 :S.497
- 13) Kocher AA, Schuster MD, Szabolcs MJ, Takuma S, Burkhoff D, Wang J, Homma S, Edwards NM, Itescu S.; “Neovascularization of ischemic myocardium by human bone-marrow-derived angioblasts prevents cardiomyocyte apoptosis, reduces remodeling and improves cardiac function.” *Nature Medicine* 2001;7:430-436
 - 35) Kohansky, Ronald A.; “Diabetes review for Endocrine Source.” Nov.4, 2002 <http://www.endotext.org/Diabetes/diabetes3/diabetes3.htm>
 - 60) Kunz-Schughart, L.A., Schroeder, J.A., Wondrak, M., van Rey, F., Lehle, K., Hofstaedter, F., Wheatley, D.N. „Potential of fibroblasts to regulate the formation of 3-D vessel-like structures from endothelial cells in vitro“. *American Journal of Physiology*, 2006; *Cell Physiol.* 290: C1385-C1398
 - 17) Liu T., Lai H, Wu W., Chinn S., Wang P., “Developing a Strategy to Define the Effects of Insulin-Like Growth Factor-1 on Gene Expression Profile in Cardiomyocytes“ in *Molecular medicine*, extract from *Circulation Research* 2001 ;88 :1231-1238
 - 11) Lin et al., 2000 : Lin Y, Weisdorf DJ, Solovey A, Hebbel RP. Origins of circulating endothelial cells and endothelial outgrowth from blood. *J Clin Invest.* 2000;105:71-7
 - 19) Löffler, Petrides, *Biochemie und Pathobiochemie* ; Georg Löffler und Petro E. Petrides, Springerverlag, 6. Auflage, ISBN : 3-540-64350-8 ; S.767-798
 - 20) Löffler, Petrides, *Biochemie und Pathobiochemie* ; Georg Löffler und Petro E. Petrides, Springerverlag, 6. Auflage, ISBN : 3-540-64350-8 ; S.851-852
 - 33) Löffler, Petrides, *Biochemie und Pathobiochemie* ; Georg Löffler und Petro E. Petrides, Springerverlag, 6. Auflage, ISBN : 3-540-64350-8 ; S.1130
 - 32) Löffler, Petrides, *Biochemie und Pathobiochemie* ; Georg Löffler und Petro E. Petrides, Springerverlag, 6. Auflage, ISBN : 3-540-64350-8 ; S.219-222
 - 36) Löffler, Petrides, *Biochemie und Pathobiochemie* ; Georg Löffler und Petro E. Petrides, Springerverlag, 6. Auflage, ISBN : 3-540-64350-8 ;S.770-780 und 1097-1100
 - 48) Löffler, Petrides, *Biochemie und Pathobiochemie* ; Georg Löffler und Petro E. Petrides, Springerverlag, 6. Auflage, ISBN : 3-540-64350-8 ; S.402
 - 49) Löffler, Petrides, *Biochemie und Pathobiochemie* ; Georg Löffler und Petro E. Petrides, Springerverlag, 6. Auflage, ISBN : 3-540-64350-8 ; S.751
 - 16) Mangi AA, Noiseux N, Kong D, He H, Rezvani M, Ingwall JS, Dzau VJ.; “Mesenchymal stem cells modified with Akt prevent remodeling and restore performance of infarcted hearts.” *Nat Med* 2003; 9:1195-1201.

- 38) Martin, Mary Beth ; Franke TF., Stoica GE., Chambon P., Franke T., Wellstein A., Czubayko F., List H.J., Reiter R., Morgan E.; “A role for AKT in Mediating the Estrogenic functions of Epidermal growth factor and Insulin-like Growth factor I .“ Endocrinology Vol 141, No12 ; 0013-7227/00/\$03.00, June 14, 2000
- 27) Murohara,T., Ikeda T., Duan J., Shintani S., Sasaki K., Imaizumi T.; Transplanted cord blood–derived endothelial precursor cells augment postnatal neovascularization.“ Journal of Clinical Investigation 2000 June 1; 105(11): 1527–1536.
- 59) O’Gorman David B., Weiss Jocelyn, Hettiaratchi Anusha, Firth Sue M., Scott Carolyn D.; “ Insulin-like Growth factor II / M6P Receptor Overexpression reduces growth of choriocarcinoma cells in vitro and in vivo”, Endocrinology 2002, Vol. 143, N. 11; 4287-4294
- 14) Ott Ilka, Keller, U., Knoedler M., Götze K.S., Fischer P., Urlbauer K., Rudelius M., Bubnoff N., Schömig A., Peschel C., and Oostendorp R.A.J.: Endothelial-like cells expanded from CD34⁺ blood cells improve left ventricular function after experimental myocardial infarction, *The FASEB Journal*. 2005;19:992-994. Article doi:10.1096/fj.04-3219fje
- 9) Peichev M, Naiyer AJ, Pereira D, Zhu Z, Lane WJ, Williams M, Oz MC, Hicklin DJ, Witte L, Moore MA, Rafii S.: Expression of VEGFR-2 and AC133 by circulating human CD34(+) cells identifies a population of functional endothelial precursors. *Blood*. 2000;95:952-8
- 43) Piao. Z .. Choi. Y .. Park. C .. Lee. W. J .. Park. J. H., and Kim. H. (1997). Deletion of the M6PIIGF2r gene in primary hepatocellular carcinoma. *Cancer Lett*. 120, 39-43.
- 51) PT 67 Producer cells: (Clontech K1060-D, RetroPack™ PT67 NIH/3T3-based packaging cell line of Clontech Laboratories Incorporate)
- 55) Qing Qiu, Jin-Yi Jiang, Michael Bell, Benjamin K Tsang, and Andrée Gruslin: “Activation of endoproteolytic processing of IGF1I in fetal, early postnatal and pregnant rats and persistence of circulating levels in postnatal life.” *Endocrinology*, doi:10.1210/en.2007-0535
- 1) Statistisches Bundesamt, Altersstandardisierte Sterbefälle im Jahr 2003 aus der Todesursachenstatistik, Heft 33, Abb. 2b, Themenhefte des GBE-Bund.
- 5) Rafii S, Lyden D.; “Therapeutic stem and progenitor cell transplantation for organ vascularization and regeneration.” *Nature Medicine* 2003;9:702-12
- 8) Rehman J, Li J, Orschell CM, March KL. Peripheral blood "endothelial progenitor cells" are derived from monocyte/macrophages and secrete angiogenic growth factors. *Circulation*. 2003;107:1164-9.
- 4) Risau W.; “Mechanisms of angiogenesis.” *Nature* 1997; 386, 671-4
- 34) Sigma-Aldrich Inc.: <http://www.sigmaaldrich.com/life-science/cell-biology/learning-center/pathfinder/pathway-maps/pi3k-signaling.html> (Stand 22.09.2008)

- 39) Skurk Carsten, Maatz H., Rocnik E., Bialik A., Force T., Walsh K.; "Glycogen-Synthase 3 β / β -Catenin Axis promotes Angiogenesis through activation of vascular endothelial Growth Factor signaling in endothelial cells." *Circulation Research*, January, 7, 2005, DOI :10.1161/01.RES.0000156273.30274.f7
- 47) Stewart CEH, Rotwein P.; "Growth, differentiation and survival:multiple physiological functions for insulin-like growth factors." *Physiology Review* 1996/ 76, 1005-1026
- 28) Test procedures SPSS software documentation and help, data test consideration chapter, SPSS- statistic software 2008 Version 15, SPSS Inc. Chicago, Illinois 60606
- 37) Torella, Daniele; Rota, M., Nurzynska D., Musso, E., Monsen A., Shiraishi I., Zias E., Walsh K., Rosenzweig A., Sussman M., Urbanek K., Nadal-Ginard B., Kajstura J., Anversa P., Leri, A., et al; "Cardiac stem cell and Myocyte aging, heart failure and Insulin-like Growth factor-1 overexpression." *Circulation research*, January 07, 2004, DOI: 10.1161/01.RES.0000117306.10142.50
- 29) Yuan J.S., Reed A., Chen F., Stewart C. N. Jr.; "Statistical Analysis of real-time PCR data." *BMC Bioinformatics*, 2006, 7/85
- 30) Stratagene Methods and Amplification Guide for Real-Time PCR Version 1.6, 01. March 2007
- 54) Western blotting techniques: Information gathered from <http://www.westernblotting.org>, online resource net, (May 2005)
- 44) Yamada. T .,De Souza. A.T., Finkelstein. S. and Jirtle.R.L.; "Loss of the gene encoding mannose 6-phosphate/insulinlike growth factor II receptor is an early event in liver carcinogenesis." *Proc. Natl. Acad. Sci. USA* 94, 10351-10355.
- 31) Zandstra, Peter W., Lauffenburger Douglas A., Eaves Connie J.; "A ligand-receptor signaling threshold model of stem cell differentiation control: a biologically conserved mechanism applicable to hematopoiesis." *Blood*, 15 August 2000, Volume 96, Number 4
- 41) Zhang, Cheng-Cheng, Harvey F. Lodish .; "Insulin-like growth factor 2 expressed in a novel fetal liver cell population is a growth factor for hematopoietic stem cells." *Blood*, October 30, 2003;DOI 10.1182/blood-2003-08-2955